Control and Alarm Systems Interplay and Co-design

by

Mohammad Hossein Roohi

A thesis submitted in partial fulfillment of the requirements for the degree of

Doctor of Philosophy
in
Control Systems

Department of Electrical and Computer Engineering

University of Alberta

Abstract

Monitoring systems are indispensable parts of industries that are responsible to guarantee the safe and proficient operation of plants. As a part of monitoring systems, alarm management systems are deployed to prevent damage to components, and improve safety and quality of products. The main concern in alarm system design is to provide a mechanism for the accurate announcement of abnormal behavior of plants. However, in reality, numerous false and missed alarms could compromise the overall proficiency.

In this thesis the effect of control systems, as a missing (but significant) actor, on the performance of alarm systems is studied. The interplay of control and alarm performance is justified and it is shown that a controller that is designed to achieve a good quality-of-control (in terms of minimum output variance) has either desirable or undesirable consequences on the performance of alarm systems. To pave the path for finding a robust controller design, a new alarm index is introduced and an analytical expression is derived to evaluate the performance of signals, known systems and systems with parameter uncertainties. A set of linear matrix inequalities (LMIs) is proposed for the controller design to satisfy the required control and alarm performance. Then, we propose a new method to obtain optimal alarm filters by incorporating the knowledge of plant and control systems. In the last part of the thesis, we propose an analytical framework to design and evaluate the performance of two types of non-linear alarm filters. Moreover, in industrial environments, many process variables are acquired. So one challenge is to identify the process

variable that provides the best alarm performance after filtering. We derive an analytical solution to this problem considering specific types of non-linear filters.

Preface

The research presented in Chapter 2 was a result of collaboration with Dr. Iman Izadi from Isfahan University of Technology, Iran. The research conducted in Chapter 3 were my original ideas. The work presented in Chapter 4 was a result of discussions with Dr. Zhe Guan who was with the University of Alberta as a visiting scholar at the time of this work and Dr. Toru Yamamoto from Hiroshima University.

- Chapter 2 has been published as: Roohi, M. H., Chen, T., Izadi, I., "$\mathcal{H}_2$ Controller Synthesis with an Alarm Performance Constraint", *IEEE International Symposium on Industrial Electronics (ISIE)*, pages 533–538, Vancouver, Canada, 2019.

- Chapter 3 has been published as: Roohi, M. H., Chen, T., Izadi, I., "Control and Alarm Interplay and Robust State-feedback Synthesis with an Alarm Performance Constraint", *Journal of Industrial & Engineering Chemistry Research*, 59(38), 16708–16719, 2020.

- Chapter 4 has been submitted for publication as: Roohi, M. H., Chen, T., Guan, Z., Yamamoto, T., "A New Approach to Design Alarm Filters Using the Plant and Controller Knowledge", *Journal of Industrial & Engineering Chemistry Research*.

- Chapter 5 has been published as: Roohi, M. H., Chen, T., "Generalized Moving Variance Filters for Industrial Alarm Systems", *Journal of Process Control*, 95, 75–85, 2020.

- Chapter 6 has been published as: Roohi, M. H., Chen, T., "Performance Assessment and Design of Quadratic Alarm Filters", *IFAC World*

Congress, Berlin, Germany, 2020.

To my beloved wife, parents and teachers.

He is a Being, but not through phenomenon of coming into being. He exists but not from non-existence. He is with everything but not in nearness. He is different from everything but not in separation.

– Ali ibn Abi Talib (p.b.u.h.)

Acknowledgements

I express my utmost gratitude to my supervisor Dr. Tongwen Chen for his continuous support, patience and exceptional guidance throughout my entire PhD program. He always encouraged me to have the wonderful sense of freedom for exploring new research ideas. It is truly a blessing for a researcher to have been trained by such a top-notch scholar. I also thank my supervisory committee members Drs. Qing Zhao and Mahdi Tavakoli for their insightful comments and constructive suggestions. My sincere thanks to Dr. Iman Izadi for his valuable comments on my work.

I would also like to thank my mother, father and my only brother for their endless love, support and encouragement, not only during the course of this work but throughout my life. No words can describe how wonderful they are and how grateful I am for their kindness.

I also extend my appreciation to my in-laws for their love and support. Finally, I can not be more grateful to have my beloved wife for her consistent trust and patience ever since we met. It was her sacrifice, moral support and compassion that made this dissertation possible.

Contents

List of Tables

List of Figures

List of Symbols

$\mathbb{R}$	Set of Real Numbers
$\mathcal{N}$	Normal (Gaussian) Distribution
$\mathcal{X}^2$	Chi-square Distribution
$\Gamma(.,.)$	Gamma Distribution
$\Gamma(.)$	Gamma Function
$\psi(.)$	Digamma Function
erf(.)	Error Function
Subscript "n"	Indicates the Normal Operation Modes
Subscript "ab"	Indicates the Abnormal Operation Modes
$\propto$ ($\propto\!\!\!\!\sim$)	Proportionality (Approximately Proportionality)
I	Identity Matrix
$\mathbf{0}$	Zero Matrix or Zero Vector
$\mathbf{1}$	One Matrix or One Vector
M^T	Transpose of Matrix M or Vector M
M^{-1}	Inverse of Matrix M
diag(.)	Diagonalization Operator of a Matrix
$\|.\|$	Euclidean-based Norm
$\prec$ ($\preceq$)	Negative Definiteness (Semi-definiteness) of a Matrix
$\succ$ ($\succeq$)	Positive Definiteness (Semi-definiteness) of a Matrix
$(.)^T$	Transposed Elements in the Symmetric Position of a Matrix

List of Acronyms

ADD	Average Detection Delay
ARX	Auto-Regressive Exogenous
AUC	Area Under the Curve
CDF	Cumulative Distribution Function
EWMA	Exponentially Moving Average Filter
FAR	False Alarm Rate
FIR	Finite Impulse Response
GMAF	Generalized Moving Average Filter
GMVF	Generalized Moving Variance Filter
HE	Heat Exchanger
HEN	Heat Exchanger Network
IID	Independently and Identically Distributed
ISA	International Society of Automation
LLR	Log-Likelihood Ratio
LMI	Linear Matrix Inequality
LTI	Linear Time-Invariant
MAR	Missed Alarm Rate
PDF	Probability Density Function
PID	Proportional–Integral–Derivative
ROC	Receiver Operating Characteristic
TEP	Tennessee Eastman Process

Chapter 1

Introduction

In this chapter, first we introduce fundamental concepts of abnormality detection systems. Then, we demonstrate current advances in abnormality detection systems, as well as the contributions of this thesis.

1.1 Motivation and Background

Safety and reliability are of great importance in industrial processes. However, they are prone to various faults and abnormal operations. To reduce failures of industrial plants, alarm systems are developed to notify operators of any possible abnormal operations or equipment malfunctions. Based on industrial standard ANSI/ISA-18.2 [92], an alarm system is the "collection of hardware and software that detects an alarm state, communicates the indication of that state to operators, and records changes in the alarm state". Detection of abnormalities is one of the most challenging tasks for alarm systems, and thus attracted the attention of practitioners as well as researchers where they utilized various methods to generate alarm signals from process variables. In an ordinary alarm system, the process variables are compared with some fixed trip-points and if they exceed that, an alarm is raised. In an ideal situation, for each abnormality, one and only one alarm should be raised. However, this is not the case in almost all industrial applications which led to the development of more sophisticated alarm detection methods. A recent study reports several company losses for up to $3.4 billion each, all incidents relating to alarm management issues [39]. The possible consequences of a defective alarm system

are not limited to financial losses or even environmental issues. In the Piper Alpha Oil rig disaster, 167 men died due to an incapacitated alarm system [13].

Aside from the advanced and automated control and monitoring systems, it is the human role to indicate whether the plant works normally or not. According to the industrial alarm standards introduced by the Engineering Equipment and Materials User Association (EEMUA) [36], human limitations should be taken into account when designing alarm management systems. Nevertheless, routinely, plant operators are exposed to overwhelming numbers of alarms to deal with [48], [82]. This may hinder a prompt and accurate reaction. It is worth noting that in practice alarms are not always notifying of a real abnormality which is referred to as the "cry wolf" effect (or false alarms) [66]. The problem of unnecessary alarms is not only limited to industries; a study conducted by [63] surprisingly shows that over 94% of alarm warnings in intensive care units are clinically worthless. Ref. [41] reported that false alarms impede clinical care in anesthesia environments. Ref. [18] stated the problem of false alarms in forest-fire detection. Ref. [1] conducted some experiments to explore the effects of missed alarms on a driver's trust in alarm systems. This phenomenon, in addition to distracting the plant operators, can also attenuate the trust of operators to alarm systems. Besides, the worst part is regarding the alarms that should have been raised but are missed. Inspired by this great demand to improve alarm systems, researchers have proposed statistical tools and data analysis methods to improve alarm systems [39], [99]. A satisfactory alarm system should reduce false alarms while announcing every abnormal situation [53].

1.2 Alarm Performance Measures

There are two generally accepted indices to quantify the accuracy of alarm systems, the false alarm rate (FAR) and missed alarm rate (MAR). False alarms happen when the plant is working normally, but the alarm system raises an alarm which can distract and mislead operators. Missed alarms

are the potential alarms that should have notified the abnormal operation of the plant but have not been raised, which can cause serious damage to the equipment. So an important design consideration of an alarm management system is to reduce false and missed alarms. To this aim, receiver operating characteristic (ROC) curves have been widely used in many publications as a metric for the accuracy of alarm systems [8], [26], [107]. An ROC curve is a plot of the missed alarms rate versus the false alarms rate when the corresponding trip-point spans over all possible values. The area under the curve (AUC) is another metric that was developed based on ROC curves [68]. The AUC is an integral measure of FAR and MAR for all trip-points. So minimizing AUC results in the minimization of FAR and MAR regardless of trip-points. In [69] the author studied an optimal alarm trip-point design problem based on a state-space model of the system and the AUC.

The aforementioned alarm performance indices (FAR, MAR and AUC) are related to the accuracy of alarm systems, However, promptness of an alarm system is also an important factor [67]. In [7], [8] an average detection delay (ADD) is considered and the trade-off among FAR, MAR and ADD is justified. The authors also proposed a method to compromise among these three indices.

1.3 Alarm System Improvement Methods

For the improvement of alarm systems many configurations have been proposed by researchers that can be categorized as basic and advanced methods. Basic methods are:

- Filters: Moving average [7], moving variance [54], quadratic [26], rank-order [90], etc.
- Deadbands: Measurement-Deadbands [49] and time-deadbands [10], [72].
- Delay-timers: On and off delay-timers [59], [111] and generalized delay-timers [6].

Advanced methods are: dynamic alarming [98], predictive alarming [51], [55], state-based alarming [73], etc.

A common issue in alarm systems is several alarms raised during a short time for a single variable which is called alarm chattering [49]. This phenomenon is related to random noise and/or disturbances on process variables that are used for alarming, mainly if values of process variables are close to the associated alarm trip-points [36]. Moreover, repeated on-off actions of control loops can cause chattering alarms by making a frequent transition between alarm and non-alarm states [97]. To tackle chattering alarms it is crucial to first detect their existence. In Ref. [74] the balance of alarm occurrences and operator response was used as an index to identify alarm chattering. Another index based on the alarm run lengths was introduced and an efficient redesign of alarm systems based on that index was proposed in [60]. In [72] the relationship of the deadband, chattering and alarm limit was discussed. Alarm shelving mechanisms are also exploited to reduce alarm chattering [12], [88].

An alarm flood is another problem which is the situation that more than 10 alarms occur during 10 or less minutes [36]. This huge amount of alarms can cause emergency plant shutdown to prevent potential damages. Similar to this benchmark, a human performance modeling study justified that operators could effectively manage at most 11 alarms per 10 minutes [78]. To solve this problem, similarity analysis [11], pattern mining [28], [62], and causal analysis [79] were introduced to reduce alarm floods. The focus of these methods was on the application of data-driven techniques to reduce alarm floods. According to Ref. [39], alarm floods could occur due to improper configurations of alarm variables, unnecessary alarms assigned for single equipment, or too many alarms configured on various process variables. In light of these major causes, instead of exploiting new techniques to reduce alarm floods, a promising solution is by improving the current alarm systems to raise less false and redundant alarms. This includes (but is not limited to) revisit of problems of alarm filter design and combining alarm signals that are set for single equipment. These points are considered in the proposed method of this thesis. Furthermore, numerous process variables are measured by deployed sensors in the plants. So it is crucial to determine the process variable that is the best representative in case of fault occurrence. As an example, Ref. [38] addressed

this problem by ranking alarm variables based on a fuzzy clustering algorithm. We also need an analytical solution to identify the optimal process variable for filtering. In the proposed analysis of this thesis, this problem is also addressed for special classes of nonlinear alarm filters.

Industrial plants are highly interconnected systems where an abnormality can propagate through the whole system and raise many alarms. So another technique to increase the efficiency of alarm systems is to investigate the relationship of raised alarms, which is called alarm root cause analysis [47], [79], [104]. According to this relationship, alarms can be categorized in some groups and the operator will receive the name of the groups instead of the whole alarms. Ref. [2] presented an approach to construct Bayesian networks for root cause analysis based on learning techniques and knowledge of plants. Bayesian networks also were used in [100] to investigate root causes of alarms in thermal power plants in a special case where alarm variables took binary values.

Owing to the large volume of industrial process data, learning based tools are also exploited to detect abnormalities. A two stage algorithm based on symbolic aggregate approximations and hidden Markov models was explored in [108]. This approach only used normal operation mode data to detect abnormalities. In [25], a random forest algorithm was suggested for the early abnormality detection of photovoltaic arrays. Ref. [56] proposed a method based on convolutional neural networks to monitor the conditions of a wind turbine gearbox. Deep belief networks were established in [109], [110] to extract some abstract information from process data for detection of abnormalities. Although these learning based methods show significant improvements in some cases, it is not straightforward to analytically determine their alarm performance. Furthermore, due to their complex structures, they should be tuned mostly based on data. Hence, the possibility of obtaining analytical performance is an advantage of classical alarm filtering methods over learning based approaches.

In this thesis, our focus is on the alarm filters and their relationship with control systems. Moving average and moving variance filters are two important

and widely used alarm filters in industrial applications. An abnormality may appear in the mean change or the variation change of some process variable, which can be detected by moving average and moving variance filters, respectively. Without imposing any constraint on the filter structure, the optimal filter is the log-likelihood ratio (LLR) filter (see [64]). However, in process industries, these filters are not as popular as moving average and variance filters. In [27], it has been proved that among all linear finite impulse response (FIR) filters with similar complexity (namely, filter order), the moving average filter is the optimal one to detect mean changes. However, the effect of filter size and coefficients on the efficiency of the alarm system was not addressed explicitly. [77] addressed the problem of mean change detection in non-stationary environments. They developed a learning-based method to obtain the optimal setting for an exponentially moving average filter (EMWA). Their proposed method could reduce the rates of false alarms and the delay of abnormality detection. Nevertheless, no calculation or estimation of the rates of false and missed alarms was given in the paper. In most situations, an abnormality changes the operating points of some process variables, which can be captured as a change in the mean value. However, there are some cases that the abnormality only affects variations of some process variables. By performing a survey, the major causes of oscillations in plants are changes in product variability [16], process interactions, aggressive controller setting, disturbances [87], and sticky behavior of control valves [29]. A moving variance filter can be used to detect this kind of abnormality. Although in some papers such filters are designed by proposing optimization algorithms (see [26], [27]), there is no explicit solution, especially for the cases that the filter coefficients are selected heterogeneously. In [44], a method for detecting variance changes was introduced, considering that the nominal variance is unknown. [58] proposed a method based on the Kantorovich distance of some principal components to detect changes of variance. Despite Kantorovich distance based filters, moving window based filters provide more intuition about the process operation for plant operators.

Some alarms may also occur due to some changes in the plant. Regarding

that, [114] improved the alarm system during the plant start-up by suppressing the alarm system. Ref. [22] introduced a method for automatic adaptation of alarm trip-points to deal with the varying process situations. A geometric process control method was proposed in [23] to obtain dynamic alarm trip-points from the best operating zones using historical data. Mode-based alarming strategies are also suggested for this issue. These methods rely on proficient knowledge of the process to avoid alarm overloading [20], [45], [46]. Inspired by the uncertainty in the models of a plant, all of these methods are either data-driven or use just a limited knowledge from the plant. As a result, the role of the physical plant and especially the controller has attracted some attention. Ref. [15] proposed a model-based approach based on particle filtering for stochastic systems, but the controller was not addressed in the paper. Ref. [35] proposed an optimization algorithm to balance the fault detectability and the closed-loop control performance by tuning the controller. The interplay of fault detectability and control performance has already been pointed out [84], [113]. The focus of these references was on the fault detection part; they either did not use any alarm performance or consider some deterministic metrics. So there is still a need for a method that utilizes statistical metrics such as FAR and MAR.

Alarm system design has already been investigated for uncorrelated process variables. But the real plants are known to be interconnected dynamical systems which result in the correlated process data even in open-loop conditions. This is definitely true for a plant when it works in the closed-loop mode. A limited number of publications proposed some techniques to attain some solutions for this problem [94], [95], [101]. These work are devoted to alarms systems with either deadbands or delay timers, and the one with filter is still an open problem. Moreover, according to the ISA standard, there are other factors outside alarm systems that are important to the effectiveness of alarm systems [52]. In addition to plant behavior, the controller dynamics can influence the overall performance of alarm systems. This motivated us to study alarm filters while taking into account plant and controller dynamics.

1.4 Thesis Contributions

The focus of this thesis is model based and data driven methods for the improvement of alarm systems. Design and analysis of this thesis are in the field of control and alarm systems, and the contributions are listed as follows. In Chapter 2, the effect of PID controllers on the performance of alarm systems is studied and a design method based on linear matrix inequalities (LMIs) is proposed. In particular, the following are the major contributions of this chapter:

- A new index for alarm signals based on FAR and MAR is introduced.
- A new approach is introduced to design a controller which guarantees a bound for the control performance as well as the alarm performance.
- It is shown that there is a trade-off between control and alarm performance.

Chapter 3 presents a new approach to design a state-feedback controller to satisfy specific requirements on control and alarm performance in the presence of model uncertainty. This chapter has the following major contributions:

- The alarm signal of the previous chapter is extended to measure the alarm performance of known systems and systems with parameter uncertainties.
- A set of LMIs is proposed for the state-space controller design to satisfy the required control and alarm performance in a robust manner.

The previous two chapters study the controller design problem. In Chapter 4 the problem of alarm filter design is studied. Major contributions of this chapter are as follows:

- A new method for obtaining optimal filter coefficients by incorporating the knowledge of plant and control systems while relaxing the independence assumption.

- It is justified that the conventional moving average filter is not optimal for the detection of mean changes when the independence assumption on process measurements is relaxed.

The rest of this thesis is devoted to data driven techniques. In the next two chapters, application of the proposed alarm index in Chapter 1 for second order alarm filters is illustrated. The major contributions of Chapter 5 are listed in what follows:

- A Gaussian approximation is derived for the output of generalized moving variance filters.
- Based on this approximation, an explicit relationship of filter parameters and the optimal solution is provided.
- It is proved that the conventional moving variance filter is the optimal configuration if only the detection accuracy is considered. But in the case study, via a counter-example, we show that this statement does not hold if we also take the detection delay into account.

Chapter 6 has the following major contributions:

- An analytic result for the alarm performance of quadratic alarm filters is derived; then the optimal solution is obtained.
- A new score is introduced, which helps the plant operators to determine an appropriate process variable for alarm purposes.
- It is demonstrated that for different filter structures, the efficient choice of process variables might be different.

1.5 Thesis Organization

The remaining of the thesis is organized as follows. Chapter 2 is on design and analysis of the PID controllers on alarm systems. In Chapter 3 a robust state-feedback controller design method is introduced by taking alarm performance into account. Chapter 4 introduces a new method to design alarm filters by

using the information from the plant and controller. In Chapter 5 a method for optimal design of the generalized moving variance filters is proposed. Chapter 6 deals with the performance evaluation and design of quadratic alarm filters. Finally, Chapter 7 provides some concluding remarks and possible future research directions.

Chapter 2

Controller Synthesis with an Alarm Performance Constraint

In this chapter, the influence of PID controllers on alarm systems will be studied in case of actuator faults. A set of linear matrix inequalities (LMIs) will be introduced to solve the problem. The LMI conditions will be obtained to achieve an $\mathcal{H}_2$ gain criterion from the control point of view and a bound for the alarm performance based on the new index. There are two parameters in the LMIs which are related to the control performance and the alarm performance. We will illustrate the effect and the trade-off of these two parameters by a numerical example.

2.1 Problem Statement

Consider a discrete-time linear time-invariant plant $\mathcal{P}$, described as

$$\begin{aligned} x_{k+1}^p &= Ax_k^p + B_u u_k + B_w w_k, \\ y_k &= Cx_k^p, \end{aligned} \tag{2.1}$$

where $x_k^p \in \mathbb{R}^n$ is the state vector, $u_k \in \mathbb{R}$ is the control input, $y_k \in \mathbb{R}$ is the measurement, $w_k \in \mathbb{R}$ is the external disturbance to the system and $A,\ B_u,\ B_w$, and C are matrices with appropriate dimensions. It is not possible to measure w_k but it is assumed to have Gaussian distributions. Furthermore, in the normal and abnormal cases it follows $\mathcal{N}(\mu_n, \sigma_w^2)$ and $\mathcal{N}(\mu_{ab}, \sigma_w^2)$, respectively. In other words, a fault will change the mean values of the distributions.

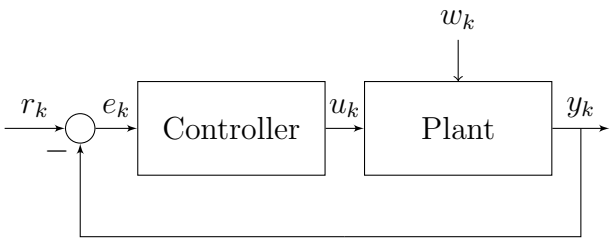

Figure 2.1: Closed-loop diagram

2.1.1 PD Controller

A discrete-time PD controller $\mathcal{C}$ is described as:

$$\begin{aligned} e_k &= r_k - y_k, \\ u_k &= k_p e_k + k_d(e_k - e_{k-1}), \end{aligned}$$

where, e_k is the error between a reference signal r_k and the measurement y_k, k_p and k_d are proportional and differential gains of the controller, respectively. We reformulate the equations to find a state space model of the controller. A state space realization of the controller can be obtained as

$$\begin{aligned} x^c_{k+1} &= e_k, \\ u_k &= -k_d x^c_k + (k_p + k_d)e_k, \end{aligned} \tag{2.2}$$

where $x^c_k \in \mathbb{R}$ is the state variable of the controller.

The diagram of the control loop that is studied in this chapter is shown in Fig. 2.1. Now assuming $r_k \equiv 0$ and combining (2.1) and (2.2), the closed-loop system from disturbance input w_k to y_k can be formulated as

$$\begin{aligned} x^c_{k+1} &= -Cx^p_k, \\ x^p_{k+1} &= (A - (k_p + k_d)B_u C)x^p_k - k_d B_u x^c_k + B_w w_k, \\ y_k &= Cx^p_k. \end{aligned}$$

Let $\bar{x}_k$ denote $\begin{bmatrix} x^c_k \\ x^p_k \end{bmatrix}$,

$$\begin{aligned} \bar{x}_{k+1} &= \begin{bmatrix} 0 & -C \\ -k_d B_u & A - (k_p + k_d)B_u C \end{bmatrix} \bar{x}_k + \begin{bmatrix} 0 \\ B_w \end{bmatrix} w_k, \\ y_k &= \begin{bmatrix} 0 & C \end{bmatrix} \bar{x}_k. \end{aligned} \tag{2.3}$$

One of our aims in designing the controller is to achieve a good quality-of-control. As the external disturbance to the system is considered to be Gaussian, to quantify the control performance we consider an upper bound η for the $\mathcal{H}_2$ norm of the plant from w_k to y_k. Let $\mathcal{G}_{yw}(z)$ denote the transfer function of the closed-loop system from w_k to y_k. So one of our goals is to satisfy

$$\|\mathcal{G}_{yw}(z)\|_{\mathcal{H}_2}^2 \leq \eta. \tag{2.4}$$

Another goal in designing the controller is to satisfy a bound on the alarm performance. For this aim, in the next subsection a new alarm index for the system is introduced.

2.1.2 Alarm Performance Index

We start with the ROC curves and the area under these curves. Two ROC curves are shown in Fig. 2.2. It is desired to have ROC curves as close as it is possible to the origin. To quantify these statement we can consider the area under these curves. So the smaller AUC means the better alarm performance. In Fig. 2.2, the curve ROC_a has a better alarm performance in comparison with the curve ROC_b. It means that for a fixed MAR (FAR), ROC_a has smaller FAR (MAR) than ROC_b. But, if an operator chooses the trip-point to achieve b_1 instead of a_3, he will get a lower FAR but a very larger MAR. A similar situation can happen for a_1 and b_3 points. However, if the operator wants to compromise between FAR and MAR, it is better to choose a_2 instead of b_2. It is worth noting that using this concept, we can make a separation between controller design problem and alarm system design problem. It means that the controller can be designed to achieve a small AUC (according to the alarm requirements) and then the alarm design problem is to choose the corresponding trip-point. The area under an ROC curve corresponding to the signal y_k with Gaussian distribution can be found by modifying a result presented in [70] as

$$\text{AUC} = 1 - \Phi\left(\frac{|\mu_{y_{ab}} - \mu_{y_n}|}{\sqrt{\sigma_{y_{ab}}^2 + \sigma_{y_n}^2}}\right), \tag{2.5}$$

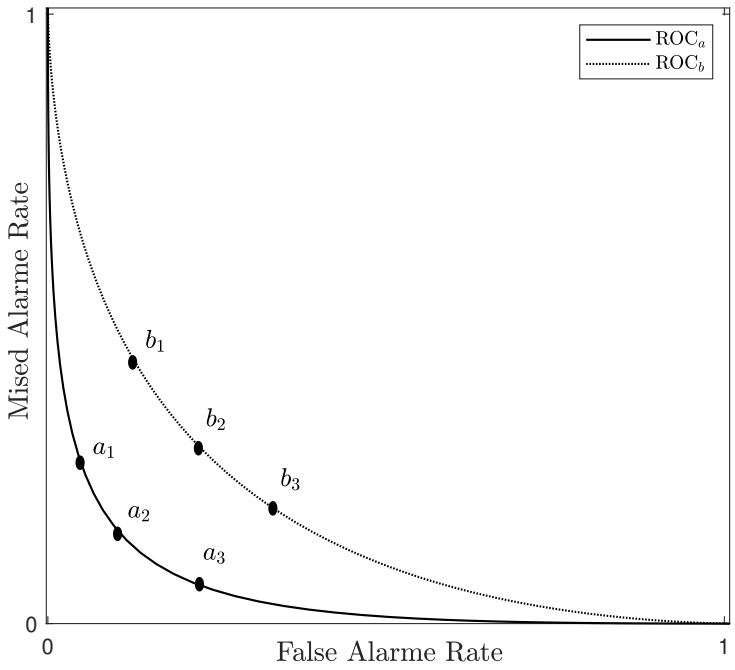

Figure 2.2: ROC curves and different trip-points

where $\mu_{y_{ab}}$ and μ_{y_n} are the expected values of the signal in abnormal and normal cases, respectively, $\sigma^2_{y_{ab}}$ and $\sigma^2_{y_n}$ are the variances of the signal in abnormal and normal cases, respectively, and the function Φ is defined as

$$\Phi(x) = \frac{1}{\sqrt{2\pi}} \int_{-\infty}^{x} e^{-\frac{1}{2}z^2} \mathrm{d}z. \tag{2.6}$$

According to the fact that Φ is a strictly increasing function and $\sup_x \Phi(x) = 1$, we can conclude that AUC is a strictly decreasing function of $|\mu_{y_{ab}} - \mu_{y_n}| \left(\sigma^2_{y_{ab}} + \sigma^2_{y_n}\right)^{\frac{-1}{2}}$. Thus, to minimize the AUC we need to maximize $|\mu_{y_{ab}} - \mu_{y_n}| \left(\sigma^2_{y_{ab}} + \sigma^2_{y_n}\right)^{\frac{-1}{2}}$. An intuition for this is that when $|\mu_{y_{ab}} - \mu_{y_n}|$ is large and $\sigma^2_{y_{ab}} + \sigma^2_{y_n}$is small it is easier to differentiate between normal and abnormal operations of the system. So the greater this $|\mu_{y_{ab}} - \mu_{y_n}|\left(\sigma^2_{y_{ab}} + \sigma^2_{y_n}\right)^{\frac{-1}{2}}$ value, the better alarm performance; and vice versa. Thus, to have a lower bound on the alarm performance, the following condition should be satisfied:

$$\frac{\sqrt{\sigma^2_{y_{ab}} + \sigma^2_{y_n}}}{|\mu_{y_{ab}} - \mu_{y_n}|} < \phi, \tag{2.7}$$

where ϕ is a design parameter corresponding to the alarm performance. A smaller ϕ results in a better alarm performance and vice versa. To add con-

dition (2.7) into the controller synthesis problem we need to reformulate it as

$$(\mu_{y_{ab}} - \mu_{y_n})^{-2}(\sigma^2_{y_{ab}} + \sigma^2_{y_n}) < \phi^2. \tag{2.8}$$

Let $\sigma^2_{w_{ab}}$ and $\sigma^2_{w_n}$ denote the variance of input noise $w(k)$ for abnormal and normal cases, respectively. For a linear single-input single output system we know that

$$\sigma^2_{y_{ab}} = \sigma^2_{w_{ab}}\sigma^2_y,\ \sigma^2_{y_n} = \sigma^2_{w_n}\sigma^2_y, \tag{2.9}$$

where σ^2_y is the output variance of the system in response to a white Gaussian noise. Furthermore, for the closed-loop system we have

$$\mathcal{G}_{yw}(z) = \frac{\mathcal{P}_{yw}(z)}{1 + \mathcal{C}_{ue}(z)\mathcal{P}_{yu}(z)}. \tag{2.10}$$

Now let us define $g \triangleq \mathcal{G}_{yw}(1)$ as the DC gain of the closed-loop system. Furthermore, let $\mu_{w_{ab}}$ and μ_{w_n} denote the expected values of input noise $w(k)$ for abnormal and normal cases, respectively. The relationship of the expected value of y_k and w_k for abnormal and normal cases can be described as

$$\mu_{y_{ab}} = g\mu_{w_{ab}},\ \mu_{y_n} = g\mu_{w_n}. \tag{2.11}$$

Using (2.9) and (2.11), the equation in (2.8) can be modified as

$$\sigma^2_y g^{-2} < \psi^2, \tag{2.12}$$

where

$$\psi = \frac{|\mu^w_{ab} - \mu^w_n|\phi}{(\sigma^2_{w_{ab}} + \sigma^2_{w_n})}.$$

Now the controller synthesis problem is to design a stabilizing PD controller $\mathcal{C}$ to guarantee an upper bound for the $\mathcal{H}_2$ norm of the system from w_k to y_k with the constraint of (2.12).

Remark 1 *Based on the new alarm index we can claim that the integral term in the classical PID controller can decrease the alarm performance significantly. Due to the integral term, the DC gain of a PID controller approaches infinity. So if we choose the PID controller structure for* $\mathcal{C}$*, according to* (2.10)

we can realize that $\mathcal{G}_{yw}(1) = 0$ *when* $\mathcal{P}_{yw}(1)$ *and* $\mathcal{P}_{yu}(1)$ *are bounded. So in view of* (2.7) *the alarm index approaches infinity regardless of the variance of the system. To gain more intuition, if the expected values for process data are the same for both normal and abnormal cases, then it is very hard to differentiate between these two cases with the trip-point.*

2.2 Controller Synthesis

In this section a set of LMIs will be introduced to solve the optimization problem. First let us find the relationship of g^{-1} from the constraint in (2.12) and system matrices. We know that $g = \mathcal{G}_{yw}(1)$ so from (2.10) we have

$$g^{-1} = \frac{1 + \mathcal{C}_{ue}(1)\mathcal{P}_{yu}(1)}{\mathcal{P}_{yw}(1)}.$$

Using the state space realization of $\mathcal{P}$ and $\mathcal{C}$ we can find the DC gains as

$$\mathcal{P}_{yu}(1) = C(I - A)^{-1}B_u,$$
$$\mathcal{P}_{yw}(1) = C(I - A)^{-1}B_w,$$

and

$$\mathcal{C}_{ue}(1) = k_p.$$

Thus, for a known plant, $\mathcal{P}_{yu}$ and $\mathcal{P}_{yw}$ are known and fixed. So we have

$$g^{-1} = \alpha + \beta k_p, \tag{2.13}$$

where $\alpha \triangleq \mathcal{P}_{yw}^{-1}(1)$ and $\beta \triangleq \mathcal{P}_{yu}(1)\mathcal{P}_{yw}^{-1}(1)$.

Now we reform the closed-loop equation in (2.3) as

$$\begin{aligned} \bar{x}_{k+1} &= (A_0 + B_0 K C_0)\bar{x}_k + \bar{B}w_k \\ y_k &= \bar{C}\bar{x}_k. \end{aligned} \tag{2.14}$$

where

$$
\begin{aligned}
A_0 &\triangleq \begin{bmatrix} 0 & -C \\ 0 & A \end{bmatrix}, \\
B_0 &\triangleq \begin{bmatrix} 0 \\ B_u \end{bmatrix}, \\
C_0 &\triangleq \begin{bmatrix} I & 0 \\ 0 & -C \end{bmatrix}, \\
\bar{B} &\triangleq \begin{bmatrix} 0 \\ B_w \end{bmatrix}, \\
\bar{C} &\triangleq \begin{bmatrix} 0 & C \end{bmatrix},
\end{aligned}
$$

and

$$K = \begin{bmatrix} -k_d & k_p + k_d \end{bmatrix}. \tag{2.15}$$

Before proceeding to the controller synthesis method, another modification should be done on (2.14). We know that for a nonzero C matrix, C_0 is of rank 2. So we can always find a transformation matrix T such that $C_0 T = [I\ 0]$. Then the new system matrices can be found as

$$
\begin{aligned}
\mathcal{A}_0 \triangleq T^{-1} A_0 T,\ \mathcal{B}_0 \triangleq T^{-1} B_0, \\
\bar{\mathcal{B}} \triangleq T^{-1} \bar{B},\ \bar{\mathcal{C}} \triangleq \bar{C} T.
\end{aligned}
$$

So (2.14) is converted to

$$\bar{x}_{k+1} = (\mathcal{A}_0 + \mathcal{B}_0 K [I\ 0]) \bar{x}_k + \bar{\mathcal{B}} w_k, \tag{2.16}$$

$$y_k = \bar{\mathcal{C}} \bar{x}_k. \tag{2.17}$$

The main result of this chapter can be summarized as in the following theorem.

Theorem 2.2.1 *Consider a plant described by* (2.1) *controlled by a PD controller in* (2.2) *and assume that* w_k *is a stochastic white noise with* $\sigma_w = 1$. *The controller is stabilizing and guarantees the control and alarm performances described by* (2.4) *and* (2.7) *if* $P \succ 0$, X_1, X_2 *and* L *can be found that satisfies the following LMIs*

$$\begin{bmatrix} P & \mathcal{A}_0 X + \mathcal{B}_0 L & \bar{\mathcal{B}} \\ (.)^T & X + X^T - P & 0 \\ (.)^T & (.)^T & 1 \end{bmatrix} \succ 0, \tag{2.18}$$

$$\begin{bmatrix} \eta & \bar{\mathcal{C}}X \\ (.)^T & X + X^T - P \end{bmatrix} \succ 0, \tag{2.19}$$

$$\begin{bmatrix} \psi^2\eta^{-1} & \alpha + \beta L \begin{bmatrix} 1 \\ 1 \\ 0 \end{bmatrix} \\ (.)^T & 1 \end{bmatrix} \succ 0, \tag{2.20}$$

where

$$L \triangleq [K\ 0], \tag{2.21}$$

and

$$X \triangleq \begin{bmatrix} I & 0 \\ X_1 & X_2 \end{bmatrix}. \tag{2.22}$$

Proof. First we introduce two lemmas which are used in the proof. The first lemma presents a set of inequalities to guarantee the stability and a bound on the output variance. The second lemma helps us to convert our inequalities to a set of LMIs.

Lemma 2.2.2 *Consider a linear time-invariant system described by* (2.16) *and* (2.17)*, where w_k is a stochastic white noise. The system is asymptotically stable and $\sigma_y^2 g^{-2} < \psi^2$ if there exists a matrix $P \succ 0$ such that*

$$(\mathcal{A}_0 + \mathcal{B}_0 K[I\ 0])P(\mathcal{A}_0 + \mathcal{B}_0 K[I\ 0])^T + \bar{\mathcal{B}}\bar{\mathcal{B}}^T \prec P, \tag{2.23}$$

$$g^{-2}\bar{\mathcal{C}}P\bar{\mathcal{C}}^T < \psi^2. \tag{2.24}$$

Proof. According to a theorem from [85] for output covariance of linear time invariant systems we know that a system is asymptotically stable if (2.23) holds and further more we have $\sigma_y^2 < \bar{\mathcal{C}}P\bar{\mathcal{C}}^T$. Also we have $g^{-2} > 0$ so $\sigma_y^2 g^{-2} < g^{-2}\bar{\mathcal{C}}P\bar{\mathcal{C}}^T$. Thus, $\sigma_y^2 g^{-2} < \psi^2$ holds if (2.24) holds. □

The closed-loop equation of the system in (2.16) can be viewed as a static output-feedback design problem. The following lemma is a result from [33] where the author introduced a new structure for the LMIs to increase degrees of freedom.

Lemma 2.2.3 *For the system described by* (2.16) *and* (2.17) *a static output-feedback controller* K *exists such that* $\|\mathcal{G}_{yw}(z)\|_{\mathcal{H}_2}^2 \leq \eta$ *from* w_k *to* y_k *if LMIs*

$$\begin{bmatrix} P & \mathcal{A}_0\mathcal{X} + \mathcal{B}_0\mathcal{L} & \bar{\mathcal{B}} \\ (.)^T & \mathcal{X} + \mathcal{X}^T - P & 0 \\ (.)^T & (.)^T & 1 \end{bmatrix} \succ 0, \tag{2.25}$$

$$\begin{bmatrix} \eta & \bar{\mathcal{C}}\mathcal{X} \\ (.)^T & \mathcal{X} + \mathcal{X}^T - P \end{bmatrix} \succ 0, \tag{2.26}$$

hold for variable matrices $P \succ 0$, $\mathcal{X}$, *and* $\mathcal{L}$ *with following structures:*

$$\mathcal{L} \triangleq \begin{bmatrix} \mathcal{L}_1 & 0 \end{bmatrix},$$
$$\mathcal{X} \triangleq \begin{bmatrix} \mathcal{X}_{11} & 0 \\ \mathcal{X}_{21} & \mathcal{X}_{22} \end{bmatrix}. \tag{2.27}$$

Then a static output-feedback can be obtained as

$$K = \mathcal{L}_1\mathcal{X}_{11}^{-1}. \tag{2.28}$$

To use this lemma we impose structure of (2.22) on (2.27) so $\mathcal{X}_{11}$ is set to be I in (2.27). Now we observe that (2.18) and (2.19) are equivalent to (2.25) and (2.26), respectively, where $X = \mathcal{X}$ $L = \mathcal{L}$.

The matrix P is positive definite; so

$$(P - X)^T P^{-1}(P - X) \succeq 0.$$

Hence

$$X^T P^{-1} X \succeq X + X^T - P. \tag{2.29}$$

From (2.18) by using Schur's complement lemma [30], we can conclude that $X + X^T - P^{-1} \succ 0$; so X should be non-singular because $P \succ 0$. Combining this fact with (2.29) yields

$$X^{-1}P(X^T)^{-1} \preceq (X + X^T - P)^{-1},$$

or

$$P \preceq X(X + X^T - P)^{-1}X^T. \tag{2.30}$$

Again by using Schur's complement lemma, the inequality (2.18) can be written as

$$P - \begin{bmatrix} \mathcal{A}_0X + \mathcal{B}_0L & \bar{\mathcal{B}} \end{bmatrix} \begin{bmatrix} (X + X^T - P)^{-1} & 0 \\ 0 & 1 \end{bmatrix} \begin{bmatrix} (\mathcal{A}_0X + \mathcal{B}_0L)^T \\ \bar{\mathcal{B}}^T \end{bmatrix} \succ 0.$$

Now using (2.21) and doing a simple matrix calculation we have

$$P \succ (\mathcal{A}_0 + \mathcal{B}_0 K[I\ 0])X(X + X^T - P)^{-1}X^T(\mathcal{A}_0 + \mathcal{B}_0 K[I\ 0])^T + \bar{\mathcal{B}}\bar{\mathcal{B}}^T. \quad (2.31)$$

Combining (2.30) and (2.31) satisfies (2.23). Again by applying Schur's complement lemma on (2.19) we can obtain

$$\eta > \bar{\mathcal{C}}X(X + X^T - P)^{-1}X^T\bar{\mathcal{C}}. \quad (2.32)$$

By comparing (2.30) and (2.32) we have

$$\eta > \bar{\mathcal{C}}P\bar{\mathcal{C}}^T. \quad (2.33)$$

Plugging (2.21) into (2.20) and applying Schur's complement lemma yields

$$\psi^2\eta^{-1} - \left(\alpha + \beta[K\ 0]\begin{bmatrix}1\\1\\0\end{bmatrix}\right)\left(\alpha + \beta[K\ 0]\begin{bmatrix}1\\1\\0\end{bmatrix}\right)^T > 0, \quad (2.34)$$

By recalling (2.15), (2.34) can be written as

$$\psi^2\eta^{-1} - (\alpha + \beta k_p)(\alpha + \beta k_p)^T > 0, \quad (2.35)$$

where $\alpha + \beta k_p$ is a scalar. (2.13) and (2.35) together yield

$$\psi^2 > g^{-2}\eta. \quad (2.36)$$

Finally, combining (2.33) and (2.36) proves (2.24), which concludes the proof. □

2.3 Simulation Result

In this section we illustrate the effectiveness of our method and the effects of η and ψ on the control and alarm performances. Consider a plant described by (2.1) where

$$A = \begin{bmatrix}-0.25 & 0\\ 0.3 & 1.18\end{bmatrix},$$

$$B_u = \begin{bmatrix}0.9\\-0.7\end{bmatrix},$$

$$B_w = \begin{bmatrix} 0.3 \\ 0.1 \end{bmatrix},$$
$$C = \begin{bmatrix} 0.8 & 0.6 \end{bmatrix}.$$

We assume that for the normal and abnormal cases w_k follows $\mathcal{N}(0,1)$ and $\mathcal{N}(2,1)$, respectively. First we design the controller such that we have a good control performance. So we set $\eta = 0.5$ and $\psi = 5$. By solving the LMIs (2.18), (2.19), and (2.20) the variable matrix K can be obtained as

$$K = \begin{bmatrix} -0.012 & -0.708 \end{bmatrix}.$$

So recalling (2.15), the PD controller can be designed as

$$u_k = -0.72e_k + 0.012(e_k - e_{k-1}).$$

The simulation result is shown in Fig. 2.3. The top plot indicates the process data y_k for 2000 samples where an abnormality happened at the 1000'th sample. The trip-point is designed based on the available data to minimize the summation of FAR and MAR. The bottom plot shows the alarm signal generated from the aforementioned process data. When the process data is greater than the trip-point, an alarm is raised and the alarm signal is set to 1; when it is smaller than the trip-point, the alarm signal is set back to 0. According to this figure, before the time that the abnormality happened, we have many alarms raised. These are considered as false alarms which are undesirable. From the other side, when the abnormality happened and stayed, the alarm signal should remain raised. However, due to the noise we can see that it is turning off and on; hence there are missed alarms.

Now let us set $\eta = 1.2$ and $\psi = 1$ to have a good alarm performance this time. By doing the same procedure we have

$$K = \begin{bmatrix} 0.088 & -0.712 \end{bmatrix},$$

and the PD controller is obtained as

$$u_k = -0.624e_k - 0.088(e_k - e_{k-1}).$$

Result of the simulation for this case is shown in Fig. 2.4. As we expected, a better alarm performance is achieved with this controller. Before happening

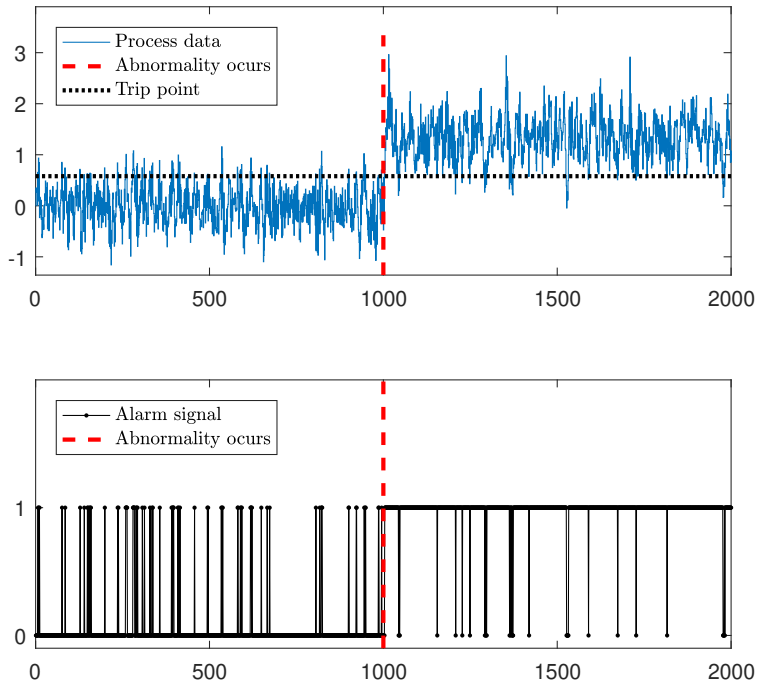

Figure 2.3: Simulation result for $\eta = 0.5$ and $\psi = 5$

of the abnormality, we have a fewer number of false alarms and also after it, we have fewer missed alarms.

We can compare two scenarios from both control and alarm points of view. Fig. 2.5 gives the ROC curves of two scenarios. The dotted line corresponds to the scenario that we designed the controller for a better control performance and the solid line is corresponding to the scenario that we wanted a better alarm performance. As a result, the AUC of the solid curve is smaller than that of the dotted curve. However, the amplitude of process data in Fig. 2.4 is smaller than Fig. 2.3 which means the controller of the first scenario rejected the effect of disturbance better than the controller of the second scenario.

It is important to note that the $\mathcal{H}_2$ controller reduces the variance of output signal which is desired both for the control and alarm systems. However, it also rejects the effect of disturbance; so the trip-point is designed with a lower magnitude. In fact, if we want a good control performance, the statistical parameters of process data for both the normal and abnormal cases

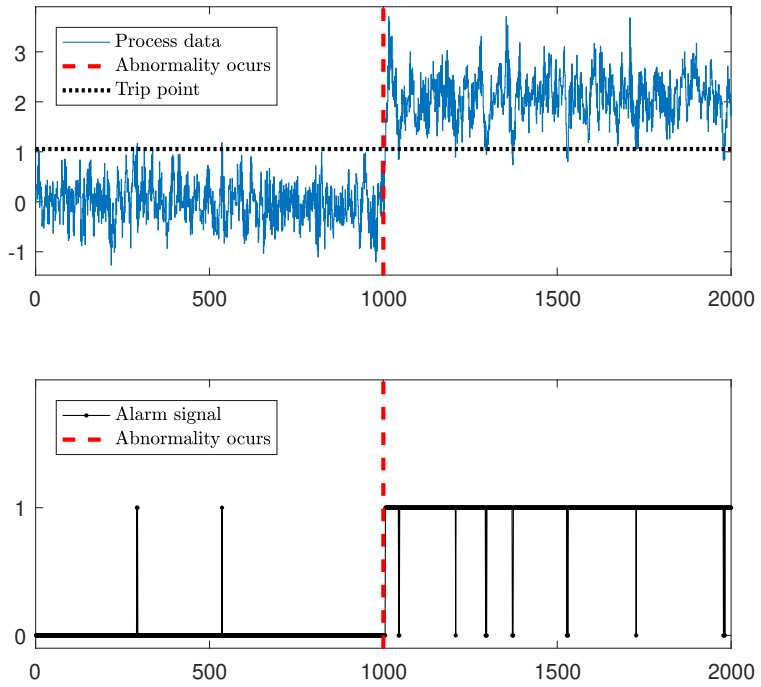

Figure 2.4: Simulation result for $\eta = 1.2$ and $\psi = 1$

will be similar; so it is harder to differentiate them. When the controller is designed to have a good alarm performance, the effect of disturbance can be seen in the process data and it is easier to differentiate between normal and abnormal cases. Thus, as a drawback we have a lower control performance in this scenario. So we can conclude that there is a trade-off for control and alarm performance.

2.4 Summary

In this chapter, we proposed a new approach to tune a PD controller which compromises both the control performance and alarm performance. The control performance is measured based on the $\mathcal{H}_2$ norm of the system. For the alarm performance, we introduced a new alarm index based on the area under ROC curves. This chapter also introduced a new framework for co-design of the control system and alarm system. A sub-optimal solution for this co-design

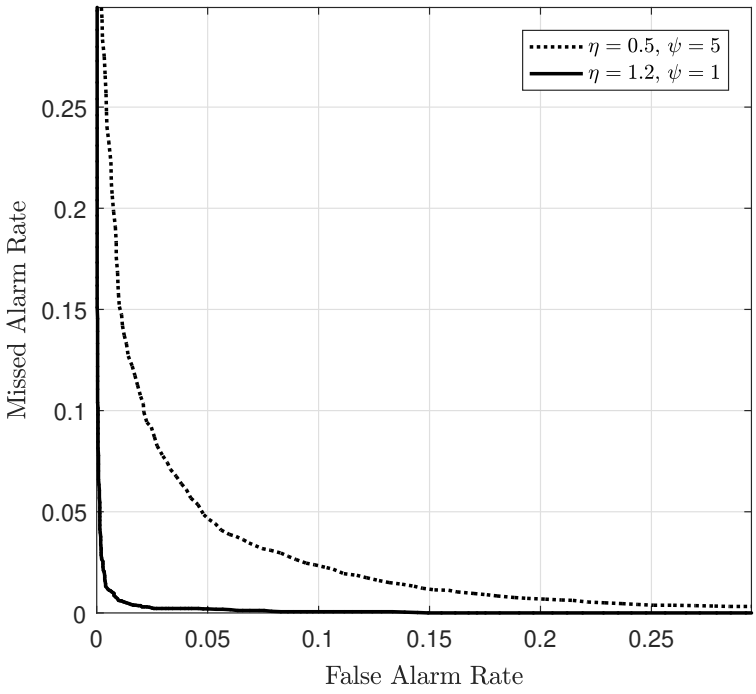

Figure 2.5: ROC curves for two sets of η and ψ

problem is given based on sufficient LMI conditions. Furthermore, the trade-off between control performance and alarm performance is illustrated using a numerical example.

Chapter 3

Control and Alarm Interplay and Robust State-feedback Design with an Alarm Performance Constraint

In this chapter, we propose a new approach to design a state-feedback controller to satisfy specific requirements on control and alarm performance in the presence of model uncertainty. The control performance is measured based on an $\mathcal{H}_2$-norm of the system. For the alarm performance, FAR and MAR are not appropriate to be used in the control design problem as a constraint. However, we use a new alarm performance index based on these two metrics, which can be either added in the cost function or as a new constraint in the controller design problem. We introduced a preliminary version of this index in Chapter 2 by exploiting area under a receiver operating characteristic (ROC) curve which is a popular measurement for efficiency of classifiers. The index proposed in Chapter 2 could only be utilized to measure alarm performance of signals. In the current chapter, we extend it to evaluate the effect of linear systems on the alarm performance of signals. This index eventually is used as an alarm performance constraint for our controller design problem. We also show how this index can be used in the presence of model uncertainty. Another contribution of this chapter is to justify the interplay of state-feedback controllers and alarm systems in case of actuator fault. Intuitively, we know that a good controller compensates the effect of abnormalities in the output

which impedes distinguishability of normal and abnormal situations. So we propose a linear matrix inequality (LMI) based solution to compromise the control and alarm performance.

3.1 Alarm Performance Index

In process industries, the most popular strategy for detecting abnormalities is based on comparing the value of a process variable with a constant alarm threshold [99]. Then the alarm triggered based on that process variable, which is referred to as an alarm variable. Let $v(k)$ and v_{th} denote the alarm variable and the associated alarm threshold, a high (low) alarm state is expressed as

$$\begin{cases} \text{alarm}, & v(k) > (<)\ v_{th}, \\ \text{no alarm}, & \text{otherwise}. \end{cases} \tag{3.1}$$

A large class of abnormalities that appear as operation point shifts of some alarm variables can be captured by this mechanism. Various alarm indices are introduced to evaluate the capability of alarm systems for distinguishing between normal and abnormal operation modes. Following the preliminary result for the new alarm performance index (or simply alarm index) that we introduced in Ref. [80], we will extend and study the alarm index in depth. The alarm index can be adopted for Gaussian alarm variables as well as systems driven by Gaussian alarm variables. In both cases it has a close relation to the classification problems where various thresholds are considered to classify a set of raw data into two categories. We start with the concept of area under the curves (AUC) for receiver operating characteristics (ROC) curves. ROC plots show the relation of the missed alarm rate (MAR) and false alarm rate (FAR) at various alarm thresholds. Then we introduce an appropriate measure for linear time-invariant (LTI) systems which can eventually lead us to design a controller that guarantees a desired level of performance for the alarm system. Suppose that $f_{v,ab}(\cdot)$ and $f_{v,n}(\cdot)$ represent the probability density function (PDF) of v in the abnormal and normal operation modes, respectively. For

high alarms (c.f. (3.1)), MAR and FAR are obtained as follows:

$$\text{MAR} = \int_{-\infty}^{v_{th}} f_{v,ab}(\tau)\ \mathrm{d}\tau,$$
$$\text{FAR} = \int_{v_{th}}^{\infty} f_{v,n}(\tau)\ \mathrm{d}\tau.$$

Here, $f_{v,ab}(\cdot)$ and $f_{v,n}(\cdot)$ can be estimated from historical process data. Now the ROC curve can be found as the plot of MAR versus FAR when the threshold v_{th} spans all real numbers. Although this formulation only holds for high alarms, a similar one can be obtained for low alarms. Likewise, the corresponding ROC curve can be plotted, thus, the AUC analysis can be applied to this case as well. For simplicity, the focus of our derivations is on high alarms. But with some slight modifications, the final result remains valid for the case of low alarms. In Fig. 3.1 the curve with closer points to the origin, corresponds to better alarm performance. Here we can measure the closeness by AUC. The AUC is classification-threshold-invariant as it measures the classification quality irrespective of what value is chosen as the threshold. Hence, it is not capable of prioritizing the minimization of FAR of MAR, which might be of interest in different applications (usually minimization of MAR is more important but some other consideration may arise due to the "cry wolf" effect [99]). However, after tuning the controller to achieve the desirable classification, the designer can make a compromise by selecting the threshold according to the design requirements. As an example, in Fig. 3.1, with no more details about the application, the design which results in the ROC_a is more desirable than the one with ROC_b. The reason is that for a particular MAR (resp. FAR), ROC_a has s smaller FAR (resp. MAR) than ROC_b. However, one may realize that b_1 (resp. b_3) has a lower FAR (resp. MAR) than a_3 (resp. a_1); but as a drawback, b_1 (resp. b_3) has a significantly greater MAR (resp. FAR) in comparison with a_3 (resp. a_1). In this example, the middle point of a curve with the lower AUC (a_2) yields a better performance than b_2. In this figure, ROC_c corresponds to the case that the mean values of the normal and abnormal cases are very close. This curve confirms that under this condition, separating these two modes can not be done with a constant threshold. It is worth emphasizing

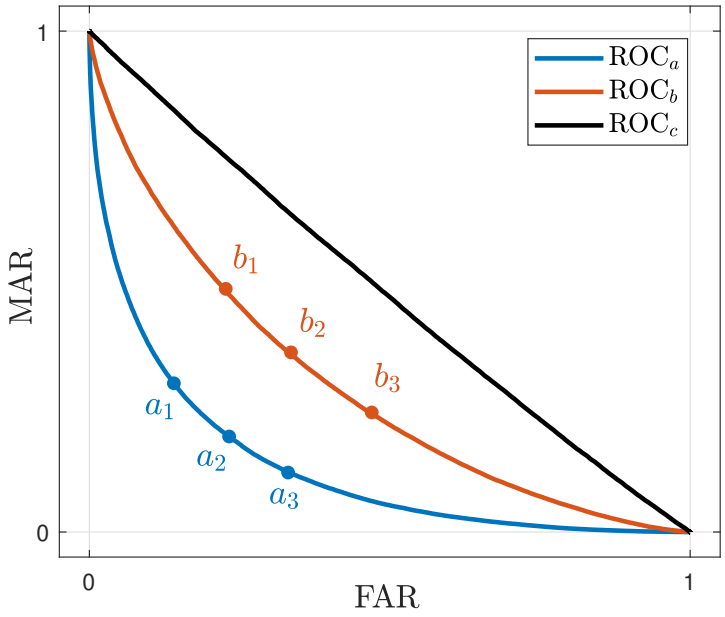

Figure 3.1: Comparison of ROC curves and different thresholds.

that using AUC made it possible to separate controller synthesis and alarm system design problems. The controller is chosen to produce a smaller AUC for the alarm system, and in the next step, the threshold of the alarm system is set to achieve the desired MAR and FAR.

3.1.1 Alarm Index for Signals

Consider a discrete-time alarm variable $v(k) \in \mathbb{R}$ with a Gaussian distribution compared with a threshold to generate an alarm signal. Let μ_v and $\bar{\mu}_v$ denote the expected values of $v(k)$ in normal and abnormal cases, respectively. Furthermore, σ_v and $\bar{\sigma}_v$ correspond to the square root of variance of $v(k)$ in normal and abnormal cases, respectively. The occurrence of abnormality can be represented as

$$v(k) \sim \begin{cases} \mathcal{N}(\mu_v, {\sigma_v}^2), & \text{normal,} \\ \mathcal{N}(\bar{\mu}_v, {\bar{\sigma}_v}^2), & \text{abnormal.} \end{cases} \tag{3.2}$$

Without loss of generality, we assume that $\bar{\mu}_v > \mu_v$. Now the rates of false and missed alarms are obtained as

$$\text{MAR} = \int_{-\infty}^{v_{th}} \frac{1}{\sqrt{2\pi}\bar{\sigma}_v} e^{-\frac{(\tau-\bar{\mu}_v)^2}{2\bar{\sigma}_v^2}} \, \mathrm{d}\tau,$$
$$\text{FAR} = \int_{v_{th}}^{\infty} \frac{1}{\sqrt{2\pi}\sigma_v} e^{-\frac{(\tau-\mu_v)^2}{2\sigma_v^2}} \, \mathrm{d}\tau.$$

The AUC for the corresponding ROC curve is given by Ref. [70] as

$$\text{AUC} = 1 - \Phi\left(\frac{|\mu_v - \bar{\mu}_v|}{\sqrt{\sigma_v^2 + \bar{\sigma}_v^2}}\right), \tag{3.3}$$

where

$$\Phi(x) \triangleq \frac{1}{\sqrt{2\pi}} \int_{-\infty}^{x} e^{-\frac{1}{2}z^2} \mathrm{d}z. \tag{3.4}$$

The function $\Phi(x)$ is strictly increasing and $\sup_x(\Phi(x)) = 1$; so according to the equation in (5.2), AUC is a strictly decreasing function of $\frac{\sqrt{\sigma_v^2+\bar{\sigma}_v^2}}{|\mu_v-\bar{\mu}_v|}$. We define the alarm performance index for the alarm variable $v(k)$ by

$$\mathcal{A}(v) \triangleq \frac{\sqrt{\sigma_v^2 + \bar{\sigma}_v^2}}{|\mu_v - \bar{\mu}_v|}. \tag{3.5}$$

This result, in comparison with FAR and MAR, simplifies the design problem and also provides more intuition about the impact of the statistical parameters of a alarm variable on the detectability of normal and abnormal operation modes. As an example, consider two alarm variables $v_1(k)$ and $v_2(k)$ in the view of (4.7) which are compared by some thresholds to generate alarm signals. We also assume that $|\mu_{v_1} - \bar{\mu}_{v_1}| > |\mu_{v_2} - \bar{\mu}_{v_2}|$ and $\sigma_{v_1}^2 + \bar{\sigma}_{v_1}^2 < \sigma_{v_2}^2 + \bar{\sigma}_{v_2}^2$. The alarm variables and the generated alarms for v_1 and v_2 are shown in Fig. 3.2 and Fig. 3.3, respectively. For both cases, the abnormality happens after 50 samples; so any alarm before this time is a false alarm and any alarm that should have occurred after that but have not occurred is a missed alarm. According to Fig. 3.2, classification of $v_1(k)$ into normal and abnormal cases results in a lower MAR and FAR and hence a better alarm performance in comparison with the one in Fig. 3.3. This is due to the fact that variations of $v_1(k)$ is small in comparison with the magnitude of abnormality. For $v_2(k)$, however, MAR and FAR are worse, because the distributions of normal and

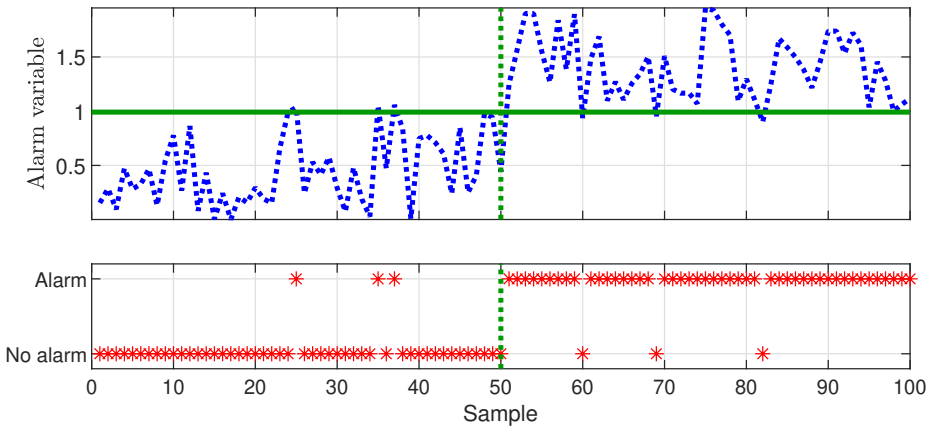

Figure 3.2: An alarm variable with a large $|\mu_{v_1} - \bar{\mu}_{v_1}|$ and a small $\sigma^2_{v_1} + \bar{\sigma}^2_{v_1}$. The solid green line indicates the alarm threshold and the green dotted line shows the time of occurrence of abnormality.

abnormal data have more overlap than the previous case, i.e., the two sets of data are more similar. The proposed alarm index can be thought of as a map between the area under the curve (which should be between 0 and 0.5) and real positive numbers. Thus, if the abnormality does not significantly change the mean value (i.e., $\mu_v \approx \bar{\mu}_v$) the proposed index approaches infinity. Also, the index is not defined when $\mu_v = \bar{\mu}_v$. Here, even though the variance may change due to the abnormality, the area under the curve remains to 0.5. Furthermore, as the considered control system and the plant together are assumed to be LTI, the controller is not able to make the classification any better, which is aligned with the view of the proposed index and the AUC index. But still, the plant operator may choose a constant threshold and notice the fault occurrence by observing the continuous switching of the alarm signal. A drawback of this method is experiencing a high rate of either false or missed alarms (or more precisely, chattering alarms). A solution to this problem is by utilizing some nonlinear filters such as those proposed by Ref. [27], [58], [81].

3.1.2 Alarm Index for Systems

We introduce the alarm index for a discrete-time LTI system $G_{y_a w}(z^{-1})$, where $w(k) \in \mathbb{R}$ denotes the input signal and $y_a(k) \in \mathbb{R}$ denotes the output of G

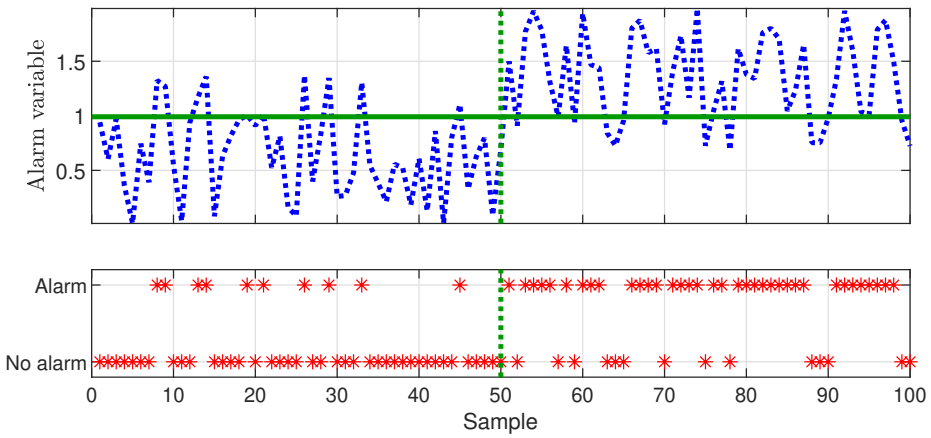

Figure 3.3: An alarm variable with a small $|\mu_{v_2} - \bar{\mu}_{v_2}|$ and a large $\sigma^2_{v_2} + \bar{\sigma}^2_{v_2}$. The solid green line indicates the alarm threshold and the green dotted line shows the time of occurrence of abnormality.

which is used to generate the alarm. Here, $w(k)$ and $y_a(k)$ follow the same distribution as (4.7). It is important to note that FAR and MAR are defined with respect to the stationary operation of the system (see for example Ref. [106]). In alarm systems, the transient behavior is captured by the average alarm detection delay (ADD). In this chapter, we focus on the accuracy of the alarm system (measured as FAR and MAR); and so we only study the stationary mode of abnormalities.

The alarm index for this system is defined as

$$\mathcal{A}(G_{y_a w}) \triangleq \frac{\mathcal{A}(y_a)}{\mathcal{A}(w)}. \tag{3.6}$$

The relation between the expected value of input and output of an LTI system driven by a Gaussian signal is given by

$$\mu_{y_a} = G_{y_a w}(1)\mu_w,$$
$$\bar{\mu}_{y_a} = G_{y_a w}(1)\bar{\mu}_w.$$

Moreover, the $\mathcal{H}_2$-norm of a system, represents the steady-state covariance of the output in response to a white Gaussian noise [32]. Hence

$$\sigma^2_{y_a} = \|G_{y_a w}\|^2_{\mathcal{H}_2}\sigma^2_w,$$
$$\bar{\sigma}^2_{y_a} = \|G_{y_a w}\|^2_{\mathcal{H}_2}\bar{\sigma}^2_w,$$

where $\|G_{y_a w}\|_{\mathcal{H}_2}$ denotes the $\mathcal{H}_2$-norm of $G_{y_a w}$. Now, (3.6) can be rewritten as

$$\mathcal{A}(G_{y_a w}) = \frac{\|G_{y_a w}\|_{\mathcal{H}_2}}{|G_{y_a w}(1)|}. \tag{3.7}$$

The proposed method results in reducing both FAR and MAR. However in most real applications, MAR is more important than FAR. To make a compromise, plant operators can manipulate the alarm threshold to achieve a lower number of missed alarms. The solution to this problem was addressed in existing work such as Ref. [106].

Remark 2 *For an LTI plant driven by $w(k)$ in the form of* (4.7) *and regardless of the distribution parameters, we can design the controller so that for the overall system, the alarm performance of the output $y_a(k)$ is improved in comparison with that of the input $w(k)$. So we use* (3.7) *as a design constraint in the control design problem.*

Remark 3 *We can clearly observe that minimizing the numerator of $\mathcal{A}(G_{y_a w})$, improves the alarm performance and is also desired from control perspective. However, this minimization can also affect the denominator of $\mathcal{A}(G_{y_a w})$. So there should be an optimal solution for the controller which compromises both the alarm and control performance. But without considering this point, one can realize that a minimum variance controller may work well in terms of alarm performance.*

Remark 4 *This index is also aligned with the optimal solution of Fisher's linear discriminant classification for Gaussian distributions [21]. In this classifier, the ratio of between-class and within-class covariances is maximized.*

Remark 5 *It is straightforward to prove that for a series connection of LTI systems $G_i,\ i = 1, \cdots, n$, the introduced alarm performance has the following property:*

$$\mathcal{A}(G_1 G_2 \cdots G_n) = \mathcal{A}(G_1)\mathcal{A}(G_2) \cdots \mathcal{A}(G_n).$$

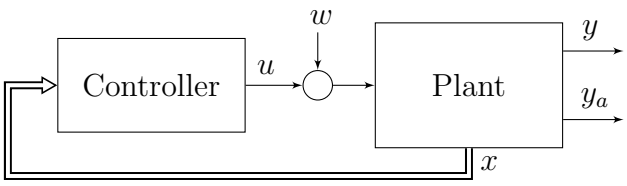

Figure 3.4: Diagram of the system.

3.2 Problem Statement

Consider a discrete-time LTI plant G with two outputs $y(k) \in \mathbb{R}$ and $y_a(k) \in \mathbb{R}$ and an input $u(k) \in \mathbb{R}$ which is corrupted by $w(k) \in \mathbb{R}$. Here, $w(k)$, which is in the form of (4.7), is used to model the abnormality in the plant's actuator. Furthermore, $y(k)$ is to evaluate the control performance, and $y_a(k)$ is to generate the alarm signal. We denote the state of the plant by $x(k) \in \mathbb{R}^n$. A diagram of the system is shown in Fig. 3.4. The controllable canonical state-space representation of the plant is given by

$$\begin{cases} x(k+1) = (A + \Delta A)x(k) + B\big(u(k) + w(k)\big), & (3.8) \\ y(k) = (C + \Delta C)x(k), & (3.9) \\ y_a(k) = C_a x(k), & (3.10) \end{cases}$$

where ΔA and ΔC represent parameter uncertainties. Furthermore, A, ΔA, and B are given by

$$A = \left[\begin{array}{c|c} 0 & I \\ \hline -a & \end{array}\right], \; \Delta A \triangleq \left[\begin{array}{c|c} 0 & I \\ \hline -\delta a & \end{array}\right], \; B = \begin{bmatrix} 0 & 0 & \cdots & 1 \end{bmatrix}^T.$$

Let us define $\bar{a} \triangleq a + \delta a$ and $\bar{C} \triangleq C + \Delta C$. In real-world applications, C_a is chosen by a designer, so it is accurately known. However, $\bar{a}$ and $\bar{C}$ are found using a system identification method, so they may have uncertainty. It is worth noting that, although C_a is accurately known, the uncertainty of $\bar{a}$ affects the alarm index.

Let δa_i and δc_i, $i \in \{1, \cdots n\}$, denote the i^{th} elements of δa and ΔC, respectively. It is reasonable to assume that

$$|\delta a_i| < \bar{\delta}_{a_i}, \tag{3.11}$$

$$|\delta c_i| < \bar{\delta}_{c_i}, \tag{3.12}$$

where $\bar{\delta}_{a_i}$ and $\bar{\delta}_{c_i}$ are uncertainty bounds corresponding to the i^{th} element of δa and ΔC, respectively and are positive. Now we find the following norm-bounded uncertainty structures:

$$\Delta A = M_a F_a, \tag{3.13}$$

and

$$\Delta C = M_c F_c, \tag{3.14}$$

where

$$M_a = \begin{bmatrix} 0 & 0 & \dots & 0 \\ 0 & 0 & \dots & 0 \\ \vdots & \vdots & \ddots & \vdots \\ \bar{\delta}_{a_n} & \bar{\delta}_{a_{n-1}} & \dots & \bar{\delta}_{a_1} \end{bmatrix}, \; F_a = \begin{bmatrix} f_{a_n} & 0 & \dots & 0 \\ 0 & f_{a_{n-1}} & \dots & 0 \\ \vdots & \vdots & \ddots & \vdots \\ 0 & 0 & \dots & f_{a_1} \end{bmatrix},$$

and

$$M_c = \begin{bmatrix} \bar{\delta}_{c_n} & \bar{\delta}_{c_{n-1}} & \dots & \bar{\delta}_{c_1} \end{bmatrix}, \; F_c = \begin{bmatrix} f_{c_n} & 0 & \dots & 0 \\ 0 & f_{c_{n-1}} & \dots & 0 \\ \vdots & \vdots & \ddots & \vdots \\ 0 & 0 & \dots & f_{c_1} \end{bmatrix}.$$

Here $|f_{a_i}| < 1, \; i = \{1, 2, \cdots, n\}$ and $|f_{c_i}| < 1, \; i = \{1, 2, \cdots, n\}$; so we have $F_a F_a^T \prec I$ and $F_c F_c^T \prec I$.

3.2.1 State-feedback Controller

A full information state-feedback controller will be designed to stabilize the system as well as to satisfy the control and alarm performance requirements. The control signal is given by

$$u(k) = Kx(k). \tag{3.15}$$

Combining (3.8) by (3.15) we can write the closed-loop equation of the system as

$$x(k+1) = (A + \Delta A + BK)x(k) + Bw(k), \tag{3.16}$$

3.2.2 Design Objectives

Our aim is to design a state-feedback controller to stabilize the plant G described by equations in (3.8), (3.9), and (3.10) which also satisfies the following conditions on the control and alarm performance:

$$\|G_{yw}\|_{\mathcal{H}_2}^2 < \eta, \tag{3.17}$$

$$\mathcal{A}^2(G_{y_a w}) < \psi, \tag{3.18}$$

where $\|G_{yw}\|_{\mathcal{H}_2}$ is the $\mathcal{H}_2$ norm from w to y and $\mathcal{A}(G_{y_a w})$ is the alarm index from w to y_a.

3.3 Controller Synthesis

In this section, a set of LMIs is given to solve the robust optimization problem. We design a state-feedback controller K for the system described in equations (3.8) to (3.10) with constraints (3.17) and (3.18). The control performance has been studied in many other publications, but to add the alarm performance constraint we need to find a unified framework to address both the control and alarm performance. We can consider the $\mathcal{H}_2$ problem as a bounded state covariance problem driven by a white Gaussian noise. Let $X(k)$ denote the covariance of the state in (3.16). Similar to the result presented in Ref. [102], $X(k)$ should satisfy

$$X(k+1) = (A + \Delta A + BK)X(k)(A + \Delta A + BK)^T + BB^T. \tag{3.19}$$

Now we define the steady-state covariances X as

$$X \triangleq \lim_{k\to\infty} X(k).$$

From Ref. [102] and Ref. [85] we know that the system in (3.16) is stable and X exists and is bounded if it satisfies the following discrete-time modified Lyapunov inequality:

$$(A + \Delta A + BK)X(A + \Delta A + BK)^T + BB^T \prec X. \tag{3.20}$$

According to the equation in (3.10), the variance of the alarm output y_a is given by

$$\sigma_{y_a}^2 = C_a X C_a^T. \tag{3.21}$$

For the alarm performance constraint, we need to find the relation between $G_{y_a w}^{-1}(1)$ and the state-feedback gain K. The equations in (3.16) and (3.10) imply that

$$G_{y_a w}^{-1}(z) = \Big(C_a\big(zI - (A + \Delta A + BK)\big)^{-1}B\Big)^{-1}. \tag{3.22}$$

We only need to consider the case when $z = 1$. Define the matrix $S \triangleq I - (A + \Delta A + BK)$ and let S_{ij} denote the ij^{th} block of S. We have

$$\left[\begin{array}{c|c} S_{11} & S_{12} \\ \hline S_{21} & S_{22} \end{array}\right] = \left[\begin{array}{ccccc|c} 1 & -1 & 0 & \cdots & 0 & 0 \\ 0 & 1 & -1 & \cdots & 0 & 0 \\ \vdots & \vdots & \ddots & \ddots & \vdots & \vdots \\ 0 & 0 & \cdots & 1 & -1 & 0 \\ 0 & 0 & \cdots & 0 & 1 & -1 \\ \hline \bar{a}_n - k_n & & \cdots & \bar{a}_2 - k_2 & \bar{a}_1 - k_1 & 1 + \bar{a}_0 - k_0 \end{array}\right],$$

where $\bar{a}_i$ and k_i are the i^{th} elements of $\bar{a}$ and K, respectively. By using Ref. [75], the inverse of S can be expressed as

$$S^{-1} = \left[\begin{array}{c|c} * & -S_{11}^{-1}S_{12}(S_{22} - S_{21}S_{11}^{-1}S_{12})^{-1} \\ \hline * & (S_{22} - S_{21}S_{11}^{-1}S_{12})^{-1} \end{array}\right],$$

where the symbol '$*$' represents a matrix block that eventually will be eliminated by multiplying with a zero element of B in (3.22). By performing some algebraic operations we obtain

$$S^{-1} = \Big(1 + \sum_{i=1}^{n} \bar{a}_i - k_i\Big)^{-1} \left[\begin{array}{c|c} * & \bar{1} \\ \hline * & 1 \end{array}\right].$$

Plugging this expression in the equation in (3.22) and setting $z = 1$ yields

$$G_{y_a w}^{-1}(1) = \left(\Big(1 + \sum_{i=1}^{n} \bar{a}_i - k_i\Big)^{-1} C_a \left[\begin{array}{c|c} * & \bar{1} \\ \hline * & 1 \end{array}\right] B\right)^{-1}.$$

Hence

$$G_{y_a w}^{-1}(1) = \left(\Big(1 + \sum_{i=1}^{n} \bar{a}_i - k_i\Big)^{-1} C_a \mathbf{1}\right)^{-1},$$

which implies

$$G^{-1}_{y_a w}(1) = \frac{1 + \sum_{i=1}^{n} \bar{a}_i - k_i}{\sum_{i=1}^{n} c_{a_i}}, \tag{3.23}$$

where c_{a_i} is the i^{th} element of C_a. The following lemma helps us to simplify the choice of C_a.

Lemma 3.3.1 *Let $G(z^{-1})$ and $\tilde{G}(z^{-1})$ be two plants described in (3.8) to (3.10) with the same parameters except for C_a where C_a and $\tilde{C}_a$ are associated with G and $\tilde{G}$, respectively. If $\tilde{C}_a = \kappa C_a,\ \kappa \in \mathbb{R}$ it holds that*

$$\mathcal{A}(G_1) = \mathcal{A}(G_2).$$

Proof. Based on the assumptions, the state-covariances of both plants are the same. According to the definition we have $\frac{\mathcal{A}(G_1)}{\mathcal{A}(G_2)} = \frac{\mathcal{A}(y_a)}{\mathcal{A}(\tilde{y}_a)}$, where y_a and $\tilde{y}_a$ are the alarm variable outputs corresponding to G and $\tilde{G}$, respectively. Let X_w and $X_{\bar{w}}$ denote the steady-state covariance corresponding to the normal and abnormal cases, respectively. Combining (6.3), (3.21) and (3.23) yields

$$\frac{\mathcal{A}(y_a)}{\mathcal{A}(\tilde{y}_a)} = \frac{\sqrt{C_a(X_w + X_{\bar{w}})C_a^T}\left|\kappa \sum_{i=1}^{n} c_{a_i}\right|}{\sqrt{\kappa^2 C_a(X_w + X_{\bar{w}})C_a^T}\left|\sum_{i=1}^{n} c_{a_i}\right|} = 1.$$

Thus, $\mathcal{A}(G_1) = \mathcal{A}(G_2)$ and the proof is complete. □

Remark 6 *Based on the result of lemma 3.3.1, without loss of generality we can always normalize C_a such that $\sum_{i=1}^{n} c_{a_i} = 1$.*

According to this remark the equation in (3.23) can be rewritten as

$$G^{-1}_{y_a w}(1) = 1 + \sum_{i=1}^{n} \bar{a}_i - k_i,$$

and due to the uncertainty we have

$$G^{-1}_{y_a w}(1) = 1 + \sum_{i=1}^{n} a_i + \delta a_i - k_i, \tag{3.24}$$

where a_i is the i^{th} element of a. Now we are ready to present the main result of this chapter.

Theorem 3.3.2 *Consider a plant described by* (3.8), (3.9) *and* (3.10) *controlled by a state-feedback controller in* (3.15) *and assume that* w_k *is a stochastic signal in view of* (4.7). *If there exist a positive definite matrix* $P \prec 2I$ *and positive scalars* ζ, ϵ_a, ϵ_c *and* ϵ_{c_a} *that satisfy the following LMIs*

$$\begin{bmatrix} -\epsilon_a I & 0 & I & 0 \\ (.)^T & -\epsilon_a I & 0 & \epsilon_a M_a^T \\ (.)^T & (.)^T & P-2I & (A+BK)^T \\ (.)^T & (.)^T & (.)^T & 2\zeta BB^T - P \end{bmatrix} \prec 0, \tag{3.25}$$

$$\begin{bmatrix} -\epsilon_c I & 0 & I & 0 \\ (.)^T & -\epsilon_c I & 0 & \epsilon_c M_c^T \\ (.)^T & (.)^T & -P & PC^T \\ (.)^T & (.)^T & (.)^T & -2\zeta\eta \end{bmatrix} \prec 0, \tag{3.26}$$

$$\begin{bmatrix} -\epsilon_{c_a} I & \sum_{i=1}^{n} \bar{\delta}_{a_i} \epsilon_{c_a} I & C_a^T \\ (.)^T & P-2I & \big(1+(a-K)\mathbf{1}\big)C_a^T \\ (.)^T & (.)^T & -2\zeta\psi \end{bmatrix} \prec 0, \tag{3.27}$$

then the controller is stabilizing and guarantees the control and alarm performance described by (3.17) *and* (3.18).

We first need the following lems to establish the proof.

Lemma 3.3.3 *For a matrix* P *where* $0 \prec P \prec 2I$, *the following inequality holds:*

$$P \preceq (2I - P)^{-1}.$$

Proof. As $P \succ 0$ we have $0 \preceq (P-I)P^{-1}(P-I)^T$, so

$$2I - P \preceq P^{-1}. \tag{3.28}$$

As $P \prec 2I$, $(2I-P)^{-1}$ exists and is positive definite. By multiplying $(2I-P)^{-1}$ to both sides of the expression in (3.28) we have

$$I \preceq P^{-1}(2I - P)^{-1}.$$

P is positive definite so by multiplying it to the above inequality we can infer that $P \preceq (2I - P)^{-1}$, and the proof is complete. □

Lemma 3.3.4 (see Ref. [105]) *Given matrices Q, E, F, and H all of appropriate dimensions with Q symmetric and $FF^T \prec I$, the inequality*

$$Q + EFH + H^T F^T E^T \prec 0$$

holds if and only if there exists some $\epsilon > 0$ such that

$$Q + \epsilon EE^T + \epsilon^{-1} H^T H \prec 0$$

Proof. [Proof of Theorem 3.3.2] A positive (small enough) ζ exists such that $X \prec \zeta^{-1} I$. Multiplying both sides of the inequality in (3.20) by 2ζ and setting $P = 2\zeta X$ yields

$$(A + \Delta A + BK)P(A + \Delta A + BK)^T + 2\zeta BB^T \prec P. \tag{3.29}$$

By applying lemma 3.3.3 we conclude that if it holds that

$$(A + \Delta A + BK)(2I - P)^{-1}(A + \Delta A + BK)^T + 2\zeta BB^T \prec P,$$

then (3.29) is satisfied. Using Schur's complement lemma (see Ref. [112]) we have

$$\begin{bmatrix} P - 2I & (A + \Delta A + BK)^T \\ A + \Delta A + BK & 2\zeta BB^T - P \end{bmatrix} \prec 0.$$

According to the norm-bounded property of the uncertainty and using the equation in (3.13) we have

$$\begin{bmatrix} P - 2I & (A + BK)^T \\ A + BK & 2\zeta BB^T - P \end{bmatrix} + \begin{bmatrix} 0 & (M_a F_a)^T \\ M_a F_a & 0 \end{bmatrix} \prec 0,$$

which holds if

$$\begin{bmatrix} P - 2I & (A + BK)^T \\ A + BK & 2\zeta BB^T - P \end{bmatrix} + \begin{bmatrix} 0 \\ M_a \end{bmatrix} F_a \begin{bmatrix} I & 0 \end{bmatrix} + \begin{bmatrix} I \\ 0 \end{bmatrix} F_a^T \begin{bmatrix} 0 & M_a^T \end{bmatrix} \prec 0.$$

Based on lemma 3.3.4, for some ϵ_a we have

$$\begin{bmatrix} P - 2I & (A + BK)^T \\ A + BK & 2\zeta BB^T - P \end{bmatrix} + \epsilon_a \begin{bmatrix} 0 \\ M_a \end{bmatrix} \begin{bmatrix} 0 & M_a^T \end{bmatrix} + \epsilon_a^{-1} \begin{bmatrix} I & 0 \end{bmatrix} \begin{bmatrix} I \\ 0 \end{bmatrix} \prec 0.$$

This condition is satisfied if

$$\begin{bmatrix} P - 2I & (A + BK)^T \\ A + BK & 2\zeta BB^T - P \end{bmatrix} + \begin{bmatrix} I & 0 \\ 0 & \epsilon_a M_a \end{bmatrix} \begin{bmatrix} \epsilon_a^{-1} & 0 \\ 0 & \epsilon_a^{-1} \end{bmatrix} \begin{bmatrix} I & 0 \\ 0 & \epsilon_a M_a^T \end{bmatrix} \prec 0.$$

By applying Schur's complement lemma we prove that if the LMI in (3.25) is satisfied, the inequality in (3.20) is also satisfied.
Now to have a bound for the control performance constraint as in (3.17), $\bar{C}X\bar{C}^T < \eta$ should be satisfied, thus

$$(C + \Delta C)X(C + \Delta C)^T < \eta.$$

Multiplying both sides by 2ζ and setting $P = 2\zeta X$ yields

$$(C + \Delta C)P(C + \Delta C)^T < 2\zeta\eta.$$

By using Schur's complement lemma we can convert it to

$$\begin{bmatrix} -P^{-1} & (C + \Delta C)^T \\ C + \Delta C & -2\zeta\eta \end{bmatrix} \prec 0.$$

For the uncertainty ΔC we know that $\Delta C = M_c F_c$, hence

$$\begin{bmatrix} -P^{-1} & C^T \\ C & -2\zeta\eta \end{bmatrix} + \begin{bmatrix} 0 \\ M_a \end{bmatrix} F_a \begin{bmatrix} I & 0 \end{bmatrix} + \begin{bmatrix} I \\ 0 \end{bmatrix} F_a^T \begin{bmatrix} 0 & M_a^T \end{bmatrix} \prec 0,$$

so according to lemma 3.3.4 for some ϵ_c we have

$$\begin{bmatrix} -P^{-1} & C^T \\ C & -2\zeta\eta \end{bmatrix} + \epsilon_c \begin{bmatrix} 0 \\ M_c \end{bmatrix} \begin{bmatrix} 0 & M_c^T \end{bmatrix} + \epsilon_c^{-1} \begin{bmatrix} I & 0 \end{bmatrix} \begin{bmatrix} I \\ 0 \end{bmatrix} \prec 0,$$

which is satisfied if

$$\begin{bmatrix} -P^{-1} & C^T \\ C & -2\zeta\eta \end{bmatrix} + \begin{bmatrix} I & 0 \\ 0 & \epsilon_a M_a \end{bmatrix} \begin{bmatrix} \epsilon_a^{-1} & 0 \\ 0 & \epsilon_a^{-1} \end{bmatrix} \begin{bmatrix} I & 0 \\ 0 & \epsilon_a M_a^T \end{bmatrix} \prec 0.$$

Applying Schur's complement lemma yields

$$\begin{bmatrix} -\epsilon_c I & 0 & I & 0 \\ 0 & -\epsilon_c I & 0 & \epsilon_c M_c^T \\ P & 0 & -P^{-1} & C^T \\ 0 & \epsilon_c M_c & C & -2\zeta\eta \end{bmatrix} \prec 0.$$

Multiplying the diagonal matrix $\text{diag}\{I,\ I,\ P,\ I\}$ from left and right to the previous inequality results in the LMI in (3.26). Now to satisfy the alarm performance constraint given by (3.18) we reform the equation in (3.7) to

$$\mathcal{A}^2(G_{y_a w}) = G_{y_a w}^{-2}(1) C_a X C_a^T.$$

Plugging (3.24) in the previous equation yields

$$\mathcal{A}^2(G_{y_a w}) = \Big(1 + \sum_{i=1}^{n} a_i + \delta a_i - k_i\Big)^2 C_a X C_a^T.$$

Now we multiply both sides of this equation by 2ζ and we set $P = 2\zeta X$. The alarm constraint in (3.18) is satisfied if the following condition holds:

$$\Big(1 + \sum_{i=1}^{n} a_i + \delta a_i - k_i\Big)^2 C_a P C_a^T < 2\zeta\psi.$$

Based on lemma 3.3.3 we know that this inequality holds if

$$\Big(1 + \sum_{i=1}^{n} a_i + \delta a_i - k_i\Big)^2 C_a (2I - P)^{-1} C_a^T < 2\zeta\psi.$$

We use Schur's complement lemma to convert it to

$$\begin{bmatrix} -(2I - P) & \Big(1 + \sum_{i=1}^{n} a_i + \delta a_i - k_i\Big) C_a^T \\ \Big(1 + \sum_{i=1}^{n} a_i + \delta a_i - k_i\Big) C_a & -2\zeta\psi \end{bmatrix} \prec 0. \tag{3.30}$$

According to the assumption in (3.11), for some scalar $\rho,\ \rho^2 < 1$ it holds that

$$\sum_{i=1}^{n} \delta a_i = \sum_{i=1}^{n} \bar{\delta}_{a_i} \rho,$$

so the inequality in (3.30) can be rewritten as

$$\begin{bmatrix} -(2I - P) & \Big(1 + \sum_{i=1}^{n} a_i - k_i\Big) C_a^T \\ \Big(1 + \sum_{i=1}^{n} a_i - k_i\Big) C_a & -2\zeta\psi \end{bmatrix} + \begin{bmatrix} \sum_{i=1}^{n} \bar{\delta}_{a_i} I \\ 0 \end{bmatrix} \rho \begin{bmatrix} 0 & C_a^T \end{bmatrix} + \begin{bmatrix} 0 \\ C_a \end{bmatrix} \rho \begin{bmatrix} \sum_{i=1}^{n} \bar{\delta}_{a_i} I & 0 \end{bmatrix} \prec 0.$$

Based on lemma 3.3.4, this inequality holds if we can find a ϵ_{c_a} such that

$$\begin{bmatrix} -(2I - P) & \Big(1 + \sum_{i=1}^{n} a_i - k_i\Big) C_a^T \\ \Big(1 + \sum_{i=1}^{n} a_i - k_i\Big) C_a & -2\zeta\psi \end{bmatrix} + \epsilon_{c_a} \begin{bmatrix} \sum_{i=1}^{n} \bar{\delta}_{a_i} I \\ 0 \end{bmatrix} \begin{bmatrix} \sum_{i=1}^{n} \bar{\delta}_{a_i} I & 0 \end{bmatrix} + \epsilon_{c_a}^{-1} \begin{bmatrix} 0 \\ C_a \end{bmatrix} \begin{bmatrix} 0 & C_a^T \end{bmatrix} \prec 0,$$

which is satisfied if the following holds:

$$\begin{bmatrix} -(2I-P) & \Big(1+\sum_{i=1}^{n} a_i - k_i\Big)C_a^T \\ \Big(1+\sum_{i=1}^{n} a_i - k_i\Big)C_a & -2\zeta\psi \end{bmatrix} + \begin{bmatrix} \sum_{i=1}^{n} \bar{\delta}_{a_i}\epsilon_{c_a} I \\ C_a \end{bmatrix} \epsilon_{c_a}^{-1} \begin{bmatrix} \sum_{i=1}^{n} \bar{\delta}_{a_i}\epsilon_{c_a} I & C_a^T \end{bmatrix} \prec 0.$$

Finally, applying Schur's complement lemma and converting $\sum_{i=1}^{n} a_i - k_i$ to the matrix form we have the LMI in (3.27) and the proof is complete. □

The LMIs of this Theorem can be used to design the controller to satisfy bounds for the performance of control and alarm systems. The LMIs are not feasible for all choices of parameters η and ψ. This is due to the trade-off between control and alarm performance. Thus, η and ψ are considered as design parameters and should be determined by a trial-and-error procedure. Furthermore, based on the LMIs in Theorem 3.3.2, one can also consider C_a as a variable to obtain a better choice of C_a. However, it leads to a bilinear matrix inequality (BMI). Unlike LMIs, there is no off-the-shelf algorithm to solve BMI problems (see Ref. [96]). On the other side, plant operators select a combination of process measurements to capture abnormality; to do that, they consider safety-related constraints and the plant's operation constraints. So it is rational to assume that in some real applications, C_a is provided by plant operators.

3.4 Case Study

We study a simulated plant model consisting of a counter-current shell-and-tube heat exchanger (HE) which is the most common type of heat exchanger in oil refineries as well as many other large chemical processes[40]. A shell-and-tube type of HE is composed of a vessel (the shell) which surrounds a tube (or a bundle of tubes). The purpose is to transfer heat from a liquid inside the shell to a liquid that flows over the tube. We consider the case

that three HEs are connected in series known as a heat exchanger network (HEN). This process is frequently used in refineries where the goal is to cool hot petroleum coming from distillation. Fig. 3.5 shows a schematic of the plant where high-temperature petroleum flows into the inner tube of the first HE and exits from the third HE with a lower temperature. The cooling water, however, flows through the shell of the third HE and exits from the shell of the first HE. The temperatures of the petroleum inlet and water streams to each HE are measured by temperature sensors. So there are 6 temperature sensors deployed in the HEN. The flow of the water stream is controlled by a control valve, and we consider the volumetric flow rate of the water fed to the shell as the manipulated value. Our aim is to design a state-feedback controller for this process to keep the temperature of the petroleum that exits from the third HE around a desired reference value which also satisfies a good alarm performance for the overall system. Starting by the discrete-time equations proposed by Ref. [19], the nominal model of the system can be found in the canonical form. According to the equations in (3.8) and (3.9) we have

$$A = \begin{bmatrix} 0 & 1 & 0 & 0 & 0 & 0 \\ 0 & 0 & 1 & 0 & 0 & 0 \\ 0 & 0 & 0 & 1 & 0 & 0 \\ 0 & 0 & 0 & 0 & 1 & 0 \\ 0 & 0 & 0 & 0 & 0 & 1 \\ -0.225 & -0.0186 & -0.0007 & 0 & 0 & 0 \end{bmatrix},$$

$$C = \begin{bmatrix} 0 & -0.48 & -0.0778 & -0.0043 & -0.0001 & 0 \end{bmatrix}.$$

Thus

$$a = \begin{bmatrix} 0.225 & 0.0186 & 0.0007 & 0 & 0 & 0 \end{bmatrix}.$$

The state of the system is given by

$$\theta(k) = \theta_m(k) - \theta_s(k),$$

where θ_m is a vector composed of temperature measurements and θ_s was the steady state value of θ_m. Here, the elements of θ are given by

$$\theta(k) = \begin{bmatrix} \theta_w^1(k) & \theta_p^1(k) & \theta_w^2(k) & \theta_p^2(k) & \theta_w^3(k) & \theta_p^3(k) \end{bmatrix}^T \tag{3.31}$$

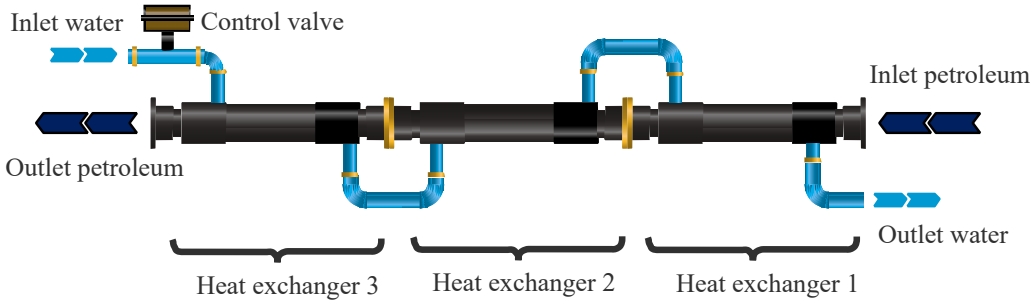

Figure 3.5: Counter-current shell-and-tube heat exchanger network consisting of three heat exchangers connected in cascade.

where the subscripts 'w' and 'p' are corresponding to the water and petroleum temperatures, respectively, and the superscripts indicate corresponding heat exchangers in Fig. 3.5.

Furthermore, we assume that the uncertainty bounds in view of (3.11) and (3.12) are given by

$$\bar{\delta}_{a_1} = 0.03,\ \bar{\delta}_{a_2} = 0.002,\ \bar{\delta}_{a_3} = 0.0001,\ \bar{\delta}_{a_4} = \bar{\delta}_{a_5} = \bar{\delta}_{a_6} = 0.0001,$$

and

$$\bar{\delta}_{c_1} = 0,\ \bar{\delta}_{c_2} = 0.048,\ \bar{\delta}_{c_3} = 0.008,\ \bar{\delta}_{c_4} = 0.0004,\ \bar{\delta}_{c_5} = 0.0001,\ \bar{\delta}_{c_6} = 0.$$

Inspired by Ref. [19], we assume that the state is measured directly from the plant using temperature sensors. To generate the alarm signal, based on the knowledge of the process the operator can choose a linear combination of these measurements which is captured by C_a. According to remark 6 we also know that only the relative weights of the measurements are important. We consider the following setting for C_a which satisfies $C_a\mathbf{1} = 1$ as

$$C_a = \begin{bmatrix} 0.19 & 0.048 & 0.238 & 0.095 & 0.286 & 0.143 \end{bmatrix}.$$

The rationale behind the selection of these weights is that, as we want to detect the abnormality faster, we assign greater weights to the water temperature measurements in comparison with the one for petroleum (c.f. (3.31)). Our assumption here is that the valve abnormality will be reflected faster on the

water temperature compared with the petroleum temperature. Moreover, the weights are sorted in descending order from the measurements of the heat exchanger that is close to the source of abnormality to the one that is far from it. Now y_a can be expressed with respect to the temperature measurements as $y_a(k) = C_a T\theta(k)$ where T denotes the transformation matrix that converts the original state-space model to the controllable canonical form. In Ref. [93], the authors presented a realistic stirred tank heater benchmark where a fault was introduced in a control valve of the process. As follow-up to this work, Ref. [9] proposed a data-driven alarm filter to detect the abnormality presented in the control valve. They modeled the operation of the control valve by two Gaussian random variables (corresponding to the normal and abnormal operation modes) where the mean and variance of the one corresponding to the abnormal situation was greater than the one for the normal situation. Moreover, in many other real-world applications, abnormalities appear as shifts in the operation point and variation of some process variables. Inspired by Ref. [9], we assume that $w(k)$ for normal and abnormal operation modes is given by

$$w(k) \sim \begin{cases} \mathcal{N}(1, 0.2), & \text{normal,} \\ \mathcal{N}(2.5, 0.6), & \text{abnormal.} \end{cases}$$

Here, $w(k)$ represents normal and abnormal operation modes of the control valve. The abnormality corresponding to the change in the valve position is modeled as the mean change in $w(k)$ after the occurrence of abnormality. Furthermore, the variance change can capture a change in the sticky behavior of the control valve or just noise.

Now we use Theorem 1 to design the controller gain K for various values of η and ψ. The achieved control and alarm performance is showed in Fig. 3.6. This figure shows the trade-off between these two indices. Now we choose two points p_1 and p_2 of this curve where p_1 corresponds to a better control performance and can be achieved by

$$K_1 = \begin{bmatrix} 0.435 & 0.086 & 0.031 & 0.014 & 0.003 & -0.027 \end{bmatrix},$$

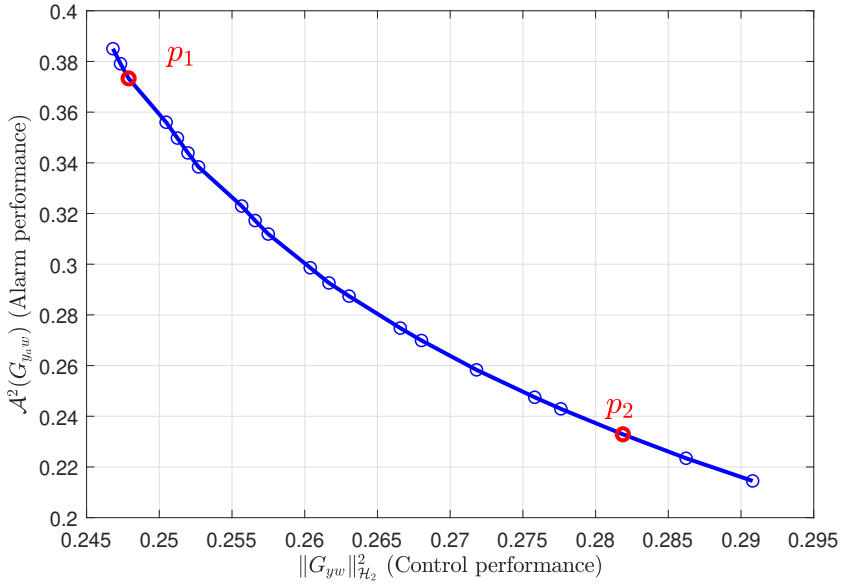

Figure 3.6: Trade-off between control and alarm performance (p_1 and p_2 are corresponding to better control and alarm performance, respectively).

and p_2 results in a better alarm performance and corresponds to

$$K_2 = \begin{bmatrix} 0.61 & 0.112 & 0.036 & 0.014 & -0.003 & -0.051 \end{bmatrix}.$$

The simulation result of these two scenarios are shown in Fig. 3.7 (for point p_1) and Fig. 3.8 (for point p_2) respectively. In both figures, the process variable is corresponding to the plant output in terms of (9), and the alarm variable shows the signal that is used for raising alarms which is represented by (10). Furthermore, the lower plots in both figures show the high alarms which are generated by comparing the alarm variable with some constant thresholds. These thresholds are not equal for both scenarios and are chosen offline, and set to a value that yields equal MAR and FAR (compromising to have low MAR and FAR at the same time). According to the simulation results, both MAR and FAR are improved in scenario p_2 by just loosing a negligible control performance. To compare the result for various thresholds, Fig. 3.9 show a part of the ROC curves of both scenarios where the curve corresponding to p_2 is closer to the origin and has a smaller area under the curve, which means a better alarm performance.

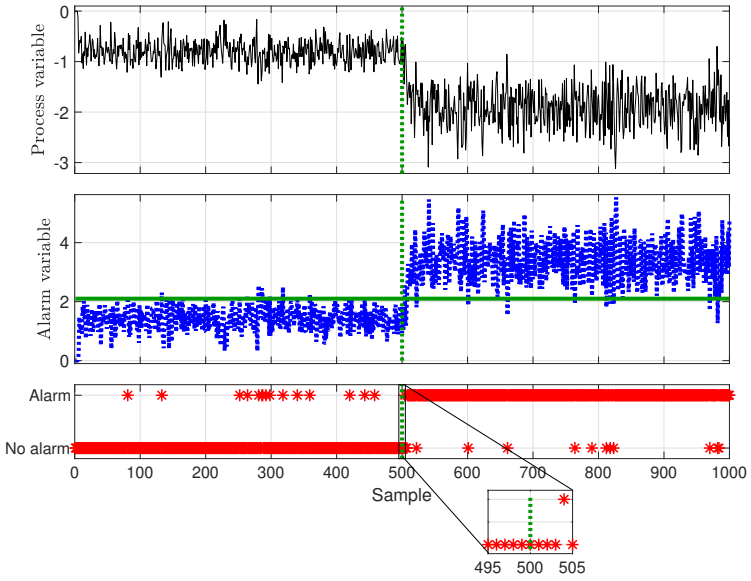

Figure 3.7: Simulation result of the design for better control performance (point p_1 in Fig. 3.6).

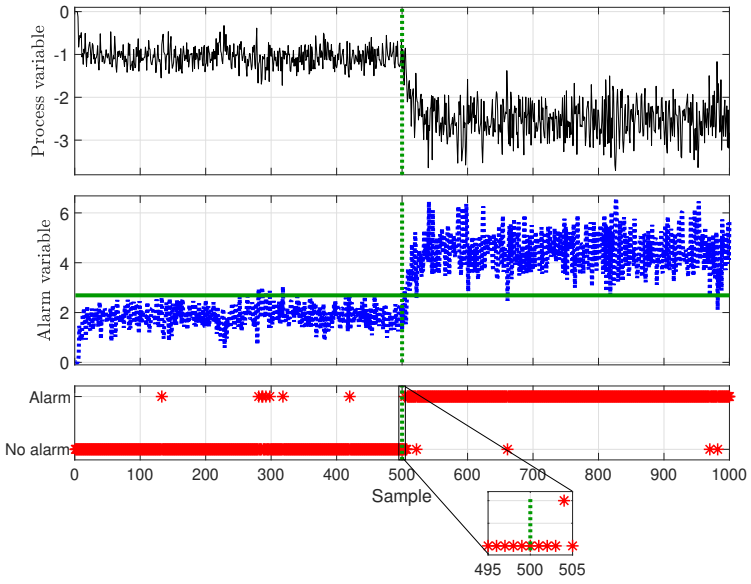

Figure 3.8: Simulation result of the design for better alarm performance (point p_2 in Fig. 3.6).

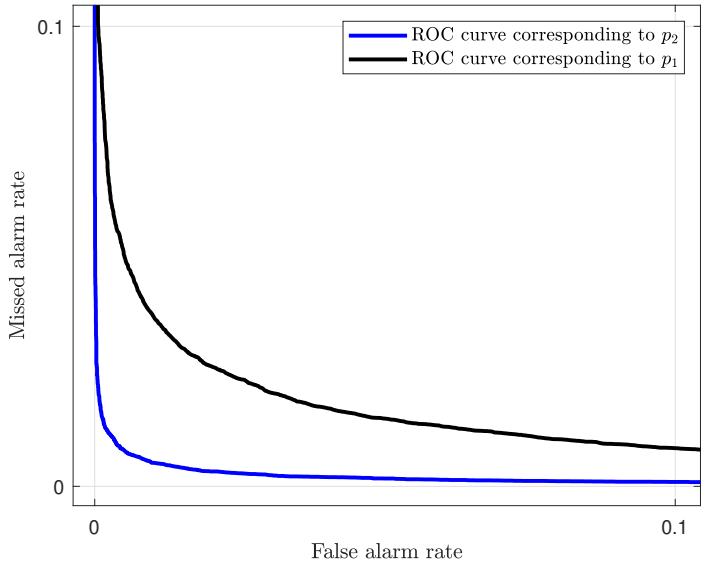

Figure 3.9: ROC curves of two design scenarios.

3.5 Summary

In this chapter, a state-feedback controller synthesis problem considering both control and alarm performance has been studied. Inspired by the presence of model uncertainty in most of industrial applications, the controller has been designed to be robust against norm-bounded uncertainty of model parameters. A new alarm index has been introduced by utilizing the concept of the area under a ROC curve. This alarm index is shown to be applicable for controller design even for uncertain systems. It also has been justified that there is an interplay between control and alarm performance for a certain type of performance indices. An LMI based method has been proposed to compromise the control and alarm performance.

*minimize

*minimize

Chapter 4

Design of Alarm Filters Based on the Plant and Controller Knowledge

In this chapter, we study the linear alarm filter design problem to detect abnormal actuator operations while the independence assumption does not hold. This is aligned with the fact that the raw data is usually acquired from a closed-loop system and are very likely to be statistically correlated. Assuming the independence assumption, the conventional moving average filter (where all filter coefficients are equal) is the optimal solution. We prove that this result can not be generalized for correlated data. We also propose a method to explicitly determine the optimal solution based on the plant and controller dynamics and the FAR/MAR design requirements. We consider a single input, single output (SISO) plant, and assume that an auto-regressive exogenous (ARX) model of the plant is available. This, together with the controller model (which is always known) and the alarm filter formulation, allows us to determine the correlation of data after filtering. The proposed method can be thought of as a multivariate alarm filter as it combines the control input and plant output to detect an abnormality. This prevents the occurrence of multiple alarms in case of an actuator fault as we have one alarm output instead of having separate ones for the input and output.

4.1 Problem Statement

In this chapter, we assume that an auto-regressive exogenous (ARX) model is available for the plant. Also, we consider a stabilizing linear controller which is precisely known and described by a transfer function. We also assume that the plant operates in two modes called normal and abnormal modes. In the abnormal operation mode, a fault occurs in the actuator. The following is the plant model:

$$\alpha(z^{-1})y(k) = \beta(z^{-1})\hat{u}(k) + \nu(k), \tag{4.1}$$

where $y(k) \in \mathbb{R}$ denotes the plant output and $\hat{u}(k)$ corresponds to the corrupted version of $u(k)$ (which is the manipulated value) due to the actuator fault. Furthermore, $\nu(k)$ is the associated measurement noise that follows the Gaussian distribution $\mathcal{N}(0, \sigma_\nu^2)$ where $\sigma_\nu^2 > 0$. Moreover,

$$\alpha(z^{-1}) = \alpha_1 + \alpha_2 z^{-1} + \cdots + \alpha_p z^{-p+1},$$
$$\beta(z^{-1}) = \beta_1 + \beta_2 z^{-1} + \cdots + \beta_q z^{-q+1}.$$

Here $\beta_1 = 0$, but we keep it as it stands for the ease of notation throughout the chapter. We also define the vectors $\boldsymbol{\alpha} = \begin{bmatrix}\alpha_1, & \alpha_2, \cdots, & \alpha_p\end{bmatrix}$ and $\boldsymbol{\beta} = \begin{bmatrix}\beta_1, & \beta_2, \cdots, & \beta_q\end{bmatrix}$. The controller is formulated as

$$u(k) = \frac{g(z^{-1})}{f(z^{-1})} y(k), \tag{4.2}$$

where

$$g(z^{-1}) = g_1 + g_2 z^{-1} + \cdots + g_n z^{-n+1},$$
$$f(z^{-1}) = f_1 + f_2 z^{-1} + \cdots + f_m z^{-m+1}.$$

To simplify the subsequent analysis, we further define $\boldsymbol{f} \triangleq \begin{bmatrix}f_1, f_2, \cdots, f_m, f_{m+1}, \cdots, f_l\end{bmatrix}$ and $\boldsymbol{g} \triangleq \begin{bmatrix}g_1, g_2, \cdots, g_n, g_{n+1}, \cdots, g_l\end{bmatrix}$. Here, $f_{m+1} = \cdots = f_l = g_{n+1} = \cdots = g_l = 0$, which are added to the vectors to make them have the same length l. Thus, l is equal to the maximum of n and m. Due to the actuator fault we have

$$\hat{u}(k) = u(k) + b, \tag{4.3}$$

where

$$b = \begin{cases} 0, & \text{normal mode,} \\ \bar{b}, & \text{abnormal mode.} \end{cases} \tag{4.4}$$

For this model, $\bar{b}$ can be identified from the historical process data or the plant knowledge. As an example, the above expression can model a partial valve closure or a deviation in pump driver voltage [91]. For the sake of simplicity, we assume that $\bar{b} > 0$ but a similar result can be derived for $\bar{b} < 0$. In many industrial applications, $\hat{u}(k)$ is not available (or even it is not possible to measure it) so the alarm signal should be constructed by using other variables. Now let $w(k)$ denote the alarm signal which is compared to a fixed alarm trip-point w_{tp}. As long as $w(k)$ falls short of the associated trip-point, no alarm is raised; otherwise, the system announces an alarm state. More formally, the normal and abnormal operation modes of the plant are distinguished as

$$\begin{cases} \text{alarm}, & w(k) \geq w_{\text{tp}}; \\ \text{no alarm}, & \text{otherwise.} \end{cases}$$

Considering the above mechanism and the inevitable measurement noise, the plant may work healthy but an alarm raises which is referred to as a false alarm. Another shortcoming is when some faults occur but the alarm system does not announce it which is called a missed alarm. We use the false and missed alarm rates (FAR/MAR) as the two commonly accepted measures for the performance of alarm systems. Suppose that $f_{w_{\text{ab}}}$ and $f_{w_{\text{n}}}$ represent the probability density functions (PDF) of w corresponding to the abnormal and normal operation modes, respectively. MAR and FAR are obtained as follows:

$$\text{MAR} = \int_{-\infty}^{w_{\text{tp}}} f_{w_{\text{ab}}}(\tau)\mathrm{d}\tau, \tag{4.5}$$

$$\text{FAR} = \int_{w_{\text{tp}}}^{\infty} f_{w_{\text{n}}}(\tau)\mathrm{d}\tau. \tag{4.6}$$

Inspired by the popularity of moving average alarm filters in industries, we apply a generalized version of it on an augmented vector composed of $y(k)$ and $u(k)$ samples. More specifically, the alarm signal is obtained as

$$w(k) = \boldsymbol{\lambda}_y \boldsymbol{y}^T(k) + \boldsymbol{\lambda}_u \boldsymbol{u}^T(k), \tag{4.7}$$

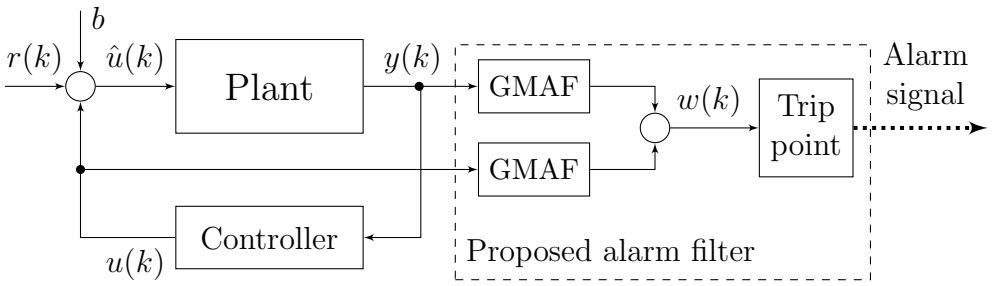

Figure 4.1: Diagram of the proposed system.

where

$$\begin{aligned}
\boldsymbol{\lambda}_y &= \big[\lambda_{y_1},\ \lambda_{y_2},\ \cdots,\ \lambda_{y_r}\big],\\
\boldsymbol{\lambda}_u &= \big[\lambda_{u_1},\ \lambda_{u_2},\ \cdots,\ \lambda_{u_r}\big],\\
\boldsymbol{y}(k) &= \big[y(k),\ y(k-1),\ \cdots,\ y(k-r+1)\big],\\
\boldsymbol{u}(k) &= \big[u(k),\ u(k-1),\ \cdots,\ u(k-r+1)\big].
\end{aligned}$$

We define the cost function as $J(\boldsymbol{\lambda}_y, \boldsymbol{\lambda}_u, w_{\text{tp}}) = \eta_m \text{MAR} + \eta_f \text{FAR}$, where $\eta_m > 0$ and $\eta_f > 0$ are design parameters to make a compromise between the rates of false and missed alarms. Typically, these parameters are selected by process safety engineers; so in this chapter we assume that they are known *a priori*. Finally, the design objective is expressed as

$$\boldsymbol{\lambda}_y, \boldsymbol{\lambda}_u, w_{\text{tp}} \quad J(\boldsymbol{\lambda}_y, \boldsymbol{\lambda}_u, w_{\text{tp}}). \tag{4.8}$$

4.2 Optimal Alarm Filter Design

In this section, we introduce the main result of this chapter which is to design optimal linear alarm filters by taking the closed-loop system dynamics into account. The proposed framework is shown in Fig. 4.1. The diagram consists of a typical control loop in which the actuator is subject to some faults. In real industrial applications, alarm filters are deployed to improve the fault distinguishability of all process variables; then the result is compared with a trip-point to check the healthy operation of the system. Considering the fact that these process variables are generated from an interconnected system we expect that they are statistically correlated. This point, however, is usually

neglected by simplifying assumptions such as the independence of the input raw data to the alarm filters. In this work, we combine the filtered version of control input $u(k)$ and plant output $y(k)$ and determine the optimal filter coefficients for this setup. It is worth noting that based on the independence assumption, the optimal filter configuration was proved to be the case that all coefficients are equal [26]. Nevertheless, by relaxing this assumption, it is essential to revisit the problem. In the problem formulation, we justified that the system of interest, in each operation mode, is driven by a Gaussian signal and a constant bias. As the closed-loop system and the alarm filters are linear, the alarm signal also follows Gaussian distribution. To determine the statistical parameters of $w(k)$ we need to obtain the closed form representation of $y(k)$ and $u(k)$. Considering the regulation problem where $r(k) \equiv 0$, and by combining the equations in (4.1), (4.2) and (4.3), after doing some manipulation we obtain

$$y(z^{-1}) = \frac{f(z^{-1})}{\alpha(z^{-1})f(z^{-1}) - \beta(z^{-1})g(z^{-1})}\nu(z^{-1}) + \frac{f(z^{-1})\beta(z^{-1})}{\alpha(z^{-1})f(z^{-1}) - \beta(z^{-1})g(z^{-1})}b, \tag{4.9}$$

and

$$u(z^{-1}) = \frac{g(z^{-1})}{\alpha(z^{-1})f(z^{-1}) - \beta(z^{-1})g(z^{-1})}\nu(z^{-1}) + \frac{g(z^{-1})\beta(z^{-1})}{\alpha(z^{-1})f(z^{-1}) - \beta(z^{-1})g(z^{-1})}b. \tag{4.10}$$

According to the filter formulation, the expected value of the alarm signal in the abnormal operation mode is given by $\mu_w = \mathbb{E}(\boldsymbol{\lambda}_y \boldsymbol{y}^T + \boldsymbol{\lambda}_u \boldsymbol{u}^T)$. Substitution of the controller formulation in this equation yields

$$\begin{aligned}\mu_w = &\mathbb{E}\Big(\frac{(\lambda_{y_1} + \cdots + \lambda_{y_r} z^{-r+1})f(z^{-1}) + (\lambda_{u_1} + \cdots + \lambda_{u_r} z^{-r+1})g(z^{-1})}{\alpha(z^{-1})f(z^{-1}) - \beta(z^{-1})g(z^{-1})}\nu\Big) \\ &+ \mathbb{E}\Big(\frac{\big((\lambda_{y_1} + \cdots + \lambda_{y_r} z^{-r+1})f(z^{-1}) + (\lambda_{u_1} + \cdots + \lambda_{u_r} z^{-r+1})g(z^{-1})\big)\beta(z^{-1})}{\alpha(z^{-1})f(z^{-1}) - \beta(z^{-1})g(z^{-1})}\bar{b}\Big).\end{aligned}$$

ν is a zero-mean Gaussian noise, so the first term in the above equation cancels out and we have

$$\mu_w = \frac{\Big(\big(\sum_{i=1}^{r}\lambda_{y_i}\big)\big(\sum_{i=1}^{m} f_i\big) + \big(\sum_{i=1}^{r}\lambda_{u_i}\big)\big(\sum_{i=1}^{n} g_i\big)\Big)\sum_{i=1}^{q}\beta_i}{\big(\sum_{i=1}^{m} f_i\big)\big(\sum_{i=1}^{p}\alpha_i\big) - \big(\sum_{i=1}^{q}\beta_i\big)\big(\sum_{i=1}^{n} g_i\big)}\bar{b}. \tag{4.11}$$

In our analysis, we assume that $\sum_{i=1}^{q} \beta_i \neq 0$. Otherwise, the abnormality does not appear as a mean change and can not be captured by the limit-checking mechanism. We also assume that $\sum_{i=1}^{m} f_i \neq 0$ and $\sum_{i=1}^{n} g_i \neq 0$. If not, there is no reason to design the associated filter coefficients (i.e., either λ_{y_i}'s or λ_{u_i}'s) as they will be canceled out. Furthermore, by design, $\sum_{i=1}^{r} \lambda_{u_i} \neq 0$ and $\sum_{i=1}^{r} \lambda_{y_i} \neq 0$. These statements together, ensure that $\mu_w \neq 0$. As we have already discussed, alarm signal $w(k)$ follows a Gaussian distribution in each operation mode. So the only parameters left to fully describe its statistical behavior is the corresponding variance that is determined by the following lemma.

Lemma 4.2.1 *Consider the plant described by* (4.1) *which is driven by the controller in* (4.2)*. The variance of alarm signal that is expressed by the equation in* (4.7) *is given by*

$$\sigma_w^2 = (\boldsymbol{\lambda_y} * \boldsymbol{f} + \boldsymbol{\lambda_u} * \boldsymbol{g})\Psi(\boldsymbol{\lambda_y} * \boldsymbol{f} + \boldsymbol{\lambda_u} * \boldsymbol{g})^T, \tag{4.12}$$

where,

$$\Psi = \sum_{i=0}^{\infty} \mathcal{A}^i \begin{bmatrix} \mathbf{0} & 1 \end{bmatrix}^T \begin{bmatrix} \mathbf{0} & 1 \end{bmatrix} (\mathcal{A}^T)^i \sigma_\nu^2, \tag{4.13}$$

and

$$\mathcal{A} = \left[\begin{array}{c|c} \mathbf{0}^T & I \\ \hline [\mathbf{0_\zeta} & \boldsymbol{\beta} * \boldsymbol{g} - \boldsymbol{\alpha} * \boldsymbol{f}] \end{array}\right].$$

Here, $\mathbf{0_\zeta}$ *is a row vector of length* $\zeta \triangleq r - \max(p, q)$*, with all elements set to zero.*

Proof. From the alarm signal formulation (see (4.7)) we obtain

$$w(z^{-1}) = \lambda_y(z^{-1})y(z^{-1}) + \lambda_u(z^{-1})u(z^{-1}),$$

where $\lambda_y(z^{-1}) = \lambda_{y_1} + \lambda_{y_2}z^{-1} + \cdots + \lambda_{y_r}z^{-r+1}$ and $\lambda_u(z^{-1}) = \lambda_{u_1} + \lambda_{u_2}z^{-1} + \cdots + \lambda_{u_r}z^{-r+1}$. Substituting (4.10) and (4.9) in the above equation yields

$$w(z^{-1}) = \frac{\lambda_y(z^{-1})f(z^{-1}) + \lambda_u(z^{-1})g(z^{-1})}{\big(\alpha(z^{-1})f(z^{-1}) - \beta(z^{-1})g(z^{-1})\big)z^{-\zeta}}\nu(z^{-1}), \tag{4.14}$$

where $z^{-\zeta}$ is added in the denominator to make the transfer function proper. The numerator degree of transfer function in (4.14) is $r+l-2$ and the denominator degree is $l+\max(p,q)-2$. So we set $\zeta = r-\max(p,q)$ to have a proper transfer function. For derivation of (4.14), the terms that are associated with b are excluded as they are constant in the steady-state and do not affect the variance. This transfer function can be represented in the state-space form where the system matrices are

$$\mathcal{A} = \left[\begin{array}{c|c} \mathbf{0}^T & I \\ \hline [\mathbf{0}_\zeta & \boldsymbol{\beta} * \boldsymbol{g} - \boldsymbol{\alpha} * \boldsymbol{f}] \end{array}\right],$$
$$\mathcal{B} = \begin{bmatrix} \mathbf{0} & 1 \end{bmatrix}^T,$$
$$\mathcal{C} = \boldsymbol{\lambda_y} * \boldsymbol{f} + \boldsymbol{\lambda_u} * \boldsymbol{g},$$
$$\mathcal{D} = 0.$$

According to Ref. [24], the state covariance of this system can be found by solving the following Lyapunov equation

$$\mathcal{A}\Psi\mathcal{A}^T - \Psi + \mathcal{B}\mathcal{B}^T = 0.$$

As we have assumed that the controller is stabilizing, the solution can be found as

$$\Psi = \sum_{i=0}^{\infty} \mathcal{A}^i \mathcal{B}^T \mathcal{B} (\mathcal{A}^T)^i.$$

Finally, the output variance is given by $\sigma_w^2 = \mathcal{C}\Psi\mathcal{C}^T\sigma_\nu^2$, which completes the proof. □

To summarize the above derivations, we can express the distribution of alarm signal $w(k)$ as

$$w(k) \sim \begin{cases} \mathcal{N}(0, \sigma_w^2), & \text{normal mode,} \\ \mathcal{N}(\mu_w, \sigma_w^2), & \text{abnormal mode.} \end{cases}$$

where μ_w and σ_w^2 are given by the equations in (4.11) and (4.12). Now we are ready to determine the optimal configuration of the alarm filters.

Remark 7 *In our analysis, we assume that $\sigma_w^2 \neq 0$. The rationale is that in the very rare cases of $\sigma_w^2 = 0$ and $\mu_w \neq 0$, the abnormal and normal operation*

modes can be distinguished perfectly (i.e., FAR = MAR = 0*) and there is no reason to use any alarm filter.*

4.2.1 Optimal Alarm Trip-point

The optimal trip-point can be obtained by setting derivative of the objective function (see the equation in (4.8)) with respect to the trip-point to zero. More formally

$$\frac{\partial}{\partial w_{tp}}(\eta_m \text{MAR} + \eta_f \text{FAR}) = 0.$$

Substituting (4.5) and (4.6) in the above equation yields

$$\eta_m \frac{\partial}{\partial w_{tp}} \int_{-\infty}^{w_{tp}} \frac{1}{\sqrt{2\pi}\sigma_w} e^{-\frac{(\tau-\mu_w)^2}{2\sigma_w^2}} \mathrm{d}\tau + \eta_f \frac{\partial}{\partial w_{tp}} \int_{w_{tp}}^{\infty} \frac{1}{\sqrt{2\pi}\sigma_w} e^{-\frac{\tau^2}{2\sigma_w^2}} \mathrm{d}\tau = 0.$$

Then we have

$$\eta_m \frac{1}{\sqrt{2\pi}\sigma_w} e^{-\frac{(w_{tp}-\mu_w)^2}{2\sigma_w^2}} - \eta_f \frac{1}{\sqrt{2\pi}\sigma_w} e^{-\frac{w_{tp}^2}{2\sigma_w^2}} = 0, \tag{4.15}$$

which can be simplified as

$$(w_{tp} - \mu_w)^2 - w_{tp}^2 - 2\sigma_w^2 \ln\left(\frac{\eta_f}{\eta_m}\right) = 0.$$

So the optimal alarm trip-point can be determined as

$$w_{\text{tp}}^* = \frac{\mu_w}{2} - \frac{\sigma_w^2}{\mu_w} \ln\left(\frac{\eta_f}{\eta_m}\right). \tag{4.16}$$

We still need to determine parameters μ_w and σ_w corresponding to the optimal filter, which will be given subsequently.

4.2.2 Optimal Solution of $\boldsymbol{\lambda_u}$ and $\boldsymbol{\lambda_y}$

In this section, we obtain the vectors $\boldsymbol{\lambda_u}$ and $\boldsymbol{\lambda_y}$ corresponding to the optimal alarm filter. Starting with $\boldsymbol{\lambda_u}$, we have

$$\frac{\partial}{\partial \boldsymbol{\lambda_u}}(\eta_m \text{MAR} + \eta_f \text{FAR}) = 0. \tag{4.17}$$

Using (4.5), the derivative of MAR with respect to $\boldsymbol{\lambda_u}$ is given by

$$\frac{\partial}{\partial \boldsymbol{\lambda_u}} \text{MAR} = \int_{-\infty}^{w_{tp}} \frac{\partial}{\partial \boldsymbol{\lambda_u}} \frac{1}{\sqrt{2\pi\sigma_w^2}} e^{-\frac{(\tau - \boldsymbol{\lambda_y} \mathbf{1}^T \mu_y - \boldsymbol{\lambda_u} \mathbf{1}^T \mu_u)^2}{2\sigma_w^2}} \mathrm{d}\tau,$$

where μ_y and μ_u indicate the expected value of y and u, respectively, in the abnormal operation mode. In the above equation we have used the vector forms of $\sum_{i=1}^{r} \lambda_{y_i}$ and $\sum_{i=1}^{r} \lambda_{u_i}$. Carrying out some manipulation yields

$$\frac{\partial}{\partial \boldsymbol{\lambda_u}}\text{MAR} = \int_{-\infty}^{w_{tp}} \Bigg(-\frac{\frac{\partial}{\partial \boldsymbol{\lambda_u}}\sigma_w^2}{2\sqrt{2\pi}\sigma_w^3} + \frac{\big(\frac{\partial}{\partial \boldsymbol{\lambda_u}}\sigma_w^2\big)(\tau - \boldsymbol{\lambda_y}\mathbf{1}^T\mu_y - \boldsymbol{\lambda_u}\mathbf{1}^T\mu_u)^2}{2\sqrt{2\pi}\sigma_w^5} + \frac{\mathbf{1}^T\mu_u(\tau - \boldsymbol{\lambda_y}\mathbf{1}^T\mu_y - \boldsymbol{\lambda_u}\mathbf{1}^T\mu_u)}{\sqrt{2\pi}\sigma_w^3} \Bigg) e^{-\frac{(\tau - \boldsymbol{\lambda_y}\mathbf{1}^T\mu_y - \boldsymbol{\lambda_u}\mathbf{1}^T\mu_u)^2}{2\sigma_w^2}} \mathrm{d}\tau.$$

After applying Lemma 4.2.2 we have

$$\frac{\partial}{\partial \boldsymbol{\lambda_u}}\text{MAR} = - \frac{2\sigma_w^2\mathbf{1}^T\mu_u + \big(\frac{\partial}{\partial \boldsymbol{\lambda_u}}\sigma_w^2\big)(w_{\text{tp}} - \boldsymbol{\lambda_y}\mathbf{1}^T\mu_y - \boldsymbol{\lambda_u}\mathbf{1}^T\mu_u)}{2\sqrt{2\pi}\sigma_w^3} e^{-\frac{(w_{\text{tp}} - \boldsymbol{\lambda_y}\mathbf{1}^T\mu_y - \boldsymbol{\lambda_u}\mathbf{1}^T\mu_u)^2}{2\sigma_w^2}}. \tag{4.18}$$

Considering the optimal trip-point, and by replacing μ_w with its expanded form (i.e., $\boldsymbol{\lambda_y}\mathbf{1}^T\mu_y - \boldsymbol{\lambda_u}\mathbf{1}^T\mu_u$) in (4.15) we obtain

$$e^{-\frac{(w_{tp}^* - \boldsymbol{\lambda_y}\mathbf{1}^T\mu_y - \boldsymbol{\lambda_u}\mathbf{1}^T\mu_u)^2}{2\sigma_w^2}} = \frac{\eta_f}{\eta_m} e^{-\frac{{w_{tp}^*}^2}{2\sigma_w^2}}.$$

Combining this equation with the one in (4.18) yields

$$\frac{\partial}{\partial \boldsymbol{\lambda_u}}\text{MAR} = -\frac{2\sigma_w^2\mathbf{1}^T\mu_u + \big(\frac{\partial}{\partial \boldsymbol{\lambda_u}}\sigma_w^2\big)(w_{\text{tp}} - \boldsymbol{\lambda_y}\mathbf{1}^T\mu_y - \boldsymbol{\lambda_u}\mathbf{1}^T\mu_u)}{2\sqrt{2\pi}\sigma_w^3} \frac{\eta_f}{\eta_m} e^{-\frac{{w_{tp}^*}^2}{2\sigma_w^2}}. \tag{4.19}$$

Now let us keep the above derivation for MAR in this form for now. Having in mind that the expected value of y and u are equal to zero in the normal operation mode, by applying a similar procedure on FAR we have

$$\frac{\partial}{\partial \boldsymbol{\lambda_u}}\text{FAR} = \int_{w_{tp}}^{\infty} \frac{\partial}{\partial \boldsymbol{\lambda_u}} \frac{1}{\sqrt{2\pi\sigma_w^2}} e^{-\frac{\tau^2}{2\sigma_w^2}} \mathrm{d}\tau.$$

Hence

$$\frac{\partial}{\partial \boldsymbol{\lambda_u}}\text{FAR} = \int_{w_{tp}}^{\infty} \left(\frac{\big(\frac{\partial}{\partial \boldsymbol{\lambda_u}}\sigma_w^2\big)\tau^2}{2\sqrt{2\pi}\sigma_w^5} - \frac{\big(\frac{\partial}{\partial \boldsymbol{\lambda_u}}\sigma_w^2\big)}{2\sqrt{2\pi}\sigma_w^3} \right) e^{-\frac{\tau^2}{2\sigma_w^2}} \mathrm{d}\tau.$$

We introduce the following lemma to calculate the above integral.

Lemma 4.2.2 *For vectors $\boldsymbol{\theta}_i$ and scalars κ_i, if $\boldsymbol{\theta_1} = -\boldsymbol{\theta_3}$ it holds that*

$$\int \left(\frac{\boldsymbol{\theta_1} + \boldsymbol{\theta_2}(\kappa_1 + \tau)}{\kappa_2^3} + \frac{\boldsymbol{\theta_3}(\kappa_1 + \tau)^2}{{\kappa_2}^5} \right) e^{-\frac{(\kappa_1+\tau)^2}{2\kappa_2^2}} \, \mathrm{d}\tau = - \frac{\boldsymbol{\theta_2}\kappa_2^2 + \boldsymbol{\theta_3}(\kappa_1 + \tau)}{\kappa_2^3} e^{-\frac{(\kappa_1+\tau)^2}{2\kappa_2^2}} + c.$$

Proof. The integral is evaluated as

$$\frac{\sqrt{\pi}}{\sqrt{2}\kappa_2^2}(\boldsymbol{\theta_1} + \boldsymbol{\theta_3})\mathrm{erf}\left(\frac{\kappa_1 + \tau}{\sqrt{2}\kappa_2} \right) - \frac{\boldsymbol{\theta_2}\kappa_2^2 + \boldsymbol{\theta_3}(\kappa_1 + \tau)}{{\kappa_2}^3} e^{-\frac{(\kappa_1+\tau)^2}{2\kappa_2^2}} + c,$$

where erf(.) indicates the error function. As $\boldsymbol{\theta_1} = -\boldsymbol{\theta_3}$, the proof is complete. □

Using this lemma the integral is determined as

$$\frac{\partial}{\partial \boldsymbol{\lambda_u}} \mathrm{FAR} = -\frac{w_{\mathrm{tp}} \left(\frac{\partial}{\partial \boldsymbol{\lambda_u}} \sigma_w^2 \right)}{2\sqrt{2\pi}\sigma_w^3} e^{\frac{w_{\mathrm{tp}}^2}{-2\sigma_w^3}}. \tag{4.20}$$

By plugging equations (4.19) and (4.20) into equation (4.17) and substituting the optimal trip-point (see (4.16)), we obtain

$$\left(\frac{\partial}{\partial \boldsymbol{\lambda_u}} \sigma_w^2 \right) (\boldsymbol{\lambda_y} \mathbf{1}^T \mu_y + \boldsymbol{\lambda_u} \mathbf{1}^T \mu_u) - 2\sigma_w^2 \mathbf{1}^T \mu_u = 0. \tag{4.21}$$

To calculate the derivative of σ_w^2 we need to rewrite the convolution terms in (4.12) as

$$\sigma_w^2 = (\boldsymbol{\lambda_y} H_f + \boldsymbol{\lambda_u} H_g) \Psi (\boldsymbol{\lambda_y} H_f + \boldsymbol{\lambda_u} H_g)^T \sigma_\nu^2, \tag{4.22}$$

where

$$H_f \triangleq \begin{bmatrix} f_1 & f_2 & \cdots & f_l & 0 & 0 & 0 & \cdots & 0 \\ 0 & f_1 & f_2 & \cdots & f_l & 0 & 0 & \cdots & 0 \\ 0 & 0 & f_1 & f_2 & \cdots & f_l & 0 & \cdots & 0 \\ \vdots & \ddots & \vdots & \vdots & \ddots & \vdots & \vdots & \ddots & \vdots \\ 0 & \cdots & 0 & f_1 & \cdots & f_{l-2} & f_{l-1} & f_l & 0 \\ 0 & \cdots & 0 & 0 & f_1 & \cdots & f_{l-2} & f_{l-1} & f_l \end{bmatrix}.$$

The above matrix has r rows and $l+r-1$ columns and H_g is defined similarly. We have

$$\frac{\partial}{\partial \boldsymbol{\lambda_u}} \sigma_w^2 = 2(\boldsymbol{\lambda_y} H_f + \boldsymbol{\lambda_u} H_g)_g^T \sigma_\nu^2.$$

Furthermore, $\mu_y = \frac{\sum_{i=1}^{m} f_i}{\sum_{i=1}^{n} g_i} \mu_u$; after some simplification, (5.21) can be reformulated as

$$\boldsymbol{\lambda} H \Psi H_g^T \left(\boldsymbol{\lambda} \mathbf{1}_{\boldsymbol{fg}}^T \right) - \left(\boldsymbol{\lambda} H \Psi H^T \boldsymbol{\lambda}^T \right) \mathbf{1} = 0, \tag{4.23}$$

where

$$\boldsymbol{\lambda} \triangleq \begin{bmatrix} \boldsymbol{\lambda_y} & \boldsymbol{\lambda_u} \end{bmatrix},$$

$$H \triangleq \begin{bmatrix} H_f \\ H_g \end{bmatrix},$$

and

$$\mathbf{1_{fg}} \triangleq \begin{bmatrix} \frac{\sum_{i=1}^{m} f_i}{\sum_{i=1}^{n} g_i}\mathbf{1} & \mathbf{1} \end{bmatrix}.$$

By conducting a similar derivation, for $\frac{\partial}{\partial \boldsymbol{\lambda_y}}(\eta_m \mathrm{MAR} + \eta_f \mathrm{FAR}) = 0$ one can show that

$$\boldsymbol{\lambda} H \Psi H_g^T (\boldsymbol{\lambda} \mathbf{1}_{\boldsymbol{gf}}^T) - (\boldsymbol{\lambda} H \Psi H^T \boldsymbol{\lambda}^T)\mathbf{1} = 0, \tag{4.24}$$

where $\mathbf{1_{gf}} \triangleq \begin{bmatrix} \mathbf{1} & \frac{\sum_{i=1}^{n} g_i}{\sum_{i=1}^{m} f_i}\mathbf{1} \end{bmatrix}$. Now we combine equations (4.24) and (4.23) and write them in the following matrix form:

$$\begin{bmatrix} \boldsymbol{\lambda} H \Psi H_f^T (\boldsymbol{\lambda} \mathbf{1}_{\boldsymbol{gf}}^T) & \boldsymbol{\lambda} H \Psi H_g^T (\boldsymbol{\lambda} \mathbf{1}_{\boldsymbol{fg}}^T) \end{bmatrix} - \begin{bmatrix} (\boldsymbol{\lambda} H \Psi H^T \boldsymbol{\lambda}^T)\mathbf{1} & (\boldsymbol{\lambda} H \Psi H^T \boldsymbol{\lambda}^T)\mathbf{1} \end{bmatrix} = 0.$$

Multiplying the above equation by matrix $\begin{bmatrix} \frac{\sum_{i=1}^{m} f_i}{\sum_{i=1}^{n} g_i} I & 0 \\ 0 & I \end{bmatrix}$ yields

$$\begin{bmatrix} \boldsymbol{\lambda} H \Psi H_f^T (\boldsymbol{\lambda} \mathbf{1}_{\boldsymbol{fg}}^T) & \boldsymbol{\lambda} H \Psi H_g^T (\boldsymbol{\lambda} \mathbf{1}_{\boldsymbol{fg}}^T) \end{bmatrix} - \begin{bmatrix} (\boldsymbol{\lambda} H \Psi H^T \boldsymbol{\lambda}^T)\left(\frac{\sum_{i=1}^{m} f_i}{\sum_{i=1}^{n} g_i}\right)\mathbf{1} & (\boldsymbol{\lambda} H \Psi H^T \boldsymbol{\lambda}^T)\mathbf{1} \end{bmatrix} = 0,$$

Note that $\boldsymbol{\lambda} \mathbf{1}_{\boldsymbol{fg}}^T$ is a scalar, so we can further simplify the above equation as

$$\boldsymbol{\lambda} H \Psi \begin{bmatrix} H_f^T & H_g^T \end{bmatrix} (\boldsymbol{\lambda} \mathbf{1}_{\boldsymbol{fg}}^T) - (\boldsymbol{\lambda} H \Psi H^T \boldsymbol{\lambda}^T) \begin{bmatrix} \left(\frac{\sum_{i=1}^{m} f_i}{\sum_{i=1}^{n} g_i}\right)\mathbf{1} & \mathbf{1} \end{bmatrix} = 0,$$

Thus

$$\boldsymbol{\lambda} H \Psi H^T (\boldsymbol{\lambda} \mathbf{1}_{\boldsymbol{fg}}^T) - (\boldsymbol{\lambda} H \Psi H^T \boldsymbol{\lambda}^T)\mathbf{1}_{\boldsymbol{fg}} = 0. \tag{4.25}$$

By defining $\bar{H} \triangleq H \Psi H^T$ and after excluding the trivial solution $\boldsymbol{\lambda} = 0$, the above equation can be written as

$$\boldsymbol{\lambda} \frac{\mathbf{1}_{\boldsymbol{fg}} \boldsymbol{\lambda}^T}{\boldsymbol{\lambda} \bar{H} \boldsymbol{\lambda}^T} \bar{H} = \mathbf{1}_{\boldsymbol{fg}}.$$

Here, $\frac{\mathbf{1_{fg}}\boldsymbol{\lambda}^T}{\boldsymbol{\lambda}\bar{H}\boldsymbol{\lambda}^T}$ is a non-zero scalar and $\bar{H}$ is a full rank square matrix, so the unique form of the answer is expressed as

$$\boldsymbol{\lambda}^* = c\mathbf{1_{fg}}\bar{H}^{-1}, \tag{4.26}$$

where $c \in \mathbb{R}\backslash\{0\}$. Here, $c = 0$ results in $\boldsymbol{\lambda} = 0$, hence, $w(k) \equiv 0$, which is not a valid answer. Furthermore, c is a free parameter and for simplicity we consider $c = 1$. Selecting any other non-zero c results in the same filter performance because it is compensated by the modification of alarm trip-point.

Now we need to show that this answer indeed is a minimum. After some math operation, the second derivative of the cost function is obtained as

$$\frac{\partial^2 J}{\partial \boldsymbol{\lambda}^*} = \big(\bar{H}\boldsymbol{\lambda}^*\mathbf{1}_{\boldsymbol{fg}}^T + \mathbf{1}_{\boldsymbol{fg}}^T\boldsymbol{\lambda}^*\bar{H} - 2\bar{H}\boldsymbol{\lambda}^{*T}\mathbf{1_{fg}}\big)\frac{e^{-\frac{{w_{tp}^*}^2}{2\sigma_w^2}}}{2\sqrt{2\pi}\sigma_w^3}. \tag{4.27}$$

Here, the term $\frac{e^{-\frac{{w_{tp}^*}^2}{2\sigma_w^2}}}{2\sqrt{2\pi}\sigma_w^3}$ is non-negative. Substituting the optimal answer in $\bar{H}\boldsymbol{\lambda}^*\mathbf{1}_{\boldsymbol{fg}}^T - \mathbf{1}_{\boldsymbol{fg}}^T\boldsymbol{\lambda}^*\bar{H} - 2\bar{H}\boldsymbol{\lambda}^{*T}\mathbf{1_{fg}}$ yields $\bar{H}(\mathbf{1_{fg}}\bar{H}^{-1}\mathbf{1}_{\boldsymbol{fg}}^T) - \mathbf{1}_{\boldsymbol{fg}}^T\mathbf{1_{fg}}$. To show that this is positive semi-definite we use Schur's complement lemma (see Ref. [112]). According to this lemma we need to prove that the following statement holds

$$\begin{bmatrix} \bar{H}(\mathbf{1_{fg}}\bar{H}^{-1}\mathbf{1}_{\boldsymbol{fg}}^T) & \mathbf{1}_{\boldsymbol{fg}}^T \\ \mathbf{1_{fg}} & 1 \end{bmatrix} \succeq 0. \tag{4.28}$$

Let us define $\Phi \triangleq \bar{H}(\mathbf{1_{fg}}\bar{H}^{-1}\mathbf{1}_{\boldsymbol{fg}}^T)$. As $\bar{H}$ is positive definite, so is $\bar{H}^{-1}$, which yields $\mathbf{1_{fg}}\bar{H}^{-1}\mathbf{1}_{\boldsymbol{fg}}^T > 0$. Hence, Φ is positive definite and invertible. The matrix in (4.28) can be decomposed as

$$\begin{bmatrix} \Phi & \mathbf{1}_{\boldsymbol{fg}}^T \\ \mathbf{1_{fg}} & 1 \end{bmatrix} = \begin{bmatrix} I \\ \mathbf{1_{fg}}\Phi^{-1} \end{bmatrix} \Phi \begin{bmatrix} I & \Phi^{-1}\mathbf{1}_{\boldsymbol{fg}}^T \end{bmatrix} + \begin{bmatrix} 0 & 0 \\ 0 & 1 - \mathbf{1_{fg}}\Phi^{-1}\mathbf{1}_{\boldsymbol{fg}}^T \end{bmatrix}.$$

It can be verified that $1 - \mathbf{1_{fg}}\Phi^{-1}\mathbf{1}_{\boldsymbol{fg}}^T = 0$. Considering the positive definiteness of Φ and based on the above equation we conclude that (4.28) holds.

It is important to note that for some configurations, the matrix $\bar{H}$ may be rank deficient (i.e., has eigenvalues equal to zero). A solution to this problem is by adding some small perturbation to replace the eigenvalues. More formally,

$$\begin{bmatrix} \boldsymbol{\lambda}_{\boldsymbol{y}}^* & \boldsymbol{\lambda}_{\boldsymbol{u}}^* \end{bmatrix} = (\bar{H} + \epsilon I)^{-1}\mathbf{1}_{\boldsymbol{fg}}^T, \tag{4.29}$$

where ϵ is a small number. Now we can obtain the optimal trip-point by manipulating the equation in (4.16). By substituting the optimal answer $\boldsymbol{\lambda}^*$, equation (4.11) can be written as

$$\mu_w^* = \frac{\mathbf{1}_{\boldsymbol{fg}}(\bar{H} + \epsilon I)^{-1}\mathbf{1}_{\boldsymbol{fg}}^T \sum_{i=1}^{m} g_i \sum_{i=1}^{p} \beta_i}{\sum_{i=1}^{m} f_i \sum_{i=1}^{p} \alpha_i - \sum_{i=1}^{m} g_i \sum_{i=1}^{p} \beta_i} \bar{b}.$$

From (4.22), we can find ${\sigma_w^2}^*$ which is the variance of the alarm signal considering the optimal filter coefficients. Finally, by plugging μ_w^* and ${\sigma_w^2}^*$ in (4.16) and after some simplification we have

$$w_{\text{tp}}^* = \mu_w^* - \frac{\sum_{i=1}^{m} f_i \sum_{i=1}^{p} \alpha_i - \sum_{i=1}^{m} g_i \sum_{i=1}^{p} \beta_i}{\bar{b} \sum_{i=1}^{m} g_i \sum_{i=1}^{p} \beta_i} \sigma_\nu^2 \ln\left(\frac{\eta_f}{\eta_m}\right). \tag{4.30}$$

It is straightforward to verify that for the moving average filters of order 1, the optimal optimal coefficients are obtained as

$$\lambda_u^* = \frac{\boldsymbol{g}\Psi\left(\boldsymbol{g}^T \frac{\sum_{i=1}^{m} f_i}{\sum_{i=1}^{n} g_i} - \boldsymbol{f}^T\right)}{\boldsymbol{f}\Psi\left(\boldsymbol{f}^T - \boldsymbol{g}^T \frac{\sum_{i=1}^{m} f_i}{\sum_{i=1}^{n} g_i}\right)} c,$$

$$\lambda_y^* = c.$$

Remark 8 *It is a common assumption that the distribution of normal and abnormal data are known. Then using the historical data we can find the expected value of $u(k)$ and $y(k)$ and identify $\bar{b}$ using the closed-loop model of the system.*

4.3 Notes on Online Application of the Method

In process industries, drift in plant characteristics or set-point adjustment usually causes performance degradation [86]. Similarly, the efficiency of the proposed alarm filter may also deteriorate due to the new condition. It was also clearly mentioned in the ISA standard that changing the controller requires the revision of the alarm system. Considering the simple form of the

final optimal solution, one may further extend it to an adaptive version. The proposed method can be used along with an adaptive controller introduced in the literature such as Ref. [57], [71]. In this case, using (4.29), the alarm filter coefficients are updated each time that the adaptive mechanism re-identifies the plant and re-tunes the controller. In light of the equation in (4.29), the optimal filter coefficients can be selected regardless of the abnormality amplitude $\bar{b}$ (see (4.4)). It means that the updated version of the plant model and the controller setting are enough to determine the new optimal alarm filter. Thus, the overall evaluation of FAR/MAR remains constant. This, however, is not true for each of FAR or MAR exclusively. From (4.30), we can verify that $\bar{b}$ has influence on the optimal trip-point. So if $\bar{b}$ deviates from its historical value, the optimal trip-point will be changed. It is worth emphasizing that by the selection of the trip-point we can adjust tradeoff between FAR and MAR. So the original design requirements of FAR and MAR may not be satisfied anymore (c.f., the $\ln\left(\frac{\eta_f}{\eta_m}\right)$ term in (4.30)). A robust solution to this problem is by obtaining the admissible range for $\bar{b}$ as $\bar{b}_{\min} < \bar{b} < \bar{b}_{\max}$; and finding the trip-point in (4.30) that guarantees the required MAR for the whole range of $\bar{b}$.

4.4 Case Study

In this section, we present the simulation result and illustrate superiority of the proposed method over the conventional version. We use the plant model that was introduced and implemented in Ref. [91]. The plant is shown in Fig. 4.2 which is composed of two tanks, a pump, a control valve, and a level meter. One of the tanks is considered as the water source. The control purpose is to maintain the water level of the second tank at a certain level. The pump and the control valve let the water flow from the source tank to the second one. This is a SISO plant where the input u and the output y are corresponding to the water flow and the water level. Inspired by the real abnormal scenarios introduced in Ref. [91], we study the valve closure fault. Our result is likewise valid for the faults corresponding to the voltage increase in the pump drive

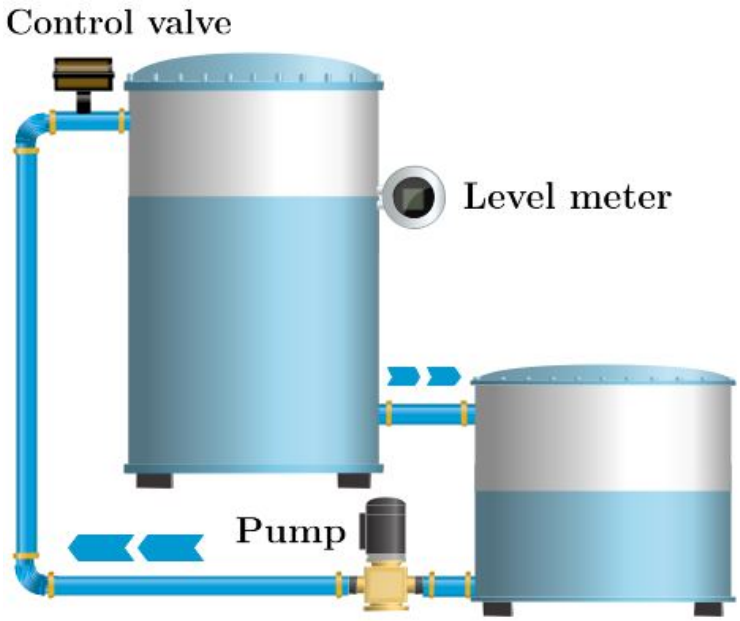

Figure 4.2: Two water tanks system

circuit. The plant model was identified in the reference as

$$y(s) = \frac{1.19}{1 + 132.80s} e^{-35s} u(s).$$

By applying the first order Padé approximation and discretizing the plant with the sampling rate of 1 second we obtain

$$y(z^{-1}) = 10^{-3} \frac{-8.426z^{-1} + 8.922z^{-2}}{1 - 1.937z^{-1} + 0.937z^{-2}} u(z^{-1}).$$

Here, the modeling error $\nu(k)$ follows $\mathcal{N}(0, 0.05^2)$. Furthermore, we assume that the following controller is used

$$u(z^{-1}) = \frac{-3 + 3.9z^{-1} - 1.2z^{-2}}{1 - 1.3z^{-1} + 0.42z^{-2}} y(z^{-1}).$$

For $\bar{b} = 20$, the normal and abnormal operation modes are represented by

$$b = \begin{cases} 0, & \text{normal mode,} \\ 20, & \text{abnormal mode.} \end{cases}$$

Using (4.29), where $\epsilon = 0.001$, for filter length $r = 5$ we determine

$$\boldsymbol{\lambda_u} = [0.11, 0.03, 0.05, 0.01, -0.18],$$

$$\boldsymbol{\lambda_y} = [0.20, 0.22, 0.15, -0.04, -0.48].$$

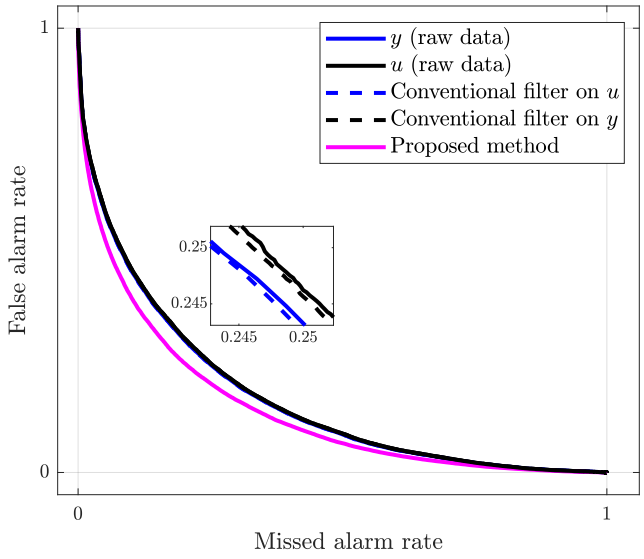

Figure 4.3: ROC curves of various alarm filter configurations where $r = 5$

A common practice to evaluate alarm filter performance is to use receiver operating characteristic (ROC) curves. An ROC curve is a plot of MAR versus FAR while the alarm trip-point spans over all possible values of its range. Using this concept, we can compare various alarm filters regardless of the alarm trip-point. Fig. 4.3 displays the simulation results for five different alarm signals. The first two signals are generated from the raw process data and are indicated as the solid blue and black curves. The dashed curves are corresponding to the filtered version of the first two signals. Here, the conventional filter that was proposed in Ref. [27] is used (where all filter coefficients are equal). The solid magenta curve shows the result of the proposed method. According to this figure, although the filter length of the conventional method and the proposed method are the same, our method outperforms the conventional filters. Furthermore, it can be seen that the alarm signals which are generated from the raw data and the conventional filter have approximately similar performance. Next, we conduct the simulation for the same closed-loop setup except that we increase the length of all filters to 35. The ROC curves for this case are shown in Fig. 4.4 We can verify the improvement of all filter configurations owing to the larger filter length. However, the conventional filter still does not show a notable improvement. Finally, the time

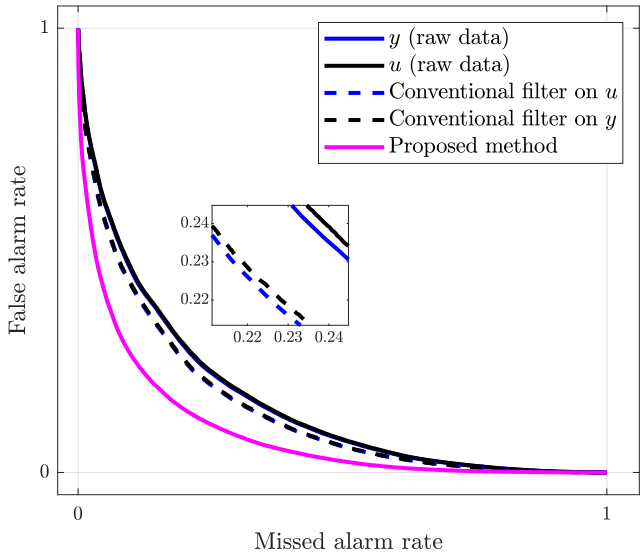

Figure 4.4: ROC curves of various alarm filter configurations where $r = 35$

trends of all alarm signals for the filter length of 35 are presented in the left part of Fig. 4.5. The alarm trip-points are obtained considering $\eta_m = \eta_f$. The right part of this figure shows the alarm states for the associated alarm signals. The alarm signal corresponding to the proposed method has a relatively higher oscillation. It may seems to be counter-intuitive at first glance as the expectation from an alarm filter is to decrease the variation. But this is only one contributing factor to the performance of an alarm filter. In fact, an alarm filter should manipulate the raw data to magnify the amplitude of the abnormality and decrease the variation at the same time.

4.5 Summary

The design problem of generalized moving average alarm filters for statistically correlated process variables has been addressed in this chapter. First, considering the ARX representation of a plant, mathematical expressions for the rates of false and missed alarms have been derived. Then, closed form solutions for the optimal design of the alarm filter and alarm trip-point has been determined. Also it have been justified that the conventional moving average filter is not the optimal answer when relaxing the independence assumption on process measurements. Furthermore, into the case of actuator faults, it has

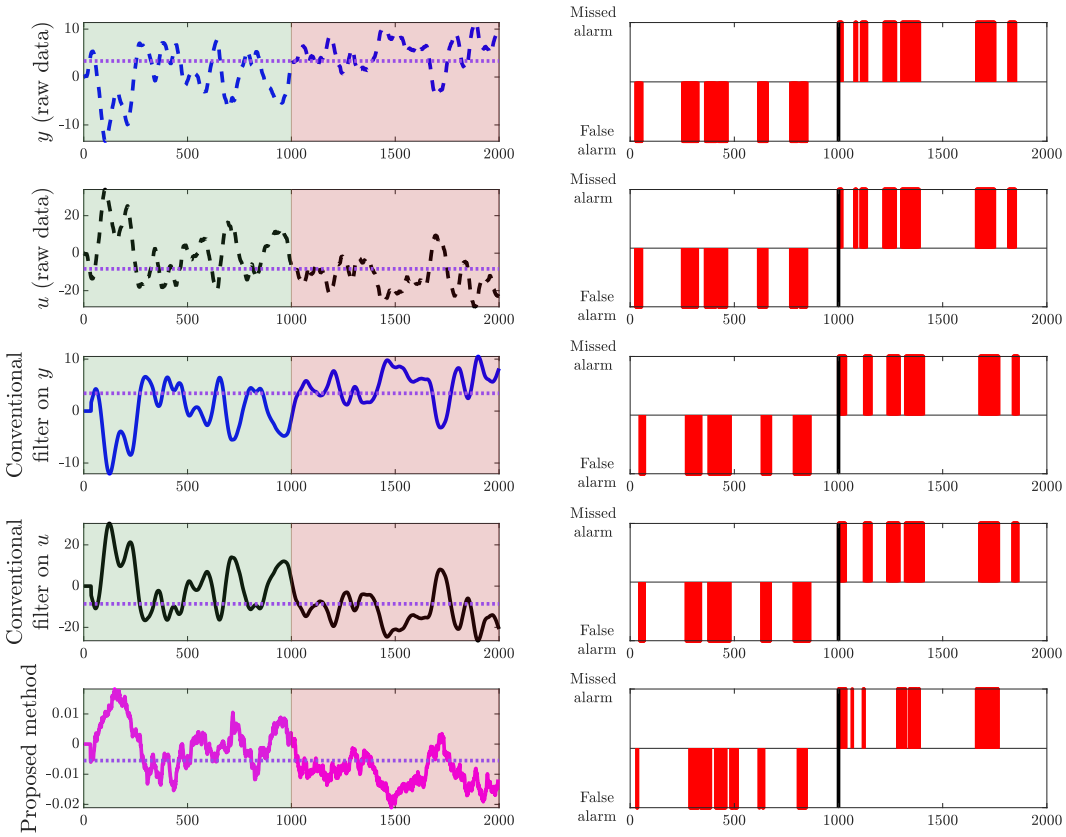

Figure 4.5: Time trends of alarm signals and the corresponding alarm states (highlighted green and red areas show the normal and abnormal operation modes, respectively, and dotted lines show the alarm trip-point)

been shown that the optimal filter coefficients can be obtained regardless of the abnormality amplitude. This result paves the path for online utilization of the proposed method.

Chapter 5

Generalized Moving Variance Filters for Industrial Alarm Systems

In this chapter, we study generalized moving average filters (GMAF) and generalized moving variance filters (GMVF). Although conventional moving variance filters have already been introduced and used, whether they are optimal was an open question. So we develop a framework for the so called *generalized filters* where the filter coefficients are allowed to be different. We prove that if the only performance measure of interest is detection accuracy, then indeed the conventional filters are the optimal ones. Our result explicitly shows how the filter performance changes with respect to the filter weights. Nevertheless, if instead, detection delay is also of interest, employing a counter-example, we show that conventional filters are outperformed by some generalized filter configurations. Considering this case, our result gives a straightforward formulation for the assessment of generalized moving variance filters. This opens the possibility for future research on finding the optimal coefficients for generalized filters that incorporate other performance indices (including but not limited to detection delay). Another contribution of this chapter is the suggestion of a measure for the impact of statistical parameters of process variables on the distinguishability of faults after filtering. Via a case study on the Tennessee Eastman process, we show that for the same level of accuracy, the generalized configuration can provide faster detection of variance changes compared to the

conventional version.

5.1 Alarm System Performance Assessment

In this section, we investigate two indices that have been regularly used by researchers as well as practitioners to evaluate the performance of alarm systems. As the alarm system design can be regarded as a classification problem, we also study the Fisher's linear discriminant classification.

5.1.1 Rates of False and Missed Alarms

Here, we introduce the performance indices from the literature. In a plant, assume that a process variable is measured and denoted by a discrete-time signal $w[k], k \in \{1, 2, \cdots\}$. To detect the faulty operation of the plant, $w[k]$ is compared with a fixed alarm trip-point $w_{\rm tp}$; and an alarm is raised if the signal exceeds this trip-point. In this scenario, some alarms may be raised while the plant works normally, which are called false alarms. Moreover, some alarms may be missed while the plant works abnormally. These two concepts have been manipulated to introduce the false alarm rate (FAR) and the missed alarm rate (MAR). Assuming that $w[k]$'s are independent and identically distributed (IID) in each operation modes (i.e., normal and abnormal modes), MAR and FAR are calculated as follows:

$$\begin{aligned} \text{MAR} &= \int_{-\infty}^{w_{\rm tp}} f_{w,\rm ab}(u)\mathrm{d}u, \\ \text{FAR} &= \int_{w_{\rm tp}}^{\infty} f_{w,\rm n}(u)\mathrm{d}u, \end{aligned}$$

where, $f_{w,\rm ab}$ (resp. $f_{w,\rm n}$) represents the PDF of process variable w in the abnormal (resp. normal) operation mode. One of the main objectives in alarm filter design is to have low MAR and FAR. However, reducing FAR (resp. MAR) causes increment of MAR (resp. FAR) in most cases. Thus, the receiver operating characteristic (ROC) curve is introduced, which is a plot of MAR versus FAR as the trip-point spans all real numbers. It can be immediately concluded that if the ROC curve is close to the origin, the associated alarm performance is desirable. For quantifying this statement, the

area under curve (AUC) has been introduced. Thus, instead of working with FAR and MAR, we can exploit AUC. It has two advantages. First, the problem is simplified to optimization with respect to one performance index (instead of two indices). Second, it splits the problem into two steps: designing an alarm filter and designing a threshold/trip-point.

For the present, assume that the probability density function of $w[k]$ are given *a priori* for both operation modes. Later, we will prove that for Gaussian distributions, the performance of moving average and moving variance filters can be assessed regardless of the input signal's statistical parameters. Let $T_{\rm ab}$ denotes the time of abnormality occurrence and assume that the distribution of $w[k]$'s are given by

$$W \sim \begin{cases} \mathcal{N}(\mu_{w,\rm n}, \sigma^2_{w,\rm n}) & k < T_{\rm ab}, \\ \mathcal{N}(\mu_{w,\rm ab}, \sigma^2_{w,\rm ab}) & k \geq T_{\rm ab}. \end{cases} \tag{5.1}$$

The AUC is calculated by [70] as

$$\mathrm{AUC}(w) = 1 - \Phi\left(\frac{|\mu_{w,\rm ab} - \mu_{w,\rm n}|}{\sqrt{\sigma^2_{w,\rm ab} + \sigma^2_{w,\rm n}}}\right), \tag{5.2}$$

where

$$\Phi(v) \triangleq \frac{1}{\sqrt{2\pi}} \int_{-\infty}^{v} e^{-\frac{1}{2}\tau^2} \mathrm{d}\tau. \tag{5.3}$$

Here, Φ has two interesting features that facilitate analysis. First, $\Phi(v)$ is an strictly increasing function of v. Second, $\Phi(v)$ is bounded from top by 1. Thus, AUC is a strictly decreasing function of $\frac{|\mu_{w,\rm ab}-\mu_{w,\rm n}|}{\sqrt{\sigma^2_{w,\rm ab}+\sigma^2_{w,\rm n}}}$. Similar to Chapter 2, for a process variable $w[k]$ in the form of (5.1), the alarm performance is defined as

$$\mathcal{A}(w) \triangleq \frac{\sigma^2_{w,\rm ab} + \sigma^2_{w,\rm n}}{(\mu_{w,\rm ab} - \mu_{w,\rm n})^2}. \tag{5.4}$$

In the next subsection, we prove that this index is aligned with the view of a special case of Fisher's linear discriminant analysis.

5.1.2 Fisher's Linear Discriminant Analysis

Now we show that the performance index considered in the Fisher's linear discriminant method in a special case is proportional to the inverse of index

$\mathcal{A}$ that we introduced to minimize the MAR and FAR performance indices. Given two classes of data, Fisher's linear discriminant classification (see [21]) is introduced for performing a separation between these classes. Let P_B and P_W denote the between-class and within-class covariance matrices; the idea is to maximize $J(z)$ with respect to the vector z, where

$$J(z) = \frac{z^T P_B z}{z^T P_W z}. \tag{5.5}$$

Let w_{n} and w_{ab} denote the collected data in normal and abnormal operation modes, and l_{n} and l_{ab} denote the length of associated data, respectively. According to [21], for the special case where P_B and P_W are scalar, one can obtain

$$P_B = (\mu_{w,\mathrm{ab}} - \mu_{w,\mathrm{n}})^2, \tag{5.6}$$

$$P_W = \sum_{k=1}^{l_{\mathrm{ab}}} \left(w_{\mathrm{ab}}[k] - \mu_{w,\mathrm{ab}}\right)^2 + \sum_{k=1}^{l_{\mathrm{n}}} \left(w_{\mathrm{n}}[k] - \mu_{w,\mathrm{n}}\right)^2. \tag{5.7}$$

Considering this specialization, we have $J(z) \equiv \bar{J}$, where $\bar{J}$ denotes the maximum of $J(z)$. From (5.7) we can see that $P_W = l_{\mathrm{ab}}\sigma^2_{w,\mathrm{ab}} + l_n\sigma^2_{w,\mathrm{n}}$. By substituting this equation and the equation in (5.7) into (5.5), we infer that $\mathcal{A} \propto \bar{J}^{-1}$ if $l_{\mathrm{ab}} = l_{\mathrm{n}}$. This represents that the view of Fisher's linear discriminant analysis is aligned with the alarm index defined in (6.3) if the length of normal and abnormal data are the same.

5.2 Generalized Moving Average Filter

Two methods have been provided in the literature for finding the optimal weights of moving average filters ([14], [27]). However, they do not reveal the relationship between the filter coefficients and its performance. In this section, we provide an intuitive method for finding the weights that explicitly reveals the influence of the weights on the alarm performance. This result can be served as a tool for plant operators to tune the alarm filters while having an intuition about the role of filter weights in the abnormality detection accuracy. A generalized moving average filter of order N with non-negative coefficients

θ_i's is described as

$$y[k] = \sum_{i=0}^{N-1} \theta_i x[k-i],\ k = N, N+1, \cdots . \tag{5.8}$$

where x and y are corresponding to the raw and filtered data, respectively. Let $T_{\rm ab}$ denote the time of abnormality occurrence and assume that all samples of the raw data are independent and identically distributed and follow

$$X \sim \begin{cases} \mathcal{N}(\mu_{x,\rm n}, \sigma^2_{x,\rm n}), & k < T_{\rm ab}, \\ \mathcal{N}(\mu_{x,\rm ab}, \sigma^2_{x,\rm ab}), & k \geq T_{\rm ab}. \end{cases} \tag{5.9}$$

To obtain filter performance, we only need to focus on the steady state (i.e., when the samples of the moving average filter correspond to either normal or abnormal operation mode, not both). Note that this is a standard assumption in almost all previous works in this area (e.g. [5], [27] and [42]). The goal is to estimate the number of missed alarms while the system is working normally for a long time. Hence, the effect of the first few samples can be neglected in the analysis. It follows that $Y = \sum_{i=0}^{N-1} \theta_i X$, where Y is a random variable corresponding to the filtered data. As the filter is linear and time-invariant, we have

$$Y \sim \begin{cases} \mathcal{N}\Big(\mu_{x,\rm n} \sum_{i=0}^{N-1} \theta_i, \sigma^2_{x,\rm n} \sum_{i=0}^{N-1} \theta_i^2\Big), & N \leq k < T_{\rm ab}, \\ \mathcal{N}\Big(\mu_{x,\rm ab} \sum_{i=0}^{N-1} \theta_i, \sigma^2_{x,\rm ab} \sum_{i=0}^{N-1} \theta_i^2\Big), & k \geq T_{\rm ab} + N. \end{cases}$$

Now the alarm index of filtered data is expressed as

$$\mathcal{A}_{\rm GMAF}(y) = \frac{(\sigma^2_{x,\rm ab} + \sigma^2_{x,\rm n}) \sum_{i=0}^{N-1} \theta_i^2}{(\mu_{x,\rm ab} - \mu_{x,\rm n})^2 \Big(\sum_{i=0}^{N-1} \theta_i \Big)^2}. \tag{5.10}$$

According to the above expression, we conclude that the alarm index is related to the statistical parameters of process variable as

$$\mathcal{A}_{\rm GMAF}(y) \propto \frac{\sigma^2_{x,\rm ab} + \sigma^2_{x,\rm n}}{(\mu_{x,\rm ab} - \mu_{x,\rm n})^2}, \tag{5.11}$$

and to the parameters of filter as

$$\mathcal{A}_{\rm GMAF}(y) \propto \frac{\sum_{i=0}^{N-1} \theta_i^2}{\Big(\sum_{i=0}^{N-1} \theta_i \Big)^2} \triangleq \mathcal{A}^{\mathcal{F}}_{\rm GMAF}. \tag{5.12}$$

One may also realize that when $\theta_i = \theta_j,\ \forall i, j$, the performance of moving average filter affected by the filter order as $\mathcal{A}_{\mathrm{GMAF}}(y) \propto \frac{1}{N}$. Moreover, the AUC corresponding to the filtered data is determined as

$$\mathrm{AUC}(y) = 1 - \Phi\Big(\mathcal{A}^{-1}_{\mathrm{GMAF}}(y)\Big). \tag{5.13}$$

According to the above results, the problem of minimizing $\mathcal{A}_{\mathrm{GMAF}}(y)$ is equivalent to the following problem:

$$\min_{\theta_0,\ldots,\theta_{N-1}} \sum_{i=0}^{N-1} \theta_i^2, \quad s.t., \ \sum_{i=0}^{N-1} \theta_i = 1.$$

So we only need to consider the filter configurations that satisfy $\sum_{i=0}^{N-1} \theta_i = 1$. Then, $\sum_{i=0}^{N-1} \theta_i^2$ can easily be considered as the performance index for generalized moving average filters.

5.3 Generalized Moving Variance Filter

The generalized moving variance filter of order N with non-negative coefficients θ_i is described by

$$y[k] = \sum_{i=0}^{N-1} \theta_i (x[k-i] - \mu_x)^2, \ k = N, N+1, \cdots . \tag{5.14}$$

This representation is different from the one in (5.9) as here only the variance is changed after the occurrence of abnormality and the mean remains unchanged. We assume that all samples of the raw data are independent and identically distributed. This is a standard simplifying assumption in the literature (see, for example, [89], [106]). However, in some cases, this simplification can be argued as the samples of process variables are measured from the industrial plants and are likely correlated. In those cases, more information about the plant and different methods are needed for the analysis. Let the samples of raw data follow

$$X \sim \begin{cases} \mathcal{N}(\mu_x, \sigma^2_{x,\mathrm{n}}), & k < T_{\mathrm{ab}}, \\ \mathcal{N}(\mu_x, \sigma^2_{x,\mathrm{ab}}), & k \geq T_{\mathrm{ab}}. \end{cases}$$

According to the equation in (5.14), the generalized moving variance filter can be reformulated as

$$y[k] = \sum_{i=0}^{N-1} \theta_i \bar{x}^2[k-i],\ k = N, N+1, \cdots . \tag{5.15}$$

Here, $\bar{x}[k]$'s are identically distributed as

$$\bar{X} \sim \begin{cases} \mathcal{N}(0, \sigma^2_{x,\mathrm{n}}), & k < T_{\mathrm{ab}}, \\ \mathcal{N}(0, \sigma^2_{x,\mathrm{ab}}), & k \geq T_{\mathrm{ab}}. \end{cases}$$

The distribution of filtered data (i.e. (5.15)) is obtained as

$$Y \sim \begin{cases} \sum\limits_{i=0}^{N-1} \theta_i \sigma^2_{x,\mathrm{n}} \mathcal{X}^2, & N \leq k < T_{\mathrm{ab}}, \\ \sum\limits_{i=0}^{N-1} \theta_i \sigma^2_{x,\mathrm{ab}} \mathcal{X}^2, & k \geq T_{\mathrm{ab}} + N, \end{cases} \tag{5.16}$$

which leads to

$$Y \sim \begin{cases} \sum\limits_{i=0}^{N-1} \Gamma(\frac{1}{2}, \theta_i \sigma^2_{x,\mathrm{n}}), & N \leq k < T_{\mathrm{ab}}, \\ \sum\limits_{i=0}^{N-1} \Gamma(\frac{1}{2}, \theta_i \sigma^2_{x,\mathrm{ab}}), & k \geq T_{\mathrm{ab}} + N. \end{cases} \tag{5.17}$$

The distribution in (5.16) is reformed to the one in (5.17) to represent the weights (i.e. $\theta_i \sigma^2_{x,\mathrm{n}}$'s and $\theta_i \sigma^2_{x,\mathrm{ab}}$'s) as the parameters of some Gamma distribution. Now we approximate the summation of independent Gamma distributions in (5.17) with a single Gamma distribution using the so called momentum matching method [31]. The approximation is expressed as

$$\widetilde{Y} \sim \begin{cases} \Gamma(\tilde{\alpha}_y, \tilde{\beta}_{y,\mathrm{n}}), & N \leq k < T_{\mathrm{ab}}, \\ \Gamma(\tilde{\alpha}_y, \tilde{\beta}_{y,\mathrm{ab}}), & k \geq T_{\mathrm{ab}} + N, \end{cases} \tag{5.18}$$

where

$$\tilde{\alpha}_y = \frac{\Big(\sum\limits_{i=0}^{N-1} \theta_i\Big)^2}{2\sum\limits_{i=0}^{N-1} \theta_i^2},$$

$$\tilde{\beta}_{y,\mathrm{n}} = \frac{\sigma^2_{x,\mathrm{n}} \sum\limits_{i=0}^{N-1} \theta_i^2}{\sum\limits_{i=0}^{N-1} \theta_i},\ \tilde{\beta}_{y,\mathrm{ab}} = \frac{\sigma^2_{x,\mathrm{ab}} \sum\limits_{i=0}^{N-1} \theta_i^2}{\sum\limits_{i=0}^{N-1} \theta_i}.$$

This result can also be achieved from the Welch-Satterthwaite equation (see [83]), which is used to approximate the effective degrees of freedom of a weighted summation of independent sample variances.

With regard to the discussions that are given in [31], we can study the accuracy of this approximation. Let $\theta_{\min}$ and $\theta_{\max}$ denote the minimum and the maximum of filter coefficients θ_i's, respectively. The following inequalities hold:

$$\theta_{\min}\sigma^2_{x,\mathrm{n}} \leq \tilde{\beta}_{y,\mathrm{n}} \leq \theta_{\max}\sigma^2_{x,\mathrm{n}}, \tag{5.19}$$

$$\frac{1}{2} < \tilde{\alpha}_y \leq \frac{N}{2}. \tag{5.20}$$

Here, the inequalities of (5.19) and the right inequality of (5.20) change to equality if θ_i's are equal. A similar statement holds for $\tilde{\beta}_{y,\mathrm{ab}}$. Under this equality condition, the approximation is perfect. Otherwise, the smaller $\theta_{\max} - \theta_{\min}$ is, the lower the approximation error.

Now we need to find a good Gaussian approximation for the distribution in (5.18). It is important to note that monotonic transformation of the random variable does not change the associated ROC curve (see [37] and [50]). By manipulating a result in [43], the m^{th} moment of $\widetilde{Y}^{\lambda}$ is obtained as

$$E(Y^{m\lambda}) = \begin{cases} \left(\tilde{\beta}_{y,\mathrm{n}}\right)^{-m\lambda} \frac{\Gamma(\tilde{\alpha}_y + m\lambda)}{\Gamma(\tilde{\alpha}_y)}, & N \leq k < T_{\mathrm{ab}}, \\ \left(\tilde{\beta}_{y,\mathrm{ab}}\right)^{-m\lambda} \frac{\Gamma(\tilde{\alpha}_y + m\lambda)}{\Gamma(\tilde{\alpha}_y)}, & k \geq T_{\mathrm{ab}} + N. \end{cases} \tag{5.21}$$

The authors of [61] discussed the accuracy of approximation when a Gamma distribution was raised to different powers of λ. More specifically, they compared the methods that are presented in [103] and [43] where the approximations were given for $\lambda = \frac{1}{3}$ and $\lambda = \frac{1}{4}$, respectively. In [61] it has been pointed out that for some cases, choosing $\lambda = \frac{1}{4}$ yields better approximation compared with setting $\lambda = \frac{1}{3}$. However, $\lambda = \frac{1}{4}$ leads to a non-monotonic function so it can not preserve the ROC curve. By setting $\lambda = \frac{1}{3}$ and using the equation in (5.21) we have

$$\widetilde{\widetilde{Y}^{\frac{1}{3}}} \sim \begin{cases} \mathcal{N}(\tilde{\mu}_{y,\mathrm{n}}, \tilde{\sigma}^2_{y,\mathrm{n}}), & N \leq k < T_{\mathrm{ab}}, \\ \mathcal{N}(\tilde{\mu}_{y,\mathrm{ab}}, \tilde{\sigma}^2_{y,\mathrm{ab}}), & k \geq T_{\mathrm{ab}} + N, \end{cases} \tag{5.22}$$

where $\widetilde{\widetilde{Y}^{\frac{1}{3}}}$ denotes the normal approximation of $\widetilde{Y}^{\frac{1}{3}}$ and

$$\tilde{\mu}_{y,\mathrm{n}} = \frac{(2\sigma_{x,\mathrm{n}}^2\eta)^{\frac{1}{3}}\Gamma(\eta+\frac{1}{3})}{\Gamma(\eta)},$$
$$\tilde{\mu}_{y,\mathrm{ab}} = \frac{(2\sigma_{x,\mathrm{ab}}^2\eta)^{\frac{1}{3}}\Gamma(\eta+\frac{1}{3})}{\Gamma(\eta)},$$
$$\tilde{\sigma}_{y,\mathrm{n}} = \frac{(\sigma_{x,\mathrm{n}}^2\eta)^{\frac{2}{3}}\Gamma(\eta+\frac{2}{3})}{\Gamma(\eta)} - \tilde{\mu}_{y,\mathrm{n}}^2,$$
$$\tilde{\sigma}_{y,\mathrm{ab}} = \frac{(\sigma_{x,\mathrm{ab}}^2\eta)^{\frac{2}{3}}\Gamma(\eta+\frac{2}{3})}{\Gamma(\eta)} - \tilde{\mu}_{y,\mathrm{ab}}^2.$$

Here, $\eta \triangleq \frac{\sum_{i=0}^{N-1}\theta_i}{2\sum_{i=0}^{N-1}\theta_i^2}$. Now by performing some algebraic operation, the alarm index of filtered data is expressed as

$$\mathcal{A}_{\mathrm{GMVF}}(y) \approx \frac{\left(\sigma_{x,\mathrm{ab}}^{\frac{4}{3}} + \sigma_{x,\mathrm{n}}^{\frac{4}{3}}\right)}{\left(\sigma_{x,\mathrm{ab}}^{\frac{2}{3}} - \sigma_{x,\mathrm{n}}^{\frac{2}{3}}\right)^2}\left(\frac{\Gamma(\eta)\Gamma(\eta+\frac{2}{3})}{\Gamma^2(\eta+\frac{1}{3})} - 1\right).$$

According to this result, the effect of the statistical parameters of x on the alarm index of the filtered data is given by

$$\mathcal{A}_{\mathrm{GMVF}}(y) \propto \frac{\sigma_{x,\mathrm{ab}}^{\frac{4}{3}} + \sigma_{x,\mathrm{n}}^{\frac{4}{3}}}{\left(\sigma_{x,\mathrm{ab}}^{\frac{2}{3}} - \sigma_{x,\mathrm{n}}^{\frac{2}{3}}\right)^2}. \tag{5.23}$$

Furthermore, the area under ROC curve corresponding to the filtered data is determined as

$$\mathrm{AUC}(y) \approx 1 - \Phi\Big(\mathcal{A}_{\mathrm{GMVF}}^{-1}(y)\Big). \tag{5.24}$$

Remark 9 *We introduced a procedure for approximating the distribution of the output samples of the moving variance filter by a Gaussian distribution. Based on the central-limit theorem, one can infer that the proposed method performs more accurate approximation as the filter order increases.*

Theorem 5.3.1 *Consider the generalized moving variance filter described by* (5.14)*. The problem of minimizing* $\mathcal{A}_{GMVF}(y)$ *is approximately equivalent to the following problem:*

$$\min_{\theta_0,\ldots,\theta_{N-1}} \sum_{i=0}^{N-1}\theta_i^2, \quad s.t., \ \sum_{i=0}^{N-1}\theta_i = 1.$$

Proof. To design the filter parameters we know that

$$\mathcal{A}_{\mathrm{GMVF}}(y) \propto \frac{\Gamma(\eta)\Gamma(\eta+\frac{2}{3})}{\Gamma^2(\eta+\frac{1}{3})} - 1 \triangleq \mathcal{A}^{\mathcal{F}}_{\mathrm{GMVF}}.$$

Derivatives of $\mathcal{A}^{\mathcal{F}}_{\mathrm{GMVF}}(y)$ with respect to η is calculated as

$$\frac{\mathrm{d}}{\mathrm{d}\eta}\mathcal{A}^{\mathcal{F}}_{\mathrm{GMVF}} = \frac{\Gamma(\eta)\Gamma\big(\eta+\frac{2}{3}\big)\big(\psi(\eta) - 2\psi(\eta+\frac{1}{3}) + \psi(\eta+\frac{2}{3})\big)}{\Gamma^2\big(\eta+\frac{1}{3}\big)}, \tag{5.25}$$

where ψ denotes the Digamma function which is defined as

$$\psi(\eta) \triangleq \frac{\mathrm{d}}{\mathrm{d}\eta}\ln\big(\Gamma(x)\big) = \frac{\Gamma'(\eta)}{\Gamma(\eta)}.$$

A series expansion for ψ is presented in [3] as

$$\psi(\eta) = -\gamma + \sum_{i=0}^{\infty}\left(\frac{1}{i} - \frac{1}{i+\eta}\right), \quad \eta \neq -1, -2, -3, \cdots,$$

where γ is the Euler-Mascheroni constant. We know that $\eta > 0$, thus we have

$$\psi(\eta) - 2\psi\Big(\eta+\frac{1}{3}\Big) + \psi\Big(\eta+\frac{2}{3}\Big) = \sum_{i=0}^{\infty}\left(\frac{2}{i+\eta+\frac{1}{3}} - \frac{1}{i+\eta} - \frac{1}{i+\eta+\frac{2}{3}}\right) < 0.$$

By comparing this inequality with (5.25), we conclude that $\frac{\mathrm{d}}{\mathrm{d}\eta}\mathcal{A}^{\mathcal{F}}_{\mathrm{GMVF}} < 0$. So we infer that $\mathcal{A}^{\mathcal{F}}_{\mathrm{GMVF}}$ is a decreasing function with respect to η. So the optimal solution is determined by maximizing η and the proof is complete. □

This result resembles the one of the generalized moving average filter. Simply, we only need to consider the filter configurations that satisfy $\sum_{i=0}^{N-1}\theta_i = 1$. Then, $\sum_{i=0}^{N-1}\theta_i^2$ can be served as the performance index for the corresponding generalized moving variance filter.

Remark 10 *The result of this theorem (in addition to determining the optimal solution) gives a compact form for the impact of filter coefficients on the alarm performance of GMVF filters. So it can be combined with other performance indices (such as alarm detection delay) or design criteria, to find the optimal filter under different circumstances.*

Remark 11 *It is worth noting that although we started by assuming that the statistical parameters of raw data are known, eventually, we relaxed this assumption. Therefore, provided that the raw data follows Gaussian distributions, optimal parameters for both GMAF and GMVF can be determined regardless of the statistical parameters.*

Remark 12 *An important advantage of the generalized filter over the conventional version is that allows for a lower detection delay, since the θ_i's can be different. The rationale is that by assigning greater weights to the more recent samples of the raw data, the effect of abnormality will appear earlier in the filtered data. This will also be illustrated in the case study. However, an analytical comparison of the detection delays relies on multivariate Gamma CDF analysis and is beyond the scope of this work.*

5.4 Implementation Notes

This section provides suggestions and discussions regarding the application of the proposed filters in the real process industry to detect an abnormality. To predict the filter performance we need to have an estimate of the mean and variance of the process variables. Thus we need some historical data with sufficient length that can represent the statistical feature of the process variables in both operation modes (namely, normal and abnormal modes). Label the historical data as $x_{\rm n}[k],\ k \in \{1, \cdots, l_{\rm n}\}$ and $x_{\rm ab}[k],\ k \in \{1, \cdots, l_{\rm ab}\}$ for the normal and abnormal operation modes, respectively. An estimation for mean values can be found as

$$\hat{\mu}_{x,{\rm n}} = \frac{1}{l_{\rm n}} \sum_{k=1}^{l_{\rm n}} x_{\rm n}[k], \quad \hat{\mu}_{x,{\rm ab}} = \frac{1}{l_{\rm ab}} \sum_{k=1}^{l_{\rm ab}} x_{\rm ab}[k],$$

and for variances as

$$\hat{\sigma}^2_{x,{\rm n}} = \frac{1}{l_{\rm n}} \sum_{k=1}^{l_{\rm n}} (x[k] - \hat{\mu}_{x,{\rm n}})^2, \quad \hat{\sigma}^2_{x,{\rm ab}} = \frac{1}{l_{\rm ab}} \sum_{k=1}^{l_{\rm ab}} (x[k] - \hat{\mu}_{x,{\rm ab}})^2.$$

The most common type of abnormality is when the operating condition of a process deviates from a steady state to a new one. This abnormality can be

captured as a shift in the mean of a process measurement from $\hat{\mu}_{\rm n}$ to $\hat{\mu}_{\rm ab}$. Here, a generalized moving average filter can be used to detect the deviation from the normal operating mode. According to (5.11), the lower $\frac{\hat{\sigma}^2_{x,\rm ab}+\hat{\sigma}^2_{x,\rm n}}{(\hat{\mu}_{x,\rm ab}-\hat{\mu}_{x,\rm n})^2}$ is, the more precise the detection is. In some other types of faults, the abnormality only becomes noticeable as a change in the variance of some process variables. More specifically, the statistical properties of the historical data is such that $\hat{\mu}_{\rm n} \approx \hat{\mu}_{\rm ab}$ and $\hat{\sigma}^2_{\rm n} \neq \hat{\sigma}^2_{\rm ab}$. This category of abnormalities can not be distinguished by a moving average filter (neither by the conventional nor the generalized one). Under this circumstance, one can utilize a generalized moving variance filter to detect the abnormality. Here, according to (5.23), the lower $\frac{\hat{\sigma}^{\frac{4}{3}}_{x,\rm ab}+\hat{\sigma}^{\frac{4}{3}}_{x,\rm n}}{\left(\hat{\sigma}^{\frac{2}{3}}_{x,\rm ab}-\hat{\sigma}^{\frac{2}{3}}_{x,\rm n}\right)^2}$ is, the more precise the detection is.

Another important point about applying generalized moving variance filters in real industrial application is regarding the parameter μ_x in the filter equation in (5.14). This parameter refers to the base case value (or operation point) of the process variable. Generally, this value is constant and can be determined from the historical knowledge of the plant. However, in particular cases, this value is changing or it is not precisely known. So we need to have an online estimation of it which can be done by utilizing a moving average filter. In this case, the filter equation in (5.14) is turned to

$$y[k] = \sum_{i=0}^{N-1} \theta_i \Big(x[k-i] - \frac{1}{N} \sum_{i=0}^{N-1} x[k-i] \Big)^2, \ k = N, N+1, \cdots .$$

Nowadays, most modern industries are equipped with distributed control systems (DCS) and supervisory control and data acquisition (SCADA). Monitoring and alarm systems with various configurations for alarm filtering are integrated into these systems. After obtaining the suitable filter type and configuration based on the historical information of the process variable, the corresponding alarm filter can be modified accordingly.

5.5 Case Studies

In this section, numerical and industrial case studies are conducted for generalized moving variance filters. Generalized moving average filters are relatively

Table 5.1: Simulation scenarios of GMVF

Scenario	**Filter weights**
1	all set to 1 (conventional moving variance filter)
2	follow an arithmetic sequence which initial term and common difference are set 1 and $1/N$, respectively
3	randomly generated numbers

straightforward and are neglected here.

5.5.1 Case I: Numerical Case Study

Suppose that $x[k]$'s are identically distributed; and follow $\mathcal{N}(0,1)$ and $\mathcal{N}(0,2)$ in normal and abnormal operation modes, respectively. We apply the generalized moving variance filter (see the equation in (5.14)) on samples of $x[k]$. Consider that the filter weights are assigned according to the scenarios given by Table 5.1 for various filter orders. Fig. 5.1 shows the approximation of AUC that is calculated analytically and the one that is obtained based on Monte Carlo simulation. As expected, the approximation error tends to vanish for higher filter length. It can also be verified by this figure that for specific filter orders in Scenario 3, the approximation error is relatively higher. This is because the θ_i's are generated randomly and for those ones, $\theta_{\max} - \theta_{\min}$ is greater.

Now we compare our method with the approaches proposed by [26] and [17]. Ref. [26] introduced the conventional moving average filter, which can be thought of as a special case of the method proposed in this chapter. In [17] the authors used the Kantorovich distance which has a relatively higher computation cost in comparison with our method and the one in [26]. The simulation results are labeled as KD, MVF and GMVF which correspond to [26], [17] and our method, respectively. We configure the filters based on the above papers. The KD method has two parameters, m, which is the number of segments, and k, which is the number of samples in each segment. For the simulation we set $m = 3$ and $k = 2$. Furthermore, the MVF filter is of order 4 and the GMVF is of order 5 (see the second case study for more details about

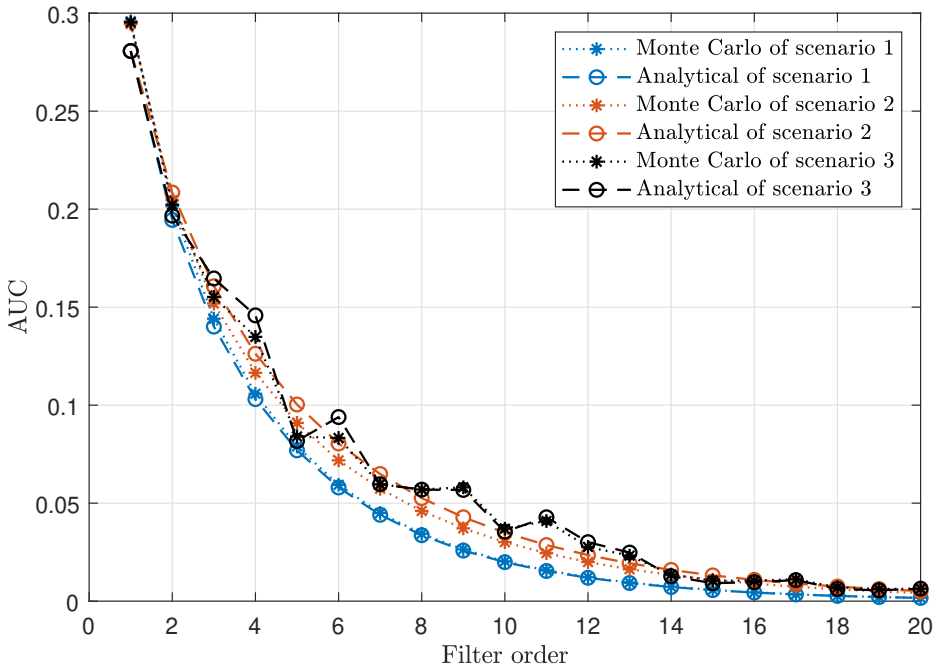

Figure 5.1: Comparison of the AUC that is evaluated analytically, and the AUC that is determined by Monte Carlo simulation.

these choices). The samples of raw data follow $\mathcal{N}(0,1)$ and $\mathcal{N}(0,2)$ in the normal and abnormal operation modes, respectively. Output amplitudes of each filter are normalized by the maximum values of the corresponding time trends. Fig. 5.2 shows that the ROC curve corresponding to our proposed method is closer to the origin, especially for the points that satisfy FAR $\approx$ MAR. From Fig. 5.3 we can observe how the summation of the rates of false and missed alarms change for various alarm trip-points. As shown in this figure, the proposed method results in better performance. We also need to check how fast are these three methods for detecting an abnormality. Thus we conduct Monte Carlo simulation to evaluate the average detection delays for various alarm trip-points. The result of this simulation is shown in Fig. 5.4. To interpret this plot we need to use the information of Fig. 5.3. To compare the detection delays of these methods, it is important to note that the best performance achieved by a lower trip-point in MVF and GMVF (according to Fig. 5.3). However, in the KD method, the optimal point can be achieved

Table 5.2: Comparison of accuracy for different constraints on average detection delay.

Method	FAR+MAR	Average detection delay
KD	0.40	< 1
MVF	0.55	
GMVF	0.45	
KD	0.39	< 2
MVF	0.41	
GMVF	0.36	

by setting a greater alarm trip-point. To make the comparison we study two design scenarios. In the first one, it is considered that the average detection delay should be less than 1 sample. For the second scenario, we relax this constraint to 2 samples. The solid red lines in Fig. 5.4 show these constraints; and the dotted black lines show the highest possible trip-point to guarantee the bounds for average detection delay. By utilizing this information, one can exploit Fig. 5.3 to judge the accuracy and swiftness of all these three methods. The summary of this comparison is given in Table 5.2. According to this table, for the tighter constraint on detection delays (i.e., less than 1), the KD method is a better choice. However, by slightly relaxing this constraint, the proposed method outperforms the others. It is also worth noting that in real industrial applications, the plant operators prefer (and need) to have a comprehensive intuition about the meaning of the filtered data with respect to their knowledge of the process. However, unlike MVF and GMVF methods, the KD method is a transformation where at each step a linear programming problem is solved; so the intuitive connection of the raw data and the filtered data is missing.

5.5.2 Case II: Study of the Tennessee Eastman process

The Tennessee Eastman Process (TEP) is a realistic industrial benchmark for evaluating process diagnosis and control methods [34]. There are five major units in the process: condenser, separator, reactor, stripper, and compressor.

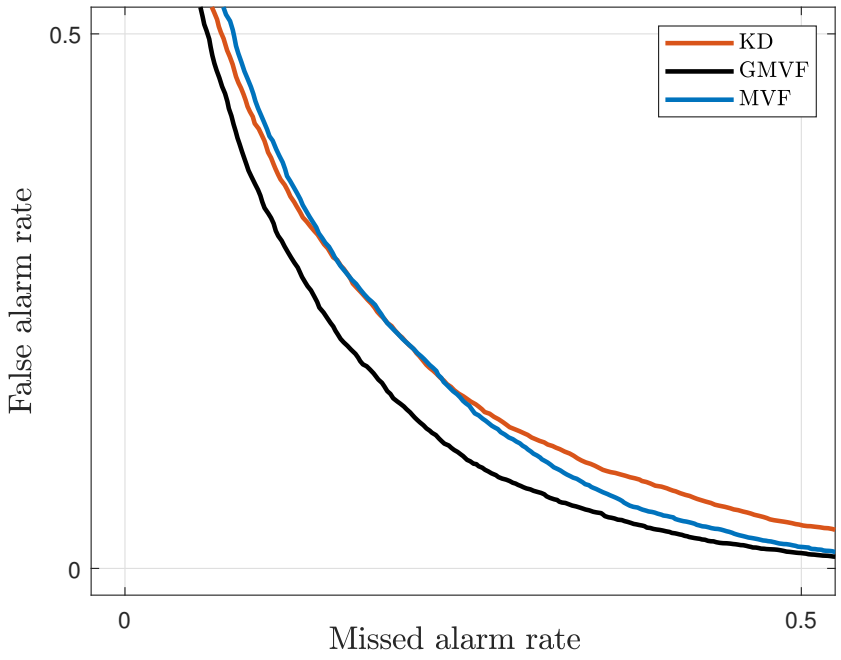

Figure 5.2: ROC curves of three different methods.

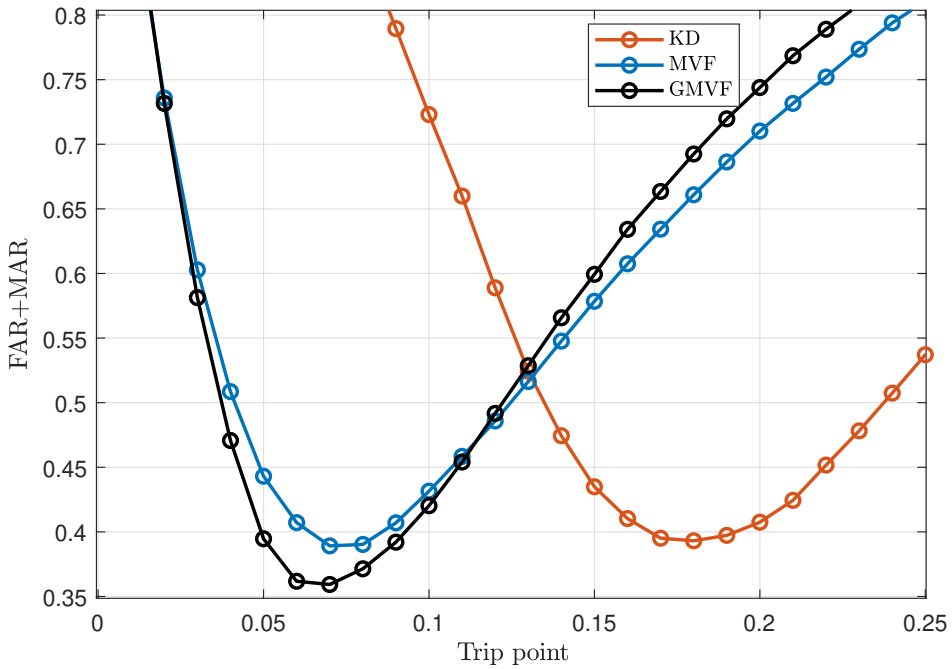

Figure 5.3: Comparison of accuracy in terms of FAR+MAR for various alarm trip-points.

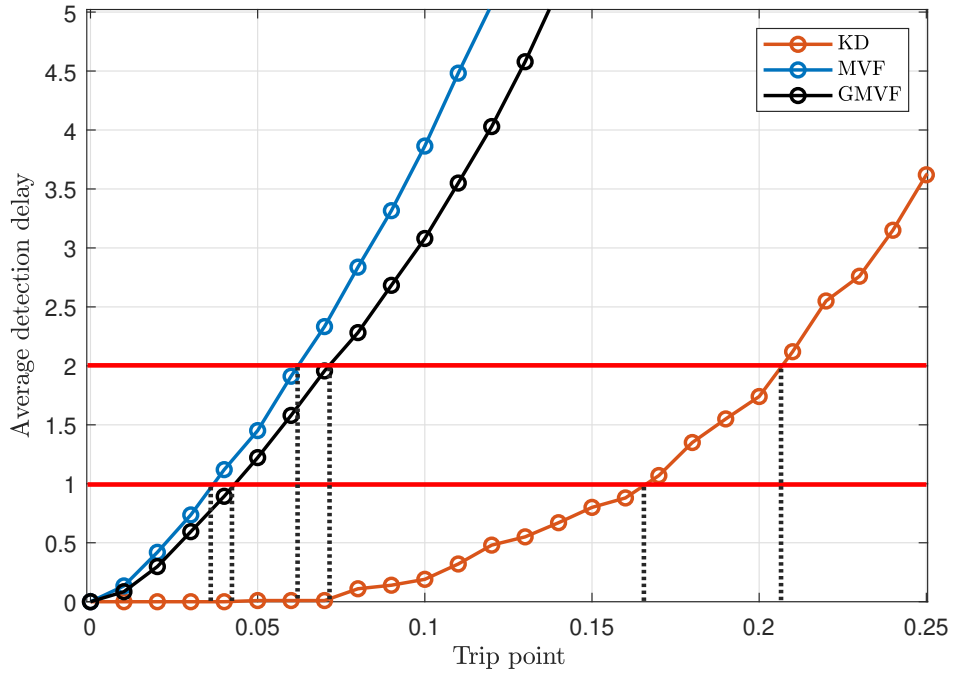

Figure 5.4: Comparison of average detection delays for various alarm trip-points. Solid red lines show the constraints on detection delays and dotted black lines indicate the corresponding bound on trip-point to achieve the appropriate detection delay.

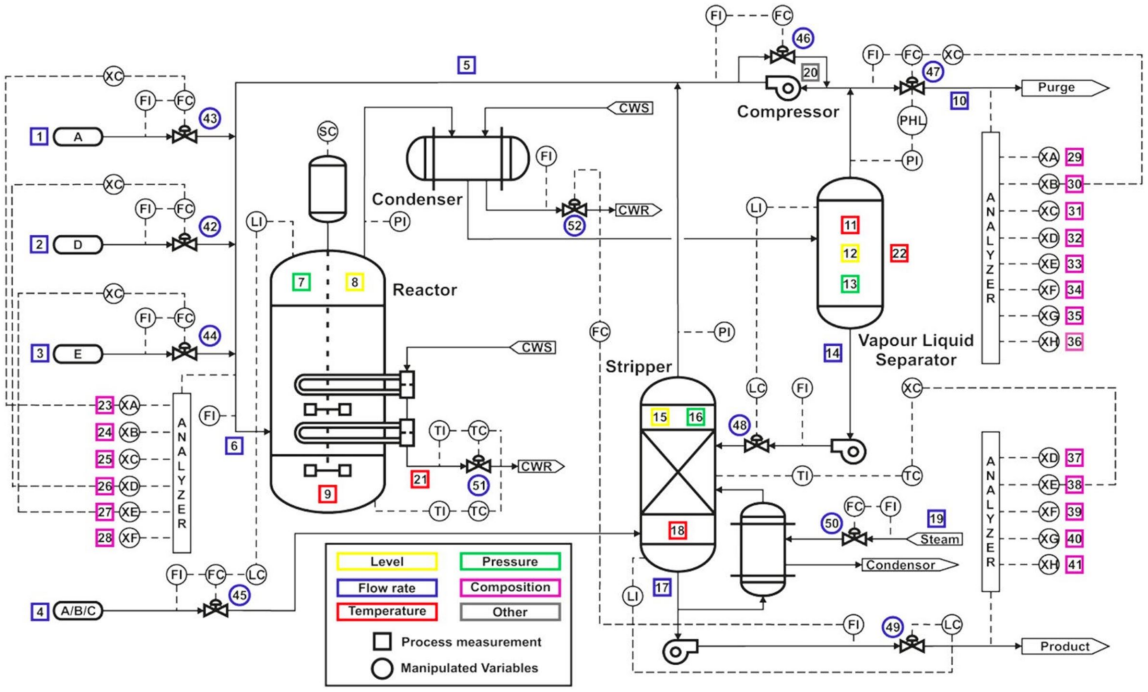

Figure 5.5: A diagram of the Tennessee Eastman process [4].

The details of the process are shown in Fig. 5.5. The process that used here is operating under closed-loop control. There are 15 known faults introduced in the TEP (represented as IDV (1)-(15)) where 12 types are corresponding to mean change (step) and variance change (random variation). Table 6.1 shows the details of these 12 faults. Generalized moving average and moving variance filters can be used to detect step change and random variation faults, respectively. According to this table, providing an analytical method for detecting random variation faults has the same degree of importance as for step faults. There are 41 measurements (namely, XMEAS (1)-(41)) available from the process; and 22 of them (namely, XMEAS (1)-(22)), are sampled with interval of 3 (min) that are listed in Table 5.4. The rest of measurements are sampled with some slower rates which may cause larger detection delays; so we only consider XMEAS (1)-(22). We study the fault corresponding to the condenser cooling water inlet temperature, which is represented as IDV (12). To detect the fault, we use the condenser coolant temperature (namely, XMEAS (22)). The base case value is given as 77.297 which remained unchanged even when an abnormality occurred. This base case value can also be substituted

Table 5.3: Fault descriptions of the Tennessee Eastman process.

Fault number	**Process variable**	**Type**
IDV (1)	A/C feed ratio, B composition constant	Step
IDV (2)	B composition, A/C ratio constant	
IDV (3)	D feed temperature	
IDV (4)	Reactor cooling water inlet temperature	
IDV (5)	Condenser cooling water inlet temperature	
IDV (6)	A feed loss	
IDV (7)	C header pressure loss-reduced availability	
IDV (8)	A, B, and C feed composition	Random variation
IDV (9)	D feed temperature	
IDV (10)	C feed temperature	
IDV (11)	Reactor cooling water inlet temperature	
IDV (12)	Condenser cooling water inlet temperature	

for μ_x in the generalized moving variance filter (see the equation in (5.14)). Even if this base case value is not available, a moving average filter can be used to estimate mean of the process variable. Fig. 5.6 shows the raw data and its distributions in normal and abnormal operation modes. Fig. 5.7 and Fig. 5.8 show the simulation results for two different filters with randomly selected coefficients and filter orders 2 and 12, respectively. Now we can compare the ROC curves using the analytical formulation proposed in (5.22) and Monte Carlo simulation which are shown in Fig. 5.9 and Fig. 5.10 for filter orders 2 and 12, respectively. There is a slight difference between the analytical results and the simulations. The reason is that the samples of raw data are not independent and do not precisely follow a Gaussian distribution in the abnormal operation mode. To verify if the raw data follows a Gaussian distribution, we use the Lilliefors test [65], which is developed based on the Kolmogorov-Smirnov test. The null hypothesis is that the data comes from a normally distributed data set. The raw data corresponding to the normal operation mode does not reject the null hypothesis at a 5% significance level. However, for the abnormal operation mode, it rejects the null hypothesis at the same significance level. This is the first source of error for the analysis.

Table 5.4: Process measurements of Tennessee Eastman process (measurements corresponding to flow rate, temperature, level, and pressure are indicated by blue, red, yellow, and green colors, respectively).

Variable number	**Variable name**	**Base case value (unit)**
XMEAS (1)	A feed rate	0.2505 (kscmh)
XMEAS (2)	D feed rate	3664.0 (kg h^{-1})
XMEAS (3)	E feed rate	4509.3 (kg h^{-1})
XMEAS (4)	A and C feed rate	9.3477 (kscmh)
XMEAS (5)	Recycle flow rate	26.902 (kscmh)
XMEAS (6)	Reactor feed rate	42.339 (kscmh)
XMEAS (7)	Reactor pressure	2705.0 (kPa gauge)
XMEAS (8)	Reactor level	75.000 (%)
XMEAS (9)	Reactor temperature	120.40 (°C)
XMEAS (10)	Purge rate	0.3371 (kscmh)
XMEAS (11)	Separator temperature	80.109 (°C)
XMEAS (12)	Separator level	50.000 (kPa gauge)
XMEAS (13)	Separator pressure	2633.7 (kPa gauge)
XMEAS (14)	Separator underflow	25.160 (m^3 h^{-1})
XMEAS (15)	Stripper level	50.000 (%)
XMEAS (16)	Stripper pressure	3102.2 (kPa gauge)
XMEAS (17)	Stripper underflow	22.949 (m^3 h^{-1})
XMEAS (18)	Stripper temperature	65.731 (°C)
XMEAS (19)	Steam flow rate	230.31 (kg h^{-1})
XMEAS (20)	Compressor work	341.43 (kw)
XMEAS (21)	Reactor coolant temperature	94.599 (°C)
XMEAS (22)	Condenser coolant temperature	77.297 (°C)

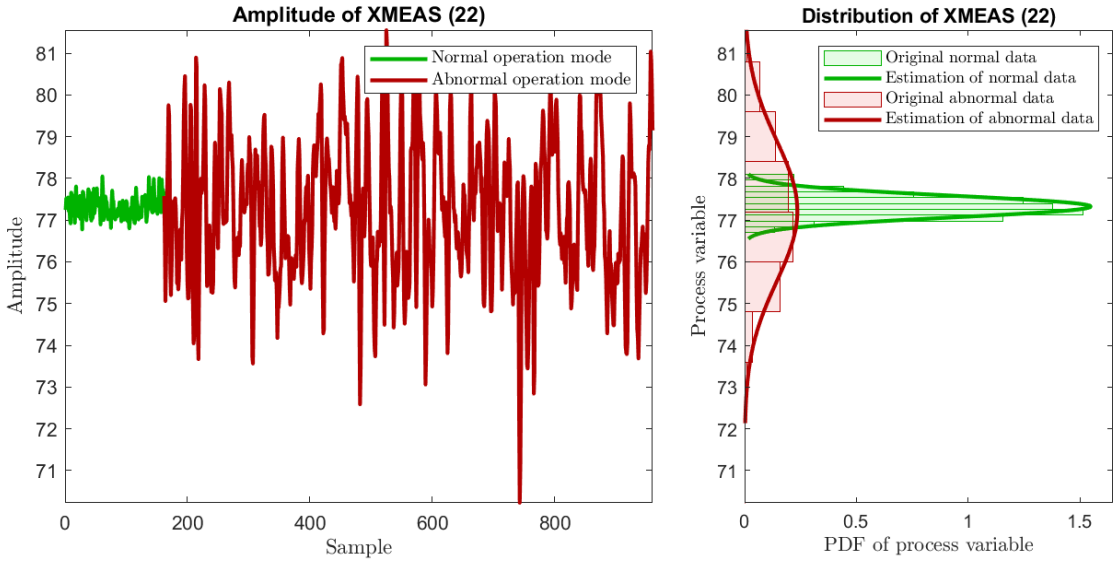

Figure 5.6: Raw data of XMEAS (22).

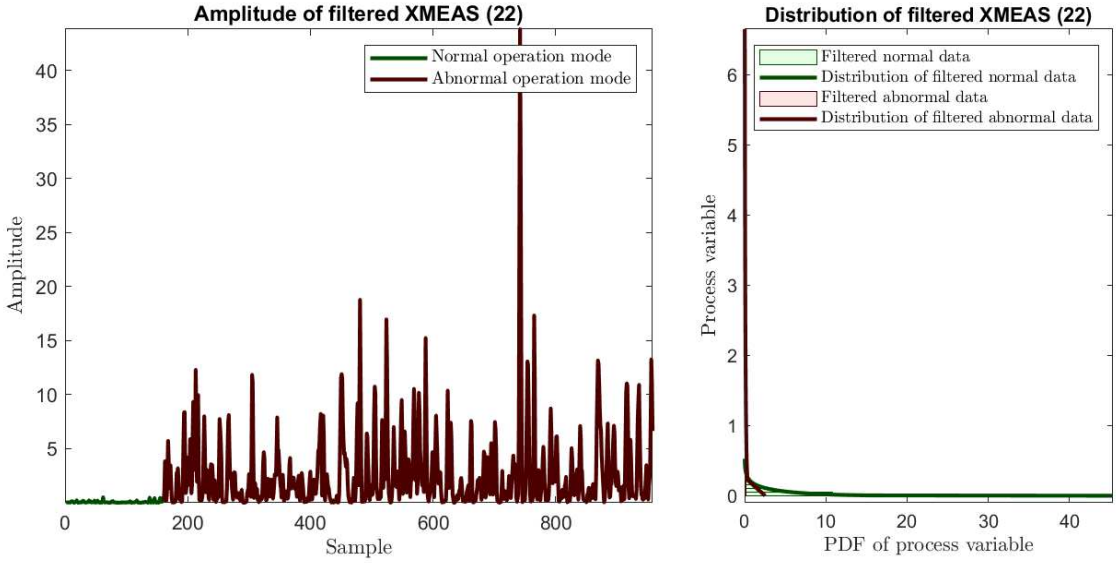

Figure 5.7: Filtered data and its distribution corresponding to XMEAS (22), considering random filter coefficients where $N = 2$.

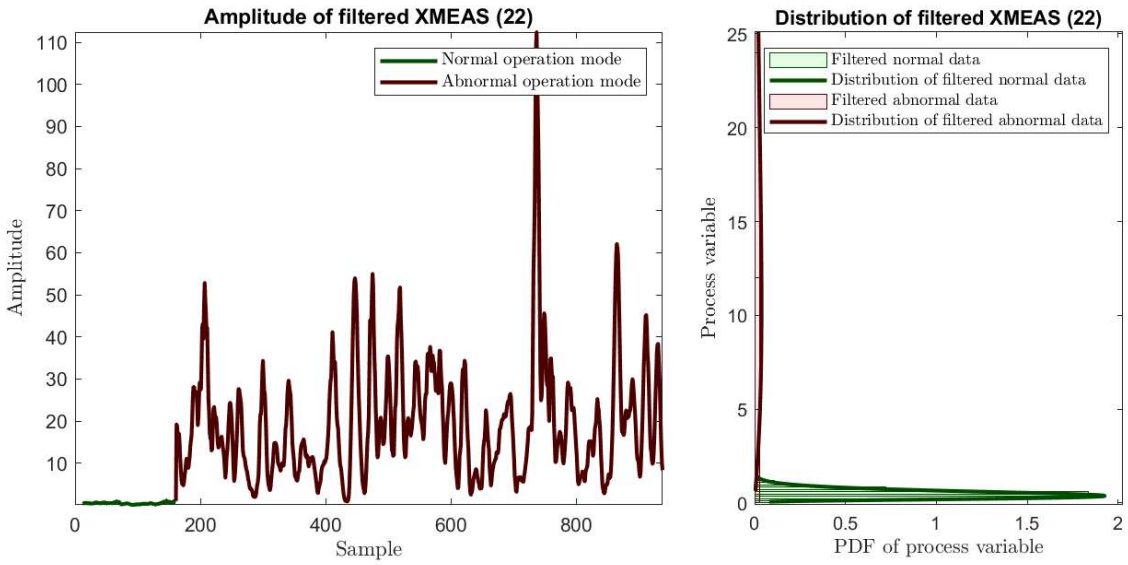

Figure 5.8: Filtered data and its distribution corresponding to XMEAS (22), considering random filter coefficients where $N = 12$.

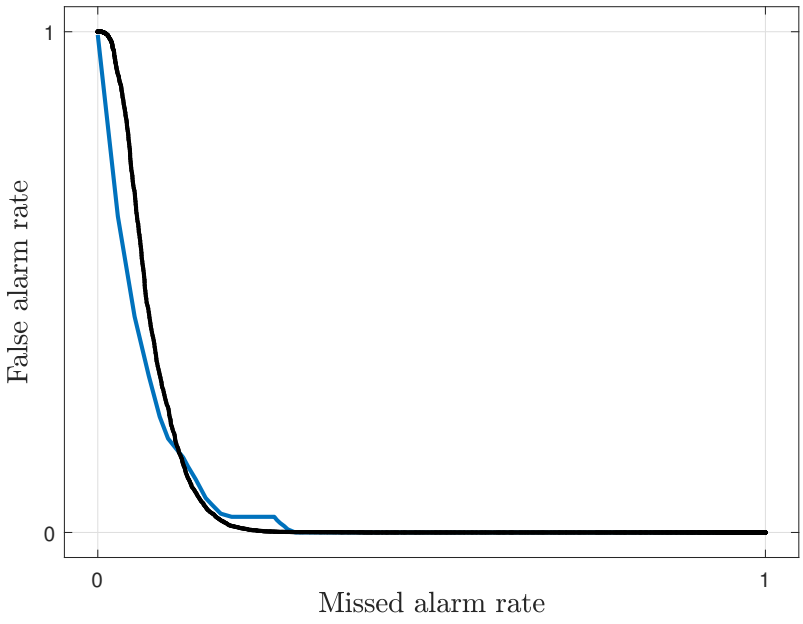

Figure 5.9: Original ROC (blue) and analytically evaluated ROC (black) of filtered data XMEAS (22), considering random coefficients where $N = 2$.

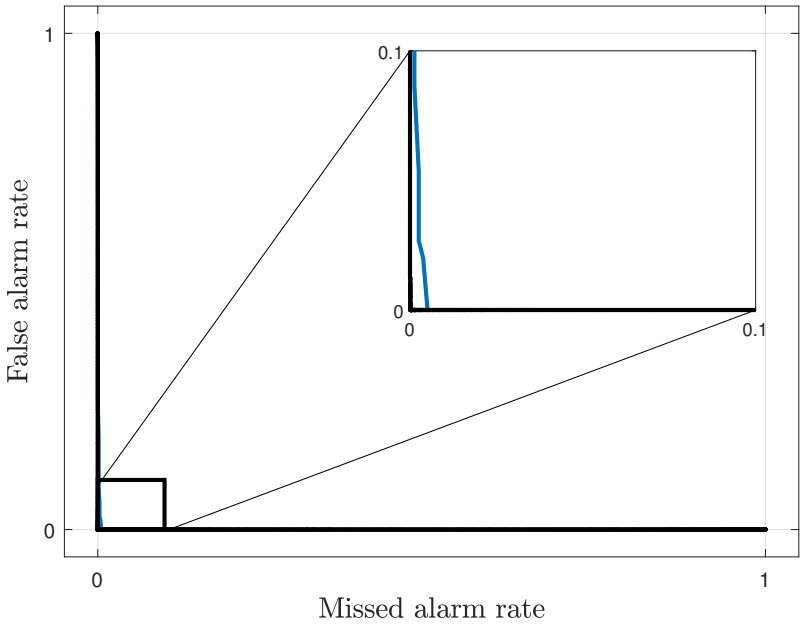

Figure 5.10: Original ROC (blue) and analytically evaluated ROC (black) of filtered data XMEAS (22), considering random coefficients where $N = 12$.

The second source is that the samples of raw data are coming from a plant and are not independent, hence the samples corresponding to each Gamma distribution in (5.17) are not independent and the approximation in (5.18) gives rise to more errors under this circumstance.

Now we apply the conventional and the generalized moving variance filters on data-set XMEAS (22) to exam the accuracy and swiftness of these filters for different configurations. For a fair comparison, similar orders are considered for both types of filters. Let Θ_4 and Θ_5 (resp. Θ'_4 and Θ'_5) denote the set of coefficients for the conventional (resp. generalized) filter of order 4 and 5, respectively. So for the conventional one we have $\Theta_4 = \{0.25, 0.25, 0.25, 0.25\}$ and $\Theta_5 = \{0.2, 0.2, 0.2, 0.2, 0.2\}$, but we need to obtain the coefficients for the generalized filters considering the filter swiftness and accuracy. As it is computationally infeasible to calculate detection delay for all combinations of filter coefficients, we limit our search domain to the combinations that follow a geometric series. So we consider $\Theta'_{(N,r)} = \{a, ar, ar^2, \cdots, ar^{N-1}\}$ where a is the start term and r is the common ratio. We want the coefficients summation to be 1 so we set $a = \frac{1-r}{1-r^N}$. Furthermore, we are specifically interested in the

generalized filters of order N which yield better accuracy than the conventional filter of order $N-1$. Thus, by applying Theorem 5.3.1 we conclude that r should satisfy

$$\sum_{i=1}^{N}\left(\frac{1-r}{1-r^N}r^{i-1}\right)^2=\frac{(r-1)(r^N+1)}{(r+1)(r^N-1)}<\frac{1}{N-1}.$$

For $N=4$ and $N=5$, we obtain $0.58<r<1$ and $0.69<r<1$, respectively ($r=1$ corresponds to the conventional filter). We know that if the coefficients associated with the recent samples of the process variable are larger than the rest, the detection can be done faster. So, the smaller the parameter r (where $0<r<1$) is, the smaller the detection delay is. Considering the lower bound for each case, we determine

$$\Theta'_{(4,0.58)}=\{0.474,0.275,0.159,0.092\},$$
$$\Theta'_{(5,0.69)}=\{0.367,0.254,0.175,0.121,0.083\}.$$

Expectedly, each of these generalized filters of order N provides the same level of accuracy as the corresponding conventional filter of order $N-1$ and at the same time results in a smaller detection delay. This result is confirmed by Fig. 5.11 which shows the ROC curves of the filtered versions of XMEAS (22). So one can conclude that here, the most accurate filter is the conventional filter of order 5, then the generalized filter of order 5, following by the conventional filter of order 4, and the worst one is the generalized filter of order 4. Now we need to investigate the swiftness of the filters in detecting the abnormality. We expect that the generalized filters detect the abnormality faster in comparison with the conventional ones. This is because in Θ'_4 and Θ'_5, the coefficients corresponding to the more recent versions of the process variable are greater than the others. By conducting Monte Carlo simulation we obtain the average detection delays corresponding to $N\in\{4,5\}$ and various r which are shown in Fig. 5.12. In this figure, the shaded blue area indicates the detection delay of generalized filters of order 5 which yields better accuracy than the conventional filter of order 4 (i.e. when $0.69<r<1$). A similar statement holds for the generalized filters of order 4 (i.e. $0.58<r<1$) which correspond to the

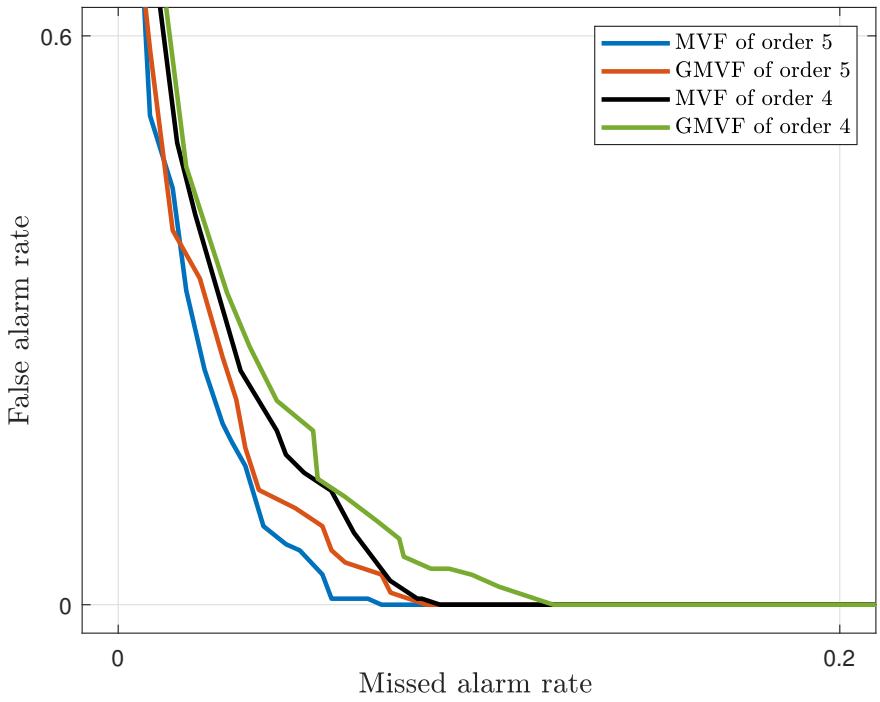

Figure 5.11: Comparison of ROC curves for two conventional and two generalized moving variance filters.

shaded green area. This figure also confirms that for both cases, the selected generalized filters result in the smallest detection delay among the filters with their coefficients forming a geometric series. In conclusion, although the conventional filter of order 5 is the best choice considering detection accuracy, it is the worst candidate with respect to detection delay. Furthermore, by investigating this figure, we conclude that the best filter in terms of swiftness is the generalized one of order 4 and then the same type of order 5. In real applications, a compromise must be made between the accuracy and the swiftness of filters. So taking both concerns into account, the generalized filter of order 5 is superior to the other ones as it is the second-best candidate with respect to accuracy and also has the second-best rank in swiftness. In other words, the accuracy level of the generalized filter of order 5 falls between the conventional filters of orders 4 and 5. Nonetheless, the detection delay of this filter is better than both of them.

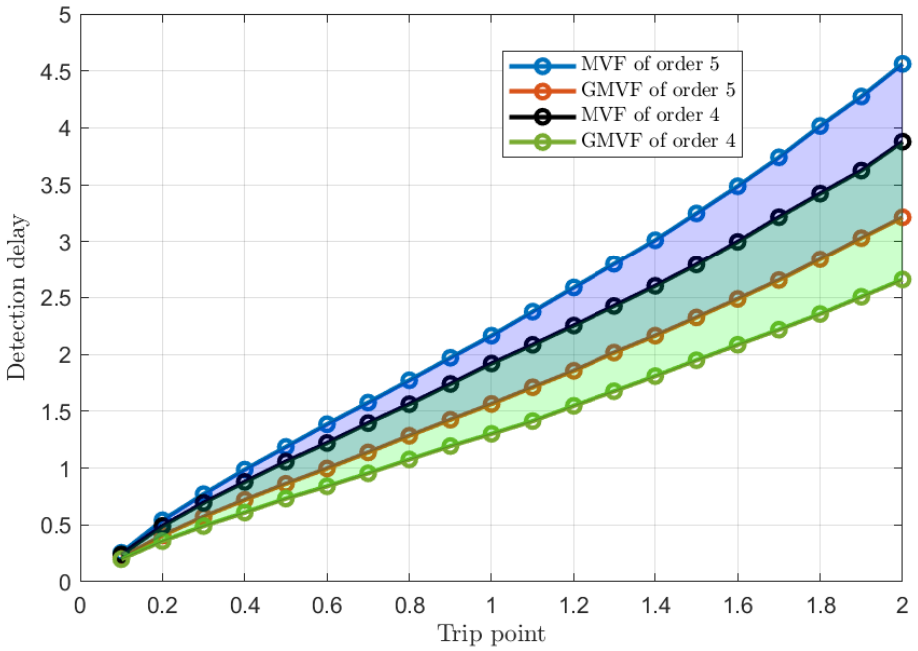

Figure 5.12: Comparison of average detection delays for conventional and generalized moving variance filters.

5.6 Summary

In this chapter, optimal alarm filter analysis and design are addressed for detecting mean and variance changes. First, the method is employed for generalized moving average filters. Then, a Gaussian approximation is derived for the output of moving variance filters. Based on this approximation, an explicit relationship of filter parameters and the optimal solution is provided. Although moving average and variance filters are structurally different, it is illustrated that a similar solution can be found for determining optimal coefficients for the filters. We also derived a formulation for the impact of statistical parameters of raw data on the performance of filtering. Furthermore, we proposed a method to estimate the ROC curves corresponding to the filtered data. The effectiveness of the method is verified by conducting simulation and a case study of the Tennessee Eastman process. Our filter is designed for stationary processes. The extension to non-stationary processes is left as future work. Similar to the existing methods in the literature in [95], one may approach

this problem by assuming a time-series model for the system.

Chapter 6

Performance Assessment and Design of Quadratic Alarm Filters

In the previous chapters we have studied the moving average and moving variance filters. We saw that a moving average (resp. moving variance) filter can detect mean (resp. variance) changes, but it can not be used to detect variance (resp. mean) changes. However, a quadratic filter can be used to detect both types of changes. Although this remarkable feature of quadratic filters has been addressed in the literature, no explicit performance analysis is performed yet. So, deriving an analytical solution for quadratic filters is of paramount importance. To this aim, we propose an analytical method for performance assessment and design of quadratic filters. On the other side, in industrial applications, many process variables are acquired. So one challenge is to identify the process variable that provides the best alarm performance after filtering. We will derive an analytical solution to this problem. Furthermore, we will prove that this optimal solution is a function of the statistical feature of historical data and alarm filter structure.

6.1 Problem Formulation

Let $x[k], k \in \{0, 1, 2, \cdots\}$, indicate a process variable that is measured in a plant. Suppose that samples of this process variable are independent, identi-

cally distributed and follow

$$\mathcal{X} \sim \begin{cases} \mathcal{N}(\mu_{x,\mathrm{n}}, \sigma^2_{x,\mathrm{n}}), & k < T_{ab}, \\ \mathcal{N}(\mu_{x,\mathrm{ab}}, \sigma^2_{x,\mathrm{ab}}), & k \geq T_{ab}, \end{cases} \tag{6.1}$$

where T_{ab} corresponds to the time of abnormality occurrence, $\sigma^2_{x,\mathrm{ab}}$ (resp. $\mu_{x,\mathrm{ab}}$) and $\sigma^2_{x,\mathrm{n}}$ (resp. $\mu_{x,\mathrm{n}}$) are corresponding to the variance (resp. mean) of x in abnormal and normal operation modes, respectively. Now let $y[k], k \in \{0, 1, 2, \cdots\}$, denote the output samples of a quadratic alarm filter. The formulation of a general quadratic filter of order N (see [26]) is given by

$$y[k] = \boldsymbol{x} Q \boldsymbol{x}^T, \tag{6.2}$$

where Q is a symmetric matrix and

$$\boldsymbol{x} \triangleq \big[x[k] \cdots x[k-N+1]\ 1\big].$$

The alarm system decides whether to raise an alarm or not based on what follows:

$$\begin{cases} \text{alarm}, & y[k] > y_{\mathrm{tp}}; \\ \text{no alarm}, & \text{otherwise}, \end{cases}$$

where y_{tp} indicates the alarm trip-point which is designed by the operator using the historical information of the plant. Based on the results of Chapter 2, we define the alarm performance index as

$$\mathcal{A}(y) \triangleq \frac{\sigma^2_{y,\mathrm{ab}} + \sigma^2_{y,\mathrm{n}}}{(\mu_{y,\mathrm{ab}} - \mu_{y,\mathrm{n}})^2}, \tag{6.3}$$

where $\sigma^2_{y,\mathrm{ab}}$ (resp. $\mu_{y,\mathrm{ab}}$) and $\sigma^2_{y,\mathrm{n}}$ (resp. $\mu_{y,\mathrm{n}}$) are corresponding to the variance (resp. mean) of y in abnormal and normal operation modes, respectively. A smaller index represents a better distinguishability of normal and abnormal operation modes. Intuitively, when the mean difference of abnormal and normal modes is large, and variance of each mode is small, it is easier to separate these two modes by using a constant trip-point. The following lemma holds for the introduced alarm index.

Lemma 6.1.1 *Suppose that $\mathcal{A}(y)$, $\mathcal{A}(y_c)$ and $\mathcal{A}(y_m)$ are associated with $y[k]$, $y[k] + c$ and $my[k]$ where $c \in \mathbb{R}$ and $m \in \mathbb{R} - \{0\}$ are known and constant. It follows that*

$$\mathcal{A}(y) = \mathcal{A}(y_c) = \mathcal{A}(y_m). \tag{6.4}$$

Proof. *The proof is straightforward from the definition of the alarm index.* □

Intuitively, if a constant value is multiplied by, or added to, a process variable, the trip-point can be modified accordingly to compensate it. According to Lemma 6.1.1, without loss of generality, we can fix the upper-left and lower-right elements of Q to 1 and 0, respectively. Now we impose some constraints on the structure of filters and study two special cases.

6.1.1 Case I: Diagonal Q

Suppose that the matrix Q has the following structure

$$Q = \begin{bmatrix} Q_1 & 0 \\ 0 & 0 \end{bmatrix}.$$

Here, Q_1 is a diagonal matrix and defined as

$$Q_1 = \begin{bmatrix} 1 & 0 & \cdots & 0 \\ 0 & q_1 & \ddots & \vdots \\ \vdots & \ddots & \ddots & 0 \\ 0 & \dots & 0 & q_{N-1} \end{bmatrix}, \tag{6.5}$$

where q_i's are non-negative weights. In this case, the filter can be reformulated as

$$y[k] = x^2[k] + \sum_{i=1}^{N-1} q_i x^2[k-i].$$

For this problem, our goal is to evaluate $\mathcal{A}(y)$, given the statistical information of x.

6.1.2 Case II: a More General Case

Inspired by [26] we assume the following structure for Q:

$$Q_2 = \begin{bmatrix} 1 & 0 & \cdots & 0 & \alpha_0 \\ 0 & q_1 & \ddots & \vdots & \alpha_1 q_1 \\ \vdots & \ddots & \ddots & 0 & \vdots \\ 0 & \dots & 0 & q_{N-1} & \alpha_{N-1} q_{N-1} \\ \alpha_0 & \alpha_1 q_1 & \dots & \alpha_{N-1} q_{N-1} & 0 \end{bmatrix}. \tag{6.6}$$

Considering this expression, one may rewrite the filter equation as

$$y'[k] = (x[k] + \alpha_0)^2 + \sum_{i=1}^{N-1} q_i (x[k-i] + \alpha_i)^2 + c,$$

where $c = -\Big(\alpha_0^2 + \sum_{i=1}^{N-1} \alpha_i^2 q_i\Big)$. It is worth noting that c does not affect the alarm performance of filter (see Lemma 6.1.1) and can be discarded in further analysis. Now the problem is to find an explicit expression for $\mathcal{A}(y')$.

6.2 Performance Assessment of Case I

For this problem, the filter can be rewritten as $\boldsymbol{x}_1 Q_1 \boldsymbol{x}_1^T$, where

$$\boldsymbol{x}_1 \triangleq \big[x[k] \cdots x[k-N+1]\big]. \tag{6.7}$$

To evaluate the alarm performance index, we first need the following lemma, which is introduced by [76].

Lemma 6.2.1 *Consider the quadratic form $P_1(\boldsymbol{x}_1) = \boldsymbol{x}_1 Q_1 \boldsymbol{x}_1^T$, where Q_1 is a symmetric matrix and $\mathcal{X}_1 \sim \mathcal{N}(\boldsymbol{\mu}, \Sigma)$, where Σ is a positive definite matrix. The r^{th} moment of $P_1(\boldsymbol{x}_1)$ for $r \in \{1, 2\}$ is expressed as*

$$\mathbb{E}(P_1(\boldsymbol{x}_1))^r = \sum_{r_1=0}^{r-1} \binom{r-1}{r_1} g^{(r-1-r_1)} \sum_{r_2=0}^{r_1-1} \binom{r_1-1}{r_2} g^{(r_1-1-r_2)}, \tag{6.8}$$

where

$$g^{(j)} = 2^j j! \big(tr(Q_1\Sigma)^{j+1} + (j+1)\boldsymbol{\mu}(Q_1\Sigma)^j Q \boldsymbol{\mu}^T\big),$$

for $j \in \{0, 1, 2, \cdots\}$.

By using this lemma, the mean and variance of $P_1(\boldsymbol{x}_1)$ is determined as

$$\begin{aligned} \mathbb{E}(P_1(\boldsymbol{x}_1)) &= \binom{0}{0} g^{(0)} \\ &= \mathrm{tr}(Q_1\Sigma) + \boldsymbol{\mu} Q_1 \boldsymbol{\mu}^T, \end{aligned} \tag{6.9}$$

and

$$\begin{aligned} \mathrm{Var}(P_1(\boldsymbol{x}_1)) &= \mathbb{E}(P_1(\boldsymbol{x}_1))^2 - \big(\mathbb{E}(P_1(\boldsymbol{x}_1))\big)^2 \\ &= \left(\binom{1}{0} g^{(1)} + \binom{1}{1} \big(g^{(0)}\big)^2\right) - \binom{0}{0} \big(g^{(0)}\big)^2 \\ &= 2\mathrm{tr}(Q_1\Sigma)^2 + 4\boldsymbol{\mu} Q_1 \Sigma Q_1 \boldsymbol{\mu}^T. \end{aligned} \tag{6.10}$$

According to the equation in (6.1), it follows that

$$\Sigma_{\boldsymbol{x}_1,\mathrm{n}} = \sigma^2_{x_n} I_N,$$

$$\Sigma_{\boldsymbol{x}_1,\mathrm{ab}} = \sigma^2_{x,\mathrm{ab}} I_N,$$

where $\Sigma_{\boldsymbol{x}_1,\mathrm{n}}$ and $\Sigma_{\boldsymbol{x}_1,\mathrm{ab}}$ are corresponding to the normal and abnormal operation modes, respectively, and I_N is an identity matrix of size N. Considering the equation in (6.5), we have

$$\begin{aligned} \mathrm{tr}(Q_1\Sigma_{\boldsymbol{x}_1,\mathrm{n}}) &= \sigma^2_{x,\mathrm{n}}\Big(1+\sum_{i=1}^{N-1} q_i\Big), \\ \mathrm{tr}(Q_1\Sigma_{\boldsymbol{x}_1,\mathrm{ab}}) &= \sigma^2_{x,\mathrm{ab}}\Big(1+\sum_{i=1}^{N-1} q_i\Big), \end{aligned} \tag{6.11}$$

and

$$\begin{aligned} \mathrm{tr}(Q_1\Sigma_{\boldsymbol{x}_1,\mathrm{n}})^2 &= \sigma^4_{x,\mathrm{n}}\Big(1+\sum_{i=1}^{N-1} q_i^2\Big), \\ \mathrm{tr}(Q_1\Sigma_{\boldsymbol{x}_1,\mathrm{ab}})^2 &= \sigma^4_{x,\mathrm{ab}}\Big(1+\sum_{i=1}^{N-1} q_i^2\Big). \end{aligned} \tag{6.12}$$

Furthermore, according to the equation in (6.1) we have

$$\begin{aligned} \boldsymbol{\mu}_{\boldsymbol{x}_1,\mathrm{n}} &= \mu_{x,\mathrm{n}}\begin{bmatrix}1 & 1 & \cdots & 1\end{bmatrix}, \\ \boldsymbol{\mu}_{\boldsymbol{x}_1,\mathrm{ab}} &= \mu_{x,\mathrm{ab}}\begin{bmatrix}1 & 1 & \cdots & 1\end{bmatrix}, \end{aligned} \tag{6.13}$$

where $\boldsymbol{\mu}_{\boldsymbol{x}_1,\mathrm{n}}$ and $\boldsymbol{\mu}_{\boldsymbol{x}_1,\mathrm{ab}}$ are corresponding to the normal and abnormal operation modes, respectively. By performing some algebraic manipulations on the equations in (6.9), (6.11) and (6.13), the mean of filtered data is determined as

$$\mu_y = \begin{cases} (\sigma^2_{x,\mathrm{n}} + \mu^2_{x,\mathrm{n}})\Big(1+\sum\limits_{i=1}^{N-1} q_i\Big), & N \le k < T_{ab}, \\ (\sigma^2_{x,\mathrm{ab}} + \mu^2_{x,\mathrm{ab}})\Big(1+\sum\limits_{i=1}^{N-1} q_i\Big), & k \ge T_{ab}+N. \end{cases} \tag{6.14}$$

Moreover, by manipulating the equations in (6.10), (6.11) and (6.13), we have

$$\sigma^2_y = \begin{cases} (2\sigma^4_{x,\mathrm{n}} + 4\mu^2_{x,\mathrm{n}}\sigma^2_{x,\mathrm{n}})\Big(1+\sum\limits_{i=1}^{N-1} q_i^2\Big), & N \le k < T_{ab}, \\ (2\sigma^4_{x,\mathrm{ab}} + 4\mu^2_{x,\mathrm{ab}}\sigma^2_{x,\mathrm{ab}})\Big(1+\sum\limits_{i=1}^{N-1} q_i^2\Big), & k \ge T_{ab}+N. \end{cases} \tag{6.15}$$

Now by substituting (6.14) and (6.15) into the definition of alarm index (see the equation in (6.3)) we have

$$\mathcal{A}(y) = \frac{\left(2(\sigma_{x,\mathrm{n}}^4 + \sigma_{x,\mathrm{ab}}^4) + 4(\mu_{x,\mathrm{n}}^2\sigma_{x,\mathrm{n}}^2 + \mu_{x,\mathrm{ab}}^2\sigma_{x,\mathrm{ab}}^2)\right)\left(1 + \sum_{i=1}^{N-1} q_i^2\right)}{\left(\sigma_{x,\mathrm{n}}^2 + \mu_{x,\mathrm{n}}^2 - (\sigma_{x,\mathrm{ab}}^2 + \mu_{x,\mathrm{ab}}^2)\right)^2\left(1 + \sum_{i=1}^{N-1} q_i\right)^2}. \tag{6.16}$$

Hence, the impact of filter weights on the alarm performance index is given by

$$\mathcal{A}(y) \propto \frac{1 + \sum_{i=1}^{N-1} q_i^2}{\left(1 + \sum_{i=1}^{N-1} q_i\right)^2}. \tag{6.17}$$

Now by setting $\left[\frac{\partial \mathcal{A}}{\partial q_1} \ \frac{\partial \mathcal{A}}{\partial q_2} \ \cdots \frac{\partial \mathcal{A}}{\partial q_{N-1}}\right] = 0$, the optimal alarm weights are determined as $q_i = q, \ \forall i \in \{1, 2, \cdots, N-1\}$, where q can be any positive real number.

Although the best performance (in the view of (6.3)) can be achieved by setting all q_i's to one, there are some cases that operators decide to change the weights due to some circumstances. An example is when operators assign higher weights to the newer samples of a process variable to reduce detection delay. For this condition, (6.17) can be exploited as a straightforward measure for the accuracy of alarm systems. Adding other constraints gives rise to a new optimization problem. The effect of statistical parameters of raw data x on the alarm performance of filtered data is obtained as

$$\mathcal{A}_y(x) \propto \frac{\left(2(\sigma_{x,\mathrm{n}}^4 + \sigma_{x,\mathrm{ab}}^4) + 4(\mu_{x,\mathrm{n}}^2\sigma_{x,\mathrm{n}}^2 + \mu_{x,\mathrm{ab}}^2\sigma_{x,\mathrm{ab}}^2)\right)}{\left(\sigma_{x,\mathrm{n}}^2 + \mu_{x,\mathrm{n}}^2 - (\sigma_{x,\mathrm{ab}}^2 + \mu_{x,\mathrm{ab}}^2)\right)^2}. \tag{6.18}$$

This expression can be utilized as a measure to help operators for exploring historical data and determining the optimal process variable for filtering. In this chapter, we call $\mathcal{A}_y(x)$, the alarm score. A smaller alarm score corresponds to a better alarm performance after filtering.

6.3 Performance Assessment of Case II

The quadratic filter associated with Case II can be reformulated as

$$P_2(\boldsymbol{x}) = \boldsymbol{x}\begin{bmatrix} Q_1 & \boldsymbol{\alpha}^T \\ \boldsymbol{\alpha} & 0 \end{bmatrix}\boldsymbol{x}^T,$$

where $\boldsymbol{x} = \begin{bmatrix}\boldsymbol{x}_1 & 1\end{bmatrix}$, $\boldsymbol{x}_1$ is introduced by the equation in (6.7), and

$$\boldsymbol{\alpha} = \begin{bmatrix}\alpha_0 & \alpha_1 q_1 & \dots & \alpha_{N-1} q_{N-1}\end{bmatrix}.$$

Furthermore, $\boldsymbol{x}_1 \boldsymbol{\alpha}^T = \boldsymbol{\alpha} \boldsymbol{x}_1^T$, thus

$$P(\boldsymbol{x}) = \boldsymbol{x}_1 Q_1 \boldsymbol{x}_1^T + 2\boldsymbol{\alpha}\boldsymbol{x}_1^T. \tag{6.19}$$

By performing some modification on a lemma presented by [76], we introduce the following lemma.

Lemma 6.3.1 *Considering the same assumptions that are made in Lemma 6.2.1, the r^{th} moment of $P_2(\boldsymbol{x})$ for $r \in \{1, 2\}$ is determined by replacing $g^{(j)}$ with $g_*^{(j)}$ in* (6.8)*, where*

$$g_*^{(j)} = \begin{cases} \frac{1}{2} j! \sum_{i=1}^{N-1} (2\lambda_i)^{j+1} + \frac{(j+1)!}{2} \sum_{i=1}^{N-1} b_i^{*2} (2\lambda_i)^{j-1}, & j \geq 1, \\ \frac{1}{2} \sum_{i=1}^{N-1} (2\lambda_i) + 2\boldsymbol{\alpha}\boldsymbol{\mu} + \boldsymbol{\mu} Q_1 \boldsymbol{\mu}^T, & j = 1. \end{cases}$$

Here,

$$\begin{bmatrix} \lambda_1 & 0 & \cdots & 0 \\ 0 & \lambda_2 & \ddots & \vdots \\ \vdots & \ddots & \ddots & 0 \\ 0 & \dots & 0 & \lambda_{N-1} \end{bmatrix} = Q_1 \Sigma,$$

and

$$\boldsymbol{b}^* \triangleq (b_1^*, b_2^*, \cdots, b_{N-1}^*) = 2\big(\Sigma^{\frac{1}{2}} \boldsymbol{\alpha} + \Sigma^{\frac{1}{2}} \boldsymbol{\mu} Q_1\big).$$

According to this lemma, the mean and variance of $P_2(x)$ is determined as

$$\mathbb{E}(P_2(\boldsymbol{x})) = \operatorname{tr}(Q_1 \Sigma) + 2\boldsymbol{\alpha}\boldsymbol{\mu} + \boldsymbol{\mu} Q_1 \boldsymbol{\mu}^T, \tag{6.20}$$

and

$$\begin{aligned} \operatorname{Var}(P_2(\boldsymbol{x})) &= \mathbb{E}(P_2(\boldsymbol{x}))^2 - \big(\mathbb{E}(P_2(\boldsymbol{x}))\big)^2 \\ &= \left(\begin{pmatrix} 1 \\ 0 \end{pmatrix} g_*^{(1)} + \begin{pmatrix} 1 \\ 1 \end{pmatrix} \big(g_*^{(0)}\big)^2 \right) - \begin{pmatrix} 0 \\ 0 \end{pmatrix} \big(g_*^{(0)}\big)^2 \\ &= 2\operatorname{tr}(\Sigma Q_1)^2 + \sum_{i=1}^{N-1} b_i^{*2}. \end{aligned} \tag{6.21}$$

Now let $\boldsymbol{b}_n^*$ be corresponding to the normal operation mode. Then

$$\boldsymbol{b}_n^* = 2\sigma_{x,\mathrm{n}}\boldsymbol{\alpha} + 2\sigma_{x,\mathrm{n}}\boldsymbol{\mu}\begin{bmatrix} 1 & 0 & \cdots & 0 \\ 0 & q_1 & \ddots & \vdots \\ \vdots & \ddots & \ddots & 0 \\ 0 & \dots & 0 & q_{N-1} \end{bmatrix}.$$

Hence

$$\begin{cases} b_{i,\mathrm{n}}^* = 2\sigma_{x,\mathrm{n}}(\alpha_i + \mu_{x,\mathrm{n}}), & i = 0, \\ b_{i,\mathrm{n}}^* = 2q_i\sigma_{x,\mathrm{n}}(\alpha_i + \mu_{x,\mathrm{n}}), & i \geq 1, \end{cases} \tag{6.22}$$

where $b_{i,\mathrm{n}}^*$'s are elements of $\boldsymbol{b}_n^*$. The same result holds for the abnormal operation modes ($b_{i,\mathrm{ab}}^*$). By substituting (6.11) and (6.13) into the equation in (6.20) and performing some algebraic manipulations, the mean of filtered data is obtained by

$$\mu_{y'} = \begin{cases} \mu_{y',\mathrm{n}} = (\sigma_{x,\mathrm{n}}^2 + \mu_{x,\mathrm{n}}^2)\Big(1 + \sum_{i=1}^{N-1} q_i\Big) + \\ \qquad\qquad 2\mu_{x,\mathrm{n}}\Big(\alpha_0 + \sum_{i=1}^{N-1}\alpha_i q_i\Big), \quad N \leq k < T_{ab}, \\ \mu_{y',\mathrm{ab}} = (\sigma_{x,\mathrm{ab}}^2 + \mu_{x,\mathrm{ab}}^2)\Big(1 + \sum_{i=1}^{N-1} q_i\Big) + \\ \qquad\qquad 2\mu_{x,\mathrm{ab}}\Big(\alpha_0 + \sum_{i=1}^{N-1}\alpha_i q_i\Big), \quad k \geq T_{ab} + N. \end{cases} \tag{6.23}$$

The variance of filtered data is determined by substituting (6.12) and (6.22) into equation (6.21):

$$\sigma_{y'}^2 = \begin{cases} \sigma_{y',\mathrm{n}}^2 = 4\sigma_{x,\mathrm{n}}^2\Big((\alpha_0 + \mu_{x,\mathrm{n}})^2 + \sum_{i=1}^{N-1} q_i^2(\alpha_i + \mu_{x,\mathrm{n}})^2\Big) + \\ \qquad\qquad 2\sigma_{x,\mathrm{n}}^4\Big(1 + \sum_{i=1}^{N-1} q_i^2\Big), \quad N \leq k < T_{ab}, \\ \sigma_{y',\mathrm{ab}}^2 = 4\sigma_{x,\mathrm{ab}}^2\Big((\alpha_0 + \mu_{x,\mathrm{ab}})^2 + \sum_{i=1}^{N-1} q_i^2(\alpha_i + \mu_{x,\mathrm{ab}})^2\Big) + \\ \qquad\qquad 2\sigma_{x,\mathrm{ab}}^4\Big(1 + \sum_{i=1}^{N-1} q_i^2\Big), \quad k \geq T_{ab} + N. \end{cases} \tag{6.24}$$

So the alarm index corresponding to the second scenario is given by

$$\mathcal{A}(y') = \frac{\sigma_{y',\mathrm{ab}}^2 + \sigma_{y',\mathrm{n}}^2}{\big(\mu_{y',\mathrm{ab}}^2 - \mu_{y',\mathrm{n}}^2\big)^2}, \tag{6.25}$$

where $\sigma_{y',\mathrm{ab}}$, $\sigma_{y',\mathrm{n}}$, $\mu_{y',\mathrm{ab}}$, and $\mu_{y',\mathrm{n}}$ are given by the equations in (6.23) and (6.24). Now consider a special case where $\alpha_i = \alpha,\ \forall i \in \{1, 2, \cdots, N\}$, and let $\tilde{y}'$ indicates the filter output, which is represented by

$$\tilde{y}'[k] = (x[k] + \alpha)^2 + \sum_{i=1}^{N-1} q_i (x[k-i] + \alpha)^2. \tag{6.26}$$

Under this assumption, we can obtain the mean and variance of $\tilde{y}'$ as

$$\mu_{\tilde{y}'} = \begin{cases} \left(\sigma^2_{x,\mathrm{n}} + \mu^2_{x,\mathrm{n}} + 2\alpha\mu_{x,\mathrm{n}}\right)\left(1 + \sum_{i=1}^{N-1} q_i\right), & N \le k < T_{ab}, \\ \left(\sigma^2_{x,\mathrm{ab}} + \mu^2_{x,\mathrm{ab}} + 2\alpha\mu_{x,\mathrm{ab}}\right)\left(1 + \sum_{i=1}^{N-1} q_i\right), & k \ge T_{ab} + N. \end{cases}$$

and

$$\sigma^2_{\tilde{y}'} = \begin{cases} \left(4\sigma^2_{x,\mathrm{n}}(\alpha + \mu_{x,\mathrm{n}})^2 + 2\sigma^4_{x,\mathrm{n}}\right)\left(1 + \sum_{i=1}^{N-1} q_i^2\right), & N \le k < T_{ab}, \\ \left(4\sigma^2_{x,\mathrm{ab}}(\alpha + \mu_{x,\mathrm{ab}})^2 + 2\sigma^4_{x,\mathrm{ab}}\right)\left(1 + \sum_{i=1}^{N-1} q_i^2\right), & k \ge T_{ab} + N. \end{cases}$$

Now the relation of q_i's and the alarm performance index is determined as

$$\mathcal{A}(\tilde{y}') \propto \frac{1 + \sum_{i=1}^{N-1} q_i^2}{\left(1 + \sum_{i=1}^{N-1} q_i\right)^2}.$$

This expression is similar to the result that we derived for Case I, so the optimal q_i's can be obtained similar to the one in Case I. By performing some calculations, the optimal value for α is determined as

$$\alpha_{\mathrm{opt}} = \frac{\Pi_1\Pi_2 - \Pi_3\Pi_4}{\Pi_1\Pi_4 - \Pi_5\Pi_2}, \quad \Pi_1\Pi_4 \neq \Pi_5\Pi_2, \tag{6.27}$$

where

$$\begin{aligned} \Pi_1 &= 2(\sigma^2_{x,\mathrm{ab}}\mu_{x,\mathrm{ab}} + \sigma^2_{x,\mathrm{n}}\mu_{x,\mathrm{n}}), \\ \Pi_2 &= (\sigma^2_{x,\mathrm{ab}} + \mu^2_{x,\mathrm{ab}}) - (\sigma^2_{x,\mathrm{n}} + \mu^2_{x,\mathrm{n}}), \\ \Pi_3 &= (\sigma^4_{x,\mathrm{ab}} + \sigma^4_{x,\mathrm{n}}) + 2(\sigma^2_{x,\mathrm{ab}}\mu^2_{x,\mathrm{ab}} + \sigma^2_{x,\mathrm{n}}\mu^2_{x,\mathrm{n}}), \\ \Pi_4 &= 2(\mu_{x,\mathrm{ab}} - \mu_{x,\mathrm{n}}), \\ \Pi_5 &= 2(\sigma^2_{x,\mathrm{ab}} + \sigma^2_{x,\mathrm{n}}). \end{aligned}$$

Hence, the effect of statistical parameters of process variable x on the alarm performance of filter data $\tilde{y}'$ is expressed as

$$\mathcal{A}_{\tilde{y}'}(x) \propto \frac{\Pi_5 \alpha_{\text{opt}}^2 + \Pi_1 \alpha_{\text{opt}} + \Pi_3}{(\Pi_4 \alpha_{\text{opt}} + \Pi_2)^2}. \tag{6.28}$$

6.4 Simulation Results

In this section, we study an example to demonstrate the effectiveness of the proposed method and verify the theoretical analysis. Consider a plant with three process variables that are sampled at discrete times. The process variables are indicated by $x_1[k]$, $x_2[k]$ and $x_3[k]$, $k \in \{1, 2, \cdots, T\}$ and are available for the alarm system to detect abnormal operation of the plant. Now assume that a fault occurred in the plant at sample $k = T_{ab}$. Mean and variance of the process variables can be estimated as

$$\mu_{x_j,\text{n}} = \frac{1}{T_{ab}} \sum_{k=0}^{T_{ab}-1} x_j[k],$$

$$\mu_{x_j,\text{ab}} = \frac{1}{T - T_{ab} + 1} \sum_{k=T_{ab}}^{T} x_j[k],$$

and

$$\sigma_{x_j,\text{n}}^2 = \frac{1}{T_{ab}} \sum_{k=0}^{T_{ab}-1} (x_j[k] - \mu_{x_j,\text{n}})^2,$$

$$\sigma_{x_j,\text{ab}}^2 = \frac{1}{T - T_{ab} + 1} \sum_{k=T_{ab}}^{T} (x_j[k] - \mu_{x_j,\text{ab}})^2,$$

where $j \in \{1, 2, 3\}$. We assume that after estimation of mean and variance, the following distributions are obtained:

$$\mathcal{X}_1 \sim \begin{cases} \mathcal{N}(0.2, 0.4^2), & k < T_{ab}, \\ \mathcal{N}(1, 1^2), & k \geq T_{ab}, \end{cases}$$

$$\mathcal{X}_2 \sim \begin{cases} \mathcal{N}(0.4, 0.3^2), & k < T_{ab}, \\ \mathcal{N}(1, 0.4^2), & k \geq T_{ab}, \end{cases}$$

$$\mathcal{X}_3 \sim \begin{cases} \mathcal{N}(0.1, 0.4^2), & k < T_{ab}, \\ \mathcal{N}(2.1, 1.4^2), & k \geq T_{ab}. \end{cases}$$

Table 6.1: Alarm score of process variables

	x_1	x_2	x_3
$\mathcal{A}_y(x)$	1.87	**0.92**	1.10
$\mathcal{A}_{\tilde{y}'}(x)$	1.63	0.69	**0.46**

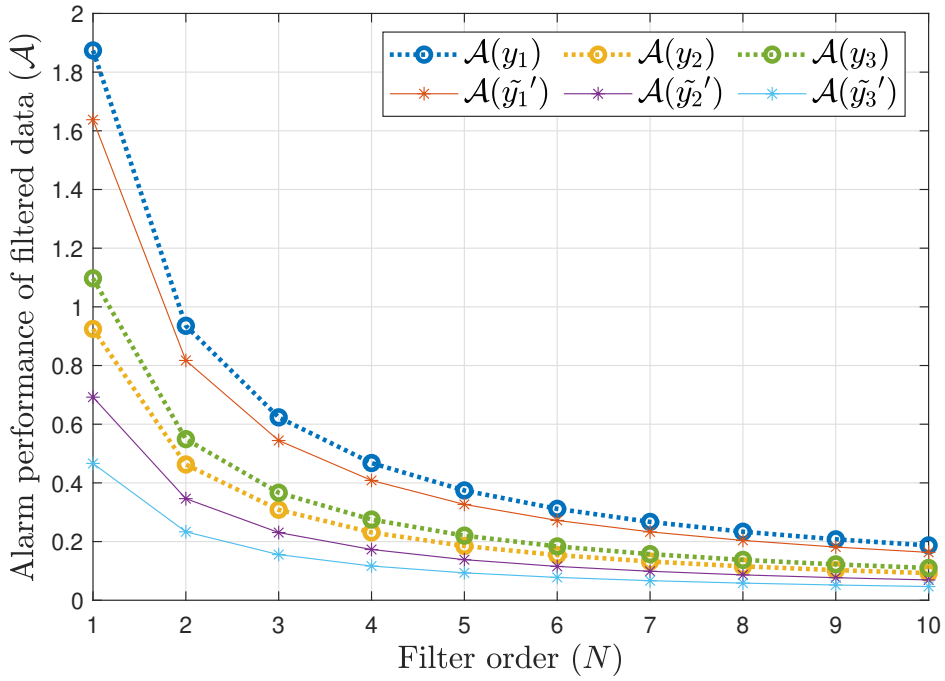

Figure 6.1: Simulation results for various filter orders, where $q_i = 1$, $\forall i \in \{1, 2, \cdots, N-1\}$, and $\alpha = \alpha_{\text{opt}}$.

Now we use the equations in (6.18) and (6.28) to obtain the appropriate process variable for fault detection. The result is presented in Table 6.1. In this table, a smaller alarm score represents a better alarm performance after filtering. This result indicates that for the filter structures of Case I and Case II, we should select x_2 and x_3, respectively. Furthermore, we can infer that x_1 is not the right choice for either filter structure. Now let y_1, y_2 and y_3 denote the filtered data corresponding to the process variables x_1, x_2 and x_3, respectively. This result can also be concluded from Fig. 6.1 which is obtained by conducting Monte Carlo simulation. Fig. 6.2 shows the alarm index of filtered data for Case I. Details of the studied scenarios are presented in Table 6.2. From Fig.

6.2, we can see that the best performance (in terms of the equation in (6.3)) can be archived by setting all q_i's to one. However, considering new constraints (see Remark 6.2), another scenario may be a good candidate. In all scenarios, the analytical result captures well the Monte Carlo simulation.

Table 6.2: Simulation scenarios

Scenario	Filter weights
1	All set to 1
2	Set according to an arithmetic sequence with initial term 1 and common difference $1/N$
3	Set according to a geometric sequence with initial term 1 and common ratio 0.6
4	Set according to a geometric sequence with initial term 1 and common ratio 0.2

For Case II, the obtained α_{opt} for each process variable is presented in Table 6.3.

Table 6.3: Optimal α for process variables

	x_1	x_2	x_3
α_{opt}	1.31	-6.64	-4.93

The simulation result of Fig. 6.3 verifies this analysis. Finally, Fig. 6.4 and Fig. 6.5 show time trends of x_2 and y_2, respectively. By comparing the histograms of x_2 and y_2, we conclude that the filter reduced the overlapped area of normal and abnormal operation modes. This implies that the separation of these two modes can be achieved with higher accuracy after filtering.

6.5 Summary

This chapter addressed the problem of optimal quadratic filter design for industrial alarm management systems. We derived an explicit solution for the

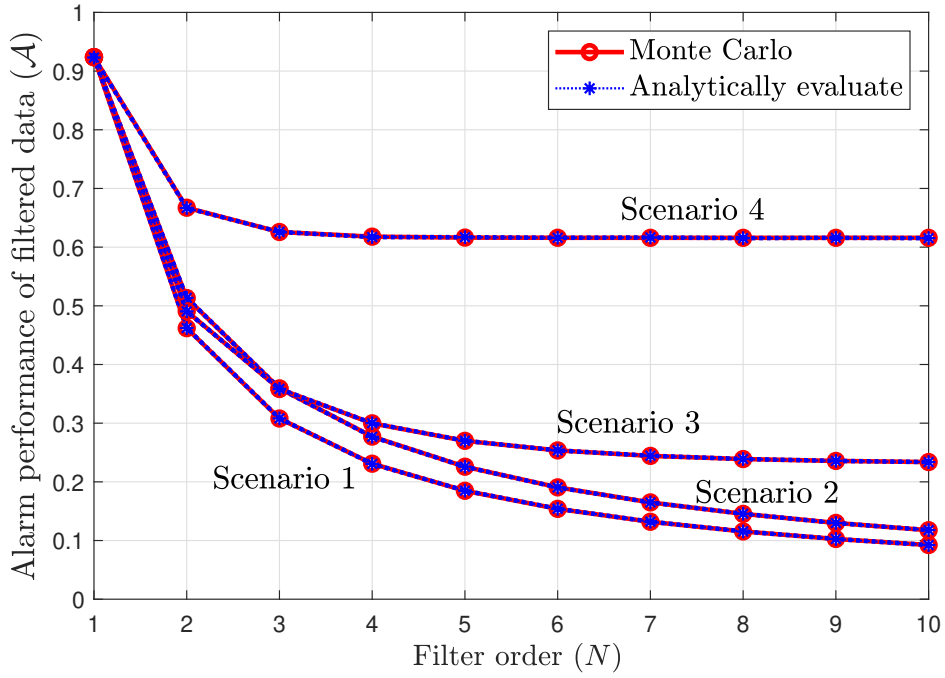

Figure 6.2: Simulation result of $\mathcal{A}(y)$ where q_i's are selected according to Table 6.2.

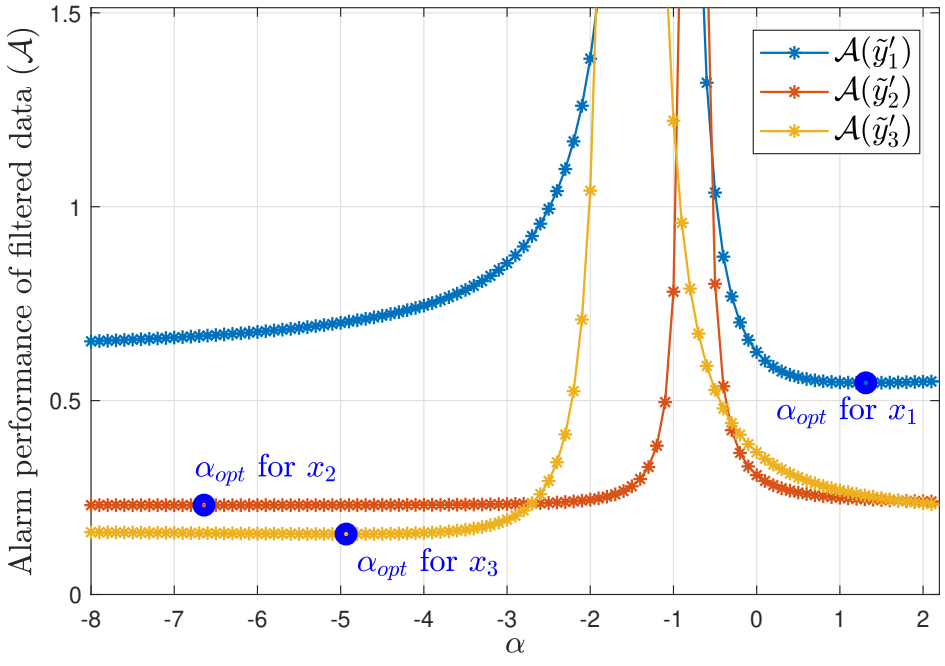

Figure 6.3: Analytically evaluated optimal α (using the equation in (6.27)) and simulation result for various choices of α with $N = 3$.

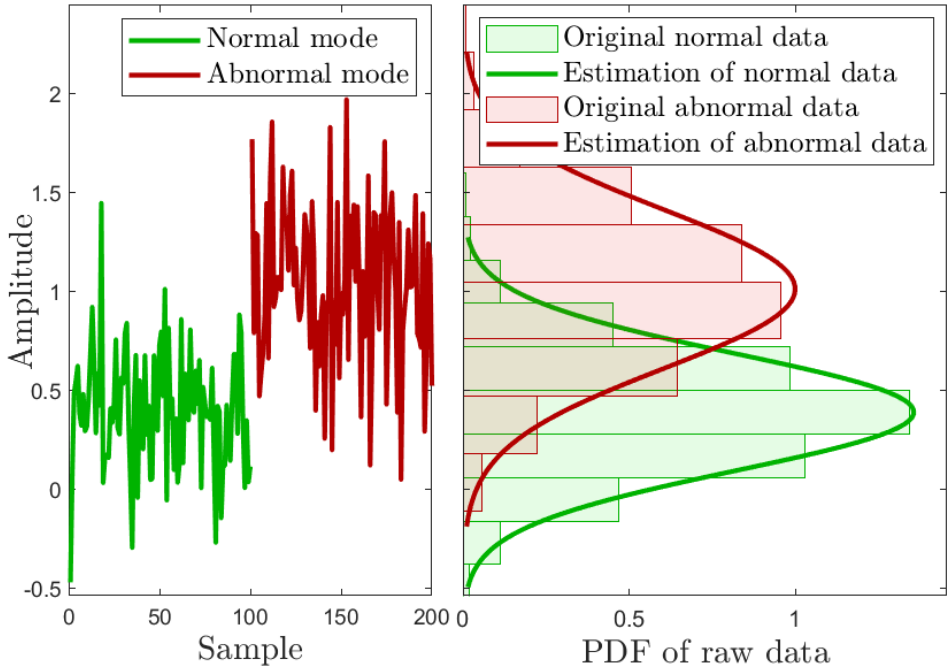

Figure 6.4: Time trend and histogram of x_2.

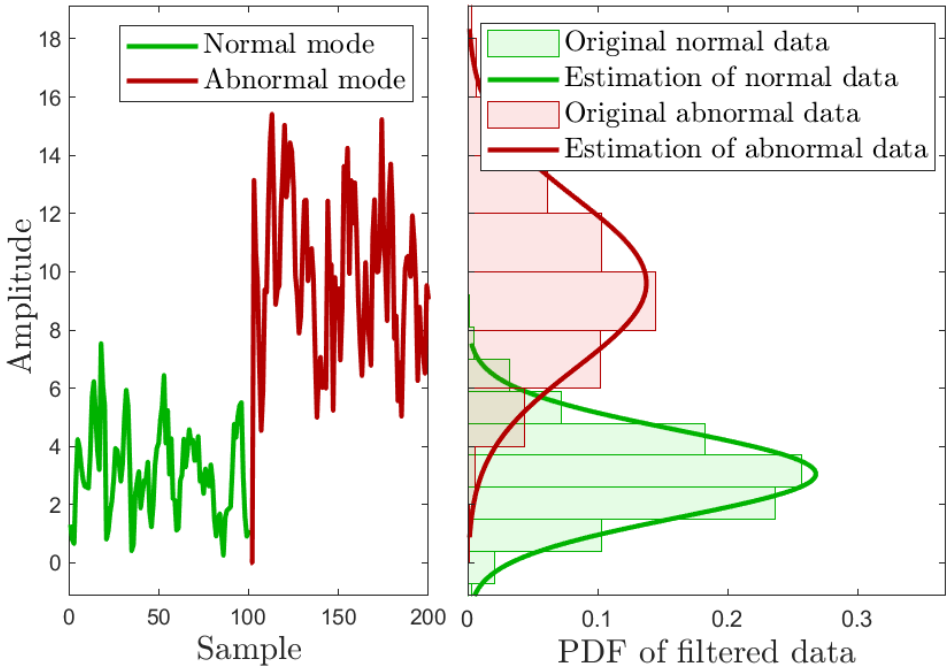

Figure 6.5: Time trend and histogram of y_2 (filtered version of x_2 according to the scenario 1 with $N = 3$).

alarm performance of quadratic filters. We introduced a new score, which can be utilized to help plant operators to determine an appropriate process variable for alarm purposes. We also demonstrated that for different filter structures, this optimal choice might be different. The analysis of this chapter can be combined with other alarm performance indices (e.g., alarm detection delay) to satisfy the requirements of various applications. It can also be served as a stepping stone to assess and design other forms of nonlinear alarm filters.

Chapter 7

Conclusions and Future Work

This chapter concludes the thesis. In the first part of this chapter, a summary of the main results is presented. After that, some potential future research directions are proposed.

7.1 Conclusions

In this thesis, PID and state-feedback controller synthesis problems considering both control and alarm performance have been studied. Inspired by the presence of model uncertainty in most of industrial applications, a state-feedback controller has been designed to be robust against norm-bounded uncertainty of model parameters. A new alarm index has been introduced by utilizing the concept of the area under a ROC curve. This alarm index is shown to be applicable for controller design even for uncertain systems. It also has been justified that there is an interplay between control and alarm performance for a certain type of performance indices. LMI based methods have been proposed to compromise the control and alarm performance.

The problem of linear alarm filters for statistically correlated process variables has also been addressed in this thesis. It has been justified that the conventional moving average filter is not the optimal answer when relaxing the independence assumption on process measurements. In the case of actuator faults, it has been shown that the optimal filter coefficients can be obtained regardless of the abnormality amplitude.

We have also addressed the problems of optimal generalized moving vari-

ance and quadratic filters for industrial alarm management systems. We derived an explicit solution for the alarm performance of quadratic filters. We introduced a new score, which can be utilized to help plant operators to determine an appropriate process variable for alarm purposes. We also demonstrated that for different filter structures, this optimal choice might be different.

7.2 Future Work

Some possible extensions and new ideas that are worth investigating as future research are listed as follows:

- The proposed controller design approach could be further extended in the various directions. In the proposed method, we have only considered mean change problem which is the most popular type of abnormality. But other types of abnormality such as ramp and variation changes can be investigated. For ramp abnormalities, instead of Gaussian distributions, one can use Gaussian mixture models to analyze the alarm performance. For variance changes, a possible solution is to derive a Gaussian approximation for alarm signals. The proposed method of Chapter 5 may be helpful to find such an approximation. Furthermore, a similar control design problem can be studied by adding alarm filters, deadbands or delay timers. The result of Chapter 4 can be utilized to deal with alarm filters. However, for deadbands or delay timers, Markov models should be used to analyze the overall performance of alarm systems. In the first two chapters, we have studied only PID and state-feedback controllers. So another possible research direction is to exploit other types of control strategies. In this case, the alarm performance index that has been introduced for systems (see Chapter 3) can be added as a constraint to the new control design problem.

- To further enhance the analysis, in addition to the accuracy measures FAR and MAR, swiftness of alarm filters in detecting abnormalities is

desirable. Average detection delay (ADD) has already been introduced in the literature which is suitable for alarm deadbands and delay timers and is hard to adopt for alarm filters. However, the definition of ADD makes it very hard to obtain a closed form solution in case of alarm filtering. The reason is that for alarm filters this index deals with multivariate Gaussian distributions where the samples are not independent; and the average is on an infinite number of cumulative distribution functions (CDFs) of these distributions. A possible direction to obtain a solution is to introduce a new index to measure the swiftness considering the structure of alarm filters.

- Industrial processes are prone to various operation mode changes. Hence, statistical parameters of process variables and associated alarm signals may also change. This may cause performance degradation of alarm filters. To address this problem, the moving variance filter design method of Chapter 5 can be generalized for non-stationary processes. Similar to the existing methods in the literature (see e.g., [95]), one may approach this problem by assuming a time-series model for the system. Furthermore, The approach of Chapter 5 can be served as a stepping-stone for analysis of other classes of nonlinear alarm filters. The simplest solution is based on the moment matching method where the output of a nonlinear filter is approximated by a Gaussian distribution. However, in some cases, more sophisticated methods can be adopted to improve the approximation accuracy.

- The distribution parameters of raw data may have uncertainties in some real applications. In Chapter 3, we have designed a controller to guarantee a robust performance for alarm systems in the presence of model uncertainties. The issue of uncertain statistical parameters of the raw data may be even more challenging for nonlinear filters. As an instance, for quadratic filters, if the parameter α is close to the mean of a process variable, a small change in the mean value can significantly deteriorate the filter performance. Thus, robust design of the quadratic and the mov-

ing variance alarm filter of Chapter 5 and Chapter 6 is also a promising research direction.

References

[1] G. Abe, M. Itoh, and T. Yamamura, "Effects of missed alarms on driver's response to a collision warning system according to alarm timings," in *International Conference on Intelligent Robotics and Applications*, Berlin, Heidelberg, 2009, pp. 245–254.

[2] L. Abele, M. Anic, T. Gutmann, J. Folmer, M. Kleinsteuber, and B. Vogel-Heuser, "Combining knowledge modeling and machine learning for alarm root cause analysis," *IFAC-PapersOnLine*, vol. 46, no. 9, pp. 1843–1848, 2013.

[3] M. Abramowitz, I. A. Stegun, and R. H. Romer, *Handbook of Mathematical Functions with Formulas, Graphs, and Mathematical Tables*. AAPT, 1988.

[4] M. Adeli and A. Mazinan, "High efficiency fault-detection and fault-tolerant control approach in tennessee eastman process via fuzzy-based neural network representation," *Complex & Intelligent Systems*, pp. 1–14, 2019.

[5] N. A. Adnan, "Performance assessment and systematic design of industrial alarm systems," *PhD thesis, University of Alberta*, 2013.

[6] N. A. Adnan, Y. Cheng, I. Izadi, and T. Chen, "Study of generalized delay-timers in alarm configuration," *Journal of Process Control*, vol. 23, no. 3, pp. 382–395, 2013.

[7] N. A. Adnan and I. Izadi, "On detection delays of filtering in industrial alarm systems," in *Mediterranean Conference on Control and Automation*, 2013, pp. 113–118.

[8] N. A. Adnan, I. Izadi, and T. Chen, "On expected detection delays for alarm systems with deadbands and delay-timers," *Journal of Process Control*, vol. 21, no. 9, pp. 1318–1331, 2011.

[9] M. S. Afzal and T. Chen, "Analysis and design of multimode delay-timers," *Chemical Engineering Research and Design*, vol. 120, pp. 179–193, 2017.

[10] M. S. Afzal, T. Chen, A. Bandehkhoda, and I. Izadi, "Performance assessment of time-deadbands," in *2017 American Control Conference (ACC)*, IEEE, 2017, pp. 4815–4820.

[11] K. Ahmed, I. Izadi, T. Chen, D. Joe, and T. Burton, "Similarity analysis of industrial alarm flood data," *IEEE Transactions on Automation Science and Engineering*, vol. 10, no. 2, pp. 452–457, 2013.

[12] J. Ahnlund, T. Bergquist, and L. Spaanenburg, "Rule-based reduction of alarm signals in industrial control," *Journal of Intelligent & Fuzzy Systems*, vol. 14, no. 2, pp. 73–84, 2003.

[13] D. A. Alexander, "Psychiatric intervention after the piper alpha disaster," *Journal of the Royal Society of Medicine*, vol. 84, no. 1, pp. 8–11, 1991.

[14] H. Alikhani, M. A. Shoorehdeli, and M. Yari, "Alarm management based fault diagnosis of v94.2 gas turbines by applying linear filters," in *International Conference on Robotics and Mechatronics*, IEEE, 2016, pp. 355–360.

[15] F. Alrowaie, R. Gopaluni, and K. Kwok, "Alarm design for nonlinear stochastic systems," in *Proceeding of Intelligent Control and Automation*, 2014, pp. 473–479.

[16] B. Arifin, Z. Li, and S. L. Shah, "Change point detection using the Kantorovich distance algorithm," *IFAC-PapersOnLine*, vol. 51, no. 18, pp. 708–713, 2018.

[17] B. Arifin, Z. Li, S. L. Shah, G. A. Meyer, and A. Colin, "A novel data-driven leak detection and localization algorithm using the kantorovich distance," *Computers & Chemical Engineering*, vol. 108, pp. 300–313, 2018.

[18] B. Arrue, A. Ollero, and J. D. Dios, "An intelligent system for false alarm reduction in infrared forest-fire detection," *Intelligent Systems and their Applications*, vol. 15, no. 3, pp. 64–73, 2000.

[19] M. Bakošová and J. Oravec, "Robust model predictive control for heat exchanger network," *Applied Thermal Engineering*, vol. 73, no. 1, pp. 924–930, 2014.

[20] S. Bhaumik, J. MacGowan, and V. Doraj, "Mode based alarm solutions at syncrude canada," *IFAC-PapersOnLine*, vol. 48, no. 8, pp. 653–656, 2015.

[21] C. M. Bishop, *Pattern Recognition and Machine Learning*. Springer, 2006.

[22] E. Bristol, "Improved process control alarm operation," *ISA Transactions*, vol. 40, no. 2, pp. 191–205, 2001.

[23] R. Brooks, R. Thorpe, and J. Wilson, "A new method for defining and managing process alarms and for correcting process operation when an alarm occurs," *Journal of Hazardous Materials*, vol. 115, no. 1-3, pp. 169–174, 2004.

[24] A. E. Bryson, *Applied Optimal Control: Optimization, Estimation and Control*. CRC Press, 1975.

[25] Z. Chen, F. Han, L. Wu, J. Yu, S. Cheng, P. Lin, and H. Chen, "Random forest based intelligent fault diagnosis for pv arrays using array voltage and string currents," *Energy Conversion and Management*, vol. 178, pp. 250–264, 2018.

[26] Y. Cheng, I. Izadi, and T. Chen, "On optimal alarm filter design," in *IEEE International Symposium on Advanced Control of Industrial Processes*, 2011, pp. 139–145.

[27] ——, "Optimal alarm signal processing: Filter design and performance analysis," *IEEE Transactions on Automation Science and Engineering*, vol. 10(2), pp. 446–451, 2013.

[28] ——, "Pattern matching of alarm flood sequences by a modified smith–waterman algorithm," *Chemical Engineering Research and Design*, vol. 91, no. 6, pp. 1085–1094, 2013.

[29] M. S. Choudhury, V. Kariwala, S. L. Shah, H. Douke, H. Takada, and N. F. Thornhill, "A simple test to confirm control valve stiction," *IFAC-PapersOnLine*, vol. 38, no. 1, pp. 81–86, 2005.

[30] R. W. Cottle, "Manifestations of the schur complement," *Linear Algebra and its Applications*, vol. 8, no. 3, pp. 189–211, 1974.

[31] S. Covo and A. Elalouf, "A novel single-Gamma approximation to the sum of independent gamma variables, and a generalization to infinitely divisible distributions," *Electronic Journal of Statistics*, vol. 8, no. 1, pp. 894–926, 2014.

[32] B. Datta, *Numerical Methods for Linear Control Systems*. Academic Press, 2004.

[33] M. C. De Oliveira, J. C. Geromel, and J. Bernussou, "Extended $\mathcal{H}_2$ and $\mathcal{H}_\infty$ norm characterizations and controller parametrizations for discrete-time systems," *International Journal of Control*, vol. 75, no. 9, pp. 666–679, 2002.

[34] J. J. Downs and E. F. Vogel, "A plant-wide industrial process control problem," *Computers & Chemical Engineering*, vol. 17, no. 3, pp. 245–255, 1993.

[35] Y. Du, H. Budman, and T. A. Duever, "Integration of fault diagnosis and control based on a trade-off between fault detectability and closed loop performance," *Journal of Process Control*, vol. 38, pp. 42–53, 2016.

[36] *EEMUA-191: A Guide to Design, Management and Procurement, Engineering Equipment and Materials Users' Association*. London, 2013.

[37] J. Egan, *Signal Detection Theory and ROC-Analysis*. Academic Press, 1975.

[38] Z. Geng, Q. Zhu, and X. Gu, "A fuzzy clustering–ranking algorithm and its application for alarm operating optimization in chemical processing," *Process Safety Progress*, vol. 24, no. 1, pp. 66–75, 2005.

[39] P. Goel, A. Datta, and M. S. Mannan, "Industrial alarm systems: Challenges and opportunities," *Journal of Loss Prevention in the Process Industries*, vol. 50, pp. 23–36, 2017.

[40] A. GopiChand, A. Sharma, G. V. Kumar, and A. Srividya, "Thermal analysis of shell and tube heat exchanger using mat lab and floefd software," *International Journal of Reasearch in Engineering and Technology*, vol. 1, no. 3, pp. 276–281, 2012.

[41] R. Hagenouw, "Should we be alarmed by our alarms?" *Current Opinion in Anesthesiology*, vol. 20, no. 6, pp. 590–594, 2007.

[42] L. Han, H. Gao, Y. Xu, and Q. Zhu, "Combining FAP and MAP and correlation analysis for multivariate alarm thresholds optimization in industrial process," *Journal of Loss Prevention in the Process Industries*, vol. 40, pp. 471–478, 2016.

[43] D. M. Hawkins and R. Wixley, "A note on the transformation of Chi-squared variables to normality," *The American Statistician*, vol. 40, no. 4, pp. 296–298, 1986.

[44] D. M. Hawkins and K. Zamba, "A change-point model for a shift in variance," *Journal of Quality Technology*, vol. 37, no. 1, pp. 21–31, 2005.

[45] W. Hu, T. Chen, and S. L. Shah, "An automated data-driven method to detect mode-based alarms," in *American Control Conference (ACC)*, IEEE, 2017, pp. 5416–5421.

[46] ——, "Discovering association rules of mode-dependent alarms from alarm and event logs," *IEEE Transactions on Control Systems Technology*, vol. 26, no. 3, pp. 971–983, 2017.

[47] W. Hu, J. Wang, T. Chen, and S. L. Shah, "Cause-effect analysis of industrial alarm variables using transfer entropies," *Control Engineering Practice*, vol. 64, pp. 205–214, 2017.

[48] A. J. Hugo, *Statistical quality control of alarm occurrences*, US Patent 7,289,935, Oct. 2007.

[49] ——, "Estimation of alarm deadbands," *IFAC Proceedings Volumes*, vol. 42, no. 8, pp. 663–667, 2009.

[50] E. Hussain, "The bi-gamma ROC curve in a straightforward manner," *Journal of Basic & Applied Sciences*, vol. 8, no. 2, pp. 309–314, 2012.

[51] S.-L. Hwang, J.-T. Lin, G.-F. Liang, Y.-J. Yau, T.-C. Yenn, and C.-C. Hsu, "Application control chart concepts of designing a pre-alarm system in the nuclear power plant control room," *Nuclear Engineering and Design*, vol. 238, no. 12, pp. 3522–3527, 2008.

[52] *ISA-18.2: Management of Alarm Systems for the Process Industries*. ISA (International Society of Automation): Durham, NC, 2009.

[53] R. Isermann, *Fault-Diagnosis Systems: an Introduction From Fault Detection to Fault Tolerance*. Springer Science & Business Media, 2006.

[54] I. Izadi, S. L. Shah, D. S. Shook, S. R. Kondaveeti, and T. Chen, "A framework for optimal design of alarm systems," *IFAC Proceedings Volumes*, vol. 42, no. 8, pp. 651–656, 2009.

[55] G.-s. Jang, S.-m. Suh, S.-k. Kim, Y.-s. Suh, and J.-y. Park, "A proactive alarm reduction method and its human factors validation test for a main control room for smart," *Annals of Nuclear Energy*, vol. 51, pp. 125–134, 2013.

[56] G. Jiang, H. He, J. Yan, and P. Xie, "Multiscale convolutional neural networks for fault diagnosis of wind turbine gearbox," *IEEE Transactions on Industrial Electronics*, vol. 66, no. 4, pp. 3196–3207, 2018.

[57] T. A. Johansen, "Adaptive control of mimo non-linear systems using local arx models and interpolation," *IFAC Proceedings Volumes*, vol. 27, no. 2, pp. 147–154, 1994.

[58] S. Kammammettu and Z. Li, "Change point and fault detection using Kantorovich distance," *Journal of Process Control*, vol. 80, pp. 41–59, 2019.

[59] S. R. Kondaveeti, I. Izadi, S. L. Shah, and T. Chen, "On the use of delay timers and latches for efficient alarm design," in *Mediterranean Conference on Control & Automation*, 2011, pp. 970–975.

[60] S. R. Kondaveeti, I. Izadi, S. L. Shah, D. S. Shook, R. Kadali, and T. Chen, "Quantification of alarm chatter based on run length distributions," *Chemical Engineering Research and Design*, vol. 91, no. 12, pp. 2550–2558, 2013.

[61] K. Krishnamoorthy, T. Mathew, and S. Mukherjee, "Normal-based methods for a Gamma distribution: Prediction and tolerance intervals and stress-strength reliability," *Technometrics*, vol. 50, no. 1, pp. 69–78, 2008.

[62] S. Lai and T. Chen, "A method for pattern mining in multiple alarm flood sequences," *Chemical Engineering Research and Design*, vol. 117, pp. 831–839, 2017.

[63] S. T. Lawless, "Crying wolf: False alarms in a pediatric intensive care unit," *Critical Care Medicine*, vol. 22, no. 6, pp. 981–985, 1994.

[64] E. L. Lehmann and J. P. Romano, *Testing Statistical Hypotheses*. Springer Science & Business Media, 2006.

[65] H. W. Lilliefors, "On the Kolmogorov-Smirnov test for normality with mean and variance unknown," *Journal of the American Statistical Association*, vol. 62, no. 318, pp. 399–402, 1967.

[66] D. Manzey, N. Gérard, and R. Wiczorek, "Decision-making and response strategies in interaction with alarms: The impact of alarm reliability, availability of alarm validity information and workload," *Ergonomics*, vol. 57, no. 12, pp. 1833–1855, 2014.

[67] M. Mariton, "Detection delays, false alarm rates and the reconfiguration of control systems," *International Journal of Control*, vol. 49, no. 3, pp. 981–992, 1989.

[68] R. A. Martin, "A state-space approach to optimal level-crossing prediction for linear gaussian processes," *IEEE Transactions on Information Theory*, vol. 56, no. 10, pp. 5083–5096, 2010.

[69] ——, "Optimal level-crossing prediction for jump linear MIMO dynamical systems," *Automatica*, vol. 49(8), pp. 2440–2445, 2013.

[70] C. Marzban, "The ROC curve and the area under it as performance measures," *Weather and Forecasting*, vol. 19, no. 6, pp. 1106–1114, 2004.

[71] E. Mosca and G. Zappa, "Arx modeling of controlled armax plants and lq adaptive controllers," *IEEE transactions on automatic control*, vol. 34, no. 3, pp. 371–375, 1989.

[72] E. Naghoosi, I. Izadi, and T. Chen, "A study on the relation between alarm deadbands and optimal alarm limits," in *American Control Conference (ACC)*, IEEE, 2011, pp. 3627–3632.

[73] C. Nihlwing and M. Kaarstad, "The development and usability test of a state based alarm system for a nuclear power plant simulator," in *Proceeding of Nuclear Plant Instrumentation, Control and Human-Machine Interface Technologies*, 2012, pp. 22–26.

[74] M. Noda, F. Higuchi, T. Takai, and H. Nishitani, "Event correlation analysis for alarm system rationalization," *Asia-Pacific Journal of Chemical Engineering*, vol. 6, no. 3, pp. 497–502, 2011.

[75] K. B. Petersen and M. S. Pedersen, *The Matrix Cookbook*. Technical University of Denmark, 2008.

[76] S. B. Provost and A. M. Mathai, *Quadratic Forms in Random Variables: Theory and Applications*. Dekker, 1992.

[77] H. Raza, G. Prasad, and Y. Li, "EWMA model based shift-detection methods for detecting covariate shifts in non-stationary environments," *Pattern Recognition*, vol. 48, no. 3, pp. 659–669, 2015.

[78] D. V. C. Reising, J. L. Downs, and D. Bayn, "Human performance models for response to alarm notifications in the process industries: An industrial case study," in *Proceedings of the Human Factors and Ergonomics Society Annual Meeting*, SAGE Publications Sage CA: Los Angeles, CA, vol. 48, 2004, pp. 1189–1193.

[79] V. Rodrigo, M. Chioua, T. Hagglund, and M. Hollender, "Causal analysis for alarm flood reduction," *IFAC-PapersOnLine*, vol. 49, no. 7, pp. 723–728, 2016.

[80] M. H. Roohi, T. Chen, and I. Izadi, "$\mathcal{H}_2$ controller synthesis with an alarm performance constraint," in *International Symposium on Industrial Electronics (ISIE)*, 2019, pp. 1–6.

[81] M. H. Roohi and T. Chen, "Performance assessment and design of quadratic alarm filters," *IFAC World Congress*, pp. 1–6, 2020.

[82] A. Salvador, "Faults diagnosis in industrial processes with a hybrid diagnostic system," in *Mexican International Conference on Artificial Intelligence*, Springer, 2002, pp. 536–545.

[83] F. E. Satterthwaite, "An approximate distribution of estimates of variance components," *Biometrics Bulletin*, vol. 2, no. 6, pp. 110–114, 1946.

[84] M. M. Seron, X. W. Zhuo, J. A. De Doná, and J. J. Martınez, "Multisensor switching control strategy with fault tolerance guarantees," *Automatica*, vol. 44, no. 1, pp. 88–97, 2008.

[85] R. E. Skelton, T. Iwasaki, and D. E. Grigoriadis, *A Unified Algebraic Approach to Control Design*. CRC Press, 1997.

[86] S. Spielberg, A. Tulsyan, N. P. Lawrence, P. D. Loewen, and R. Bhushan Gopaluni, "Toward self-driving processes: A deep reinforcement learning approach to control," *AIChE Journal*, vol. 65, no. 10, e16689, 2019.

[87] B. Srinivasan, U. Nallasivam, and R. Rengaswamy, "Diagnosis of root cause for oscillations in closed-loop chemical process systems," *IFAC-PapersOnLine*, vol. 44, no. 1, pp. 13 145–13 150, 2011.

[88] R. Srinivasan, J. Liu, K. Lim, K. Tan, and W. Ho, "Intelligent alarm management in a petroleum refinery," *Hydrocarbon Processing*, vol. 83, no. 11, pp. 47–54, 2004.

[89] J. Taheri-Kalani, G. Latif-Shabgahi, and M. A. Shooredeli, "On the use of penalty approach for design and analysis of univariate alarm systems," *Journal of Process Control*, vol. 69, pp. 103–113, 2018.

[90] W. Tan, Y. Sun, I. I. Azad, and T. Chen, "Design of univariate alarm systems via rank order filters," *Control Engineering Practice*, vol. 59, pp. 55–63, 2017.

[91] D. Tena and I. Peñarrocha-Alós, "A simple procedure for fault detectors design in siso systems," *Control Engineering Practice*, vol. 96, p. 104 302, 2020.

[92] *The International Society of Automation (ISA), Management of Alarm Systems for the Process Industries*. ANSI/ISA Standard 18.2, 2016.

[93] N. F. Thornhill, S. C. Patwardhan, and S. L. Shah, "A continuous stirred tank heater simulation model with applications," *Journal of Process Control*, vol. 18, no. 3-4, pp. 347–360, 2008.

[94] A. Tulsyan, F. Alrowaie, and B. Gopaluni, "Design and assessment of delay timer alarm systems for nonlinear chemical processes," *AIChE Journal*, vol. 64, no. 1, pp. 77–90, 2018.

[95] A. Tulsyan and R. B. Gopaluni, "Univariate model-based deadband alarm design for nonlinear processes," *Industrial & Engineering Chemistry Research*, vol. 58, no. 26, pp. 11 295–11 302, 2019.

[96] J. G. Vanantwerp and R. D. Braatz, "A tutorial on linear and bilinear matrix inequalities," *Journal of Process Control*, vol. 10, no. 4, pp. 363–385, 2000.

[97] J. Wang and T. Chen, "An online method for detection and reduction of chattering alarms due to oscillation," *Computers & Chemical Engineering*, vol. 54, pp. 140–150, 2013.

[98] ——, "An online method to remove chattering and repeating alarms based on alarm durations and intervals," *Computers & Chemical Engineering*, vol. 67, pp. 43–52, 2014.

[99] J. Wang, F. Yang, T. Chen, and S. L. Shah, "An overview of industrial alarm systems: Main causes for alarm overloading, research status, and open problems," *IEEE Transactions on Automation Science and Engineering*, vol. 13, no. 2, pp. 1045–1061, 2015.

[100] J. Wang, Z. Yang, J. Su, Y. Zhao, S. Gao, X. Pang, and D. Zhou, "Root-cause analysis of occurring alarms in thermal power plants based on bayesian networks," *International Journal of Electrical Power & Energy Systems*, vol. 103, pp. 67–74, 2018.

[101] Z. Wang, X. Bai, J. Wang, and Z. Yang, "Indexing and designing deadbands for industrial alarm signals," *IEEE Transactions on Industrial Electronics*, vol. 66, no. 10, pp. 8093–8103, 2018.

[102] Z. Wang, D. W. Ho, and X. Liu, "Variance-constrained filtering for uncertain stochastic systems with missing measurements," *IEEE Transactions on Automatic control*, vol. 48, no. 7, pp. 1254–1258, 2003.

[103] E. B. Wilson and M. M. Hilferty, "The distribution of Chi-square," *Proceedings of the National Academy of Sciences*, vol. 17, no. 12, pp. 684–688, 1931.

[104] P. Wunderlich and O. Niggemann, "Structure learning methods for bayesian networks to reduce alarm floods by identifying the root cause," in *International Conference on Emerging Technologies and Factory Automation*, 2017, pp. 1–8.

[105] L. Xie, "Output-feedback $\mathcal{H}_2$ control of systems with parameter uncertainty," *International Journal of Control*, vol. 63, pp. 741–750, Mar. 1996.

[106] J. Xu, J. Wang, I. Izadi, and T. Chen, "Performance assessment and design for univariate alarm systems based on FAR, MAR, and AAD," *IEEE Transactions on Automation Science and Engineering*, vol. 9, no. 2, pp. 296–307, 2011.

[107] F. Yang, S. L. Shah, and D. Xiao, "Correlation analysis of alarm data and alarm limit design for industrial processes," in *American Control Conference (ACC)*, IEEE, 2010, pp. 5850–5855.

[108] C. Yiakopoulos, K. Gryllias, M. Chioua, M. Hollender, and I. Antoniadis, "An on-line sax and hmm-based anomaly detection and visualization tool for early disturbance discovery in a dynamic industrial process," *Journal of Process Control*, vol. 44, pp. 134–159, 2016.

[109] J. Yu and X. Yan, "Active features extracted by deep belief network for process monitoring," *ISA transactions*, vol. 84, pp. 247–261, 2019.

[110] ——, "Modeling large-scale industrial processes by multiple deep belief networks with lower-pressure and higher-precision for status monitoring," *IEEE Access*, vol. 8, pp. 20 439–20 448, 2020.

[111] H. Zang, F. Yang, and D. Huang, "Design and analysis of improved alarm delay-timers," *IFAC-PapersOnLine*, vol. 48, no. 8, pp. 669–674, 2015.

[112] F. Zhang, *The Schur Complement and its Applications*. Springer Science & Business Media, 2006.

[113] P. Zhang and S. X. Ding, "An integrated trade-off design of observer based fault detection systems," *Automatica*, vol. 44, no. 7, pp. 1886–1894, 2008.

[114] B. Zhou, W. Hu, and T. Chen, "A new method for alarm monitoring of equipment start-up operations with applications to pumps," *Industrial & Engineering Chemistry Research*, vol. 58, no. 26, pp. 11 251–11 260, 2019.